

UNIVERSITY OF CALIFORNIA

Los Angeles

Capturing the Diversity and Evolution of Color and Color Patterns Across Reef Fishes

A dissertation submitted in partial satisfaction
of the requirements for the degree Doctor of Philosophy
in Biology

by

Elizabeth Anne Karan

2023

© Copyright by

Elizabeth Anne Karan

2023

ABSTRACT OF THE DISSERTATION

Capturing the Diversity and Evolution of Color and Color Patterns Across Reef Fishes

by

Elizabeth Anne Karan

Doctor of Philosophy in Biology

University of California, Los Angeles, 2023

Professor Michael Edward Alfaro, Chair

Marine fishes comprise one of the most colorful assemblages of living vertebrates. The diversity of color mechanisms and color patterns is an interesting metric to consider within evolutionary history, however the actual diversity has never been quantified broadly across fishes. Although previous studies have linked diversity of color and color patterns in reef fish to factors ranging from sexual selection and communication with conspecifics to predator-prey interactions, these hypotheses have not been tested in a comparative evolutionary framework. I intend to quantify diversity of color mechanisms and patterns across marine acanthomorphs, which encompass a wide range of morphological, ecological, behavioral, and trophic diversity. This research will apply phylogenetic comparative methods to reef fish color data, integrating phenotypic data with biotic and abiotic factors that contribute to observed color and pattern diversity, to adequately test multiple hypotheses within an evolutionary framework. The aim of this research is to determine how and when diversity in color and color patterns was assembled at different comparative phylogenetic scales. The relative influence of biotic and abiotic factors in determining observed levels of diversity will be quantified to determine the proportional impacts of ecology and life history on color diversity.

The dissertation of Elizabeth Anne Karan is approved.

Karen Elizabeth Sears

Gregory F. Grether

Felipe Hoyos Zapata

Allison Shultz

Michael Edward Alfaro, Committee Chair

University of California, Los Angeles

2023

DEDICATION

To my parents: thank you so much for cultivating and supporting my interests in science.

TABLE OF CONTENTS

	Page
LIST OF FIGURES	vii
LIST OF TABLES	xi
ACKNOWLEDGMENTS	xiii
VITA	xiv
1 Predator avoidance and morphology shape the evolution of false eyespots and eye coverage in butterflyfishes (Chaetodontidae)	1
1.1 Introduction	1
1.2 Methods	6
1.3 Results	13
1.4 Discussion	18
1.5 Conclusion	21
2 Comparative evolution of color pattern across sexual strategies in wrasses (Labridae)	22
2.1 Introduction	22
2.2 Methods	26
2.3 Results	31
2.4 Discussion	36

2.5	Conclusion	38
3	Global spatial patterns and phylogeography of color and color pattern diversity across fishes	55
3.1	Introduction	55
3.2	Methods	58
3.3	Results	61
3.4	Discussion	65
3.5	Conclusion	67

LIST OF FIGURES

	Page
1.1 Examples of eyespot types found throughout the butterflyfish tree: (a) <i>C. unimaculatus</i> with a large oculus on the side body, (b) <i>C. ocellicaudus</i> with a small eyespot on the caudal peduncle, (c) <i>C. rostratus</i> with an ocellus on the dorsal fin, (d) <i>C. auriga</i> with an ovular eyespot on the dorsal fin, (e) <i>F. longirostrus</i> with a small eyespot on the anal fin, (f) <i>C. speculum</i> with a large, ovular eyespot on the side body, and (g) <i>C. bennetti</i> with a large ocellus on the side body.	2
1.2 Hypothesized eyespot properties, eye covering color patterns, and defensive morphology involved in aposematism, predator mimicry, and automimicry. .	4
1.3 (a) The two types of eyespots we considered: simple eyespots (round and uniformly dark) and ocelli (dark spots surrounded by a ring of a lighter color). (b) Possible locations of eyespots on the butterflyfish body. (c) Eye coverage color pattern types included: a vertical stripe, spot, and mask.	7
1.4 The proportional distribution of (a) eyespots and (b) eye coverage across butterflyfishes (97 sp.). Ancestral state reconstructions of (c) eyespots and (d) eye coverage (97 sp.) Eyespots emerge multiple times on the tree. The stripe type eye coverage is ubiquitous and ancestral for most of the family. .	15

1.5	Phylogenetic regression (PGLS) of distance of eyespot from the body's center (eyespot distance from body center) against (a) eyespot diameter and (b) eyespot diameter / eye diameter (all raw trait values, not size-standardized), with lines representing linear models fit to PGLS. The dashed line (a) is a nonsignificant relationship between eyespot distance from body center and eyespot diameter ($t_{1,21} = -1.228817$, $p = 0.2341$). The solid line (b) represents a significant relationship between eyespot distance from body center and the ratio of eyespot diameter over eye diameter ($t_{1,21} = -2.195171$, $p = 0.0408$).	17
2.1	Diagnostic plots of <i>Anampses chrysocephalus</i> , <i>Sparisoma aurofrenatum</i> , and <i>Scarus taeniopterus</i> . Each includes the original image, the discrete color categories determined, the image input for 'pavo' color pattern analysis, and the number of colors (k) to input into 'pavo'	28
2.2	Discrete color categories present across the wrasse tree for (a) males vs (b) females	39
2.3	Continuous map of ancestral states for color pattern transition complexity (m) across the wrasse tree for (a) males vs (b) females.	40
2.4	Continuous map of ancestral states for aspect ratio (A) across the wrasse tree for (a) males vs (b) females.	41
2.5	Continuous map of ancestral states for scaled Simpson color class diversity (Jc) across the wrasse tree for (a) males vs (b) females.	42
2.6	Continuous map of ancestral states for scaled Simpson transition diversity (Jt) across the wrasse tree for (a) males vs (b) females.	43
2.7	Continuous map of ancestral states for chromatic boundary strength (m_dS) across the wrasse tree for (a) males vs (b) females.	44
2.8	Continuous map of ancestral states for achromatic boundary strength (m_dL) across the wrasse tree for (a) males vs (b) females.	45

2.9	Phylogenetic reduced major axis regression of male (x) vs female (y) rates of evolution of color classes (k). Reduced major axis regression ($y = 0.449x + 0.007$; $R^2=0.85776$) is significant ($T = 18.86480$, $df = 57.28805$, $p < 0.00001$) .	46
2.10	Phylogenetic reduced major axis regression of male (x) vs female (y) rates of evolution of scaled Simpson transition diversity (Jt). Reduced major axis regression ($y = 0.791x - 0.001$; $R^2=0.838$) is significant ($T = 5.179$, $df = 57.682$, $P = 3 \times 10^{-6}$.)	47
2.11	Phylogenetic reduced major axis regression of male (x) vs female (y) rates of evolution of achromatic boundary strength (m.dL). Reduced major axis regression ($y = 0.757x - 6.73 \times 10^{-4}$; $R^2=0.981$) is significant ($T = 18.049$, $df = 54.999$, $P < 0.0001$.)	48
2.12	Color pattern morphospace of PC1 (x) vs PC2 (y) for (a) males and (b) females with individuals and hulls colored by habitat type: coral reef associated (red), coral reef exclusive (green), and non coral reef (blue)	49
2.13	Color pattern morphospace of PC3 (x) vs PC4 (y) for (a) males and (b) females with individuals and hulls colored by habitat type: coral reef associated (red), coral reef exclusive (green), and non coral reef (blue)	50
2.14	Color pattern morphospace of PC1 (x) vs PC2 (y) for (a) males and (b) females with individuals and hulls colored by sex allocation type: diandric (red), gonochorous (green), and monandric (blue)	51
2.15	Color pattern morphospace of PC3 (x) vs PC4 (y) for (a) males and (b) females with individuals and hulls colored by sex allocation type: diandric (red), gonochorous (green), and monandric (blue)	52
2.16	Color pattern morphospace of PC1 (x) vs PC2 (y) for (a) males and (b) females with individuals and hulls colored by mating strategy: harem (red), lek-like (green), and promiscuous (blue)	53

2.17	Color pattern morphospace of PC3 (x) vs PC4 (y) for (a) males and (b) females with individuals and hulls colored by mating strategy: haremnic (red), lek-like (green), and promiscuous (blue)	54
3.1	Violin plot of the proportions of each color class (k) displayed by individuals sampled within each species.	62
3.2	Mean species transition complexity (m), pattern aspect ratio (A), scaled Simpson color class diversity (Jc), scaled Simpson transition diversity (Jt), chromatic boundary strength (m_dS), achromatic boundary strength (m_dL), and number of color classes (k) for marine fish assemblages at the global scale. .	69
3.3	Mean species transition complexity (m), pattern aspect ratio (A), scaled Simpson color class diversity (Jc), scaled Simpson transition diversity (Jt), chromatic boundary strength (m_dS), achromatic boundary strength (m_dL), and number of color classes (k) for marine fish assemblages at the global scale for shallow water species only.	70
3.4	Mean species transition complexity (m), pattern aspect ratio (A), scaled Simpson color class diversity (Jc), scaled Simpson transition diversity (Jt), chromatic boundary strength (m_dS), achromatic boundary strength (m_dL), and number of color classes (k) for marine fish assemblages at the global scale for deep water species only	71
3.5	Color pattern morphospace of PC1 (x) vs PC2 (y) with individuals and hulls colored by climate type: temperate (red) vs tropical and subtropical (blue) .	72
3.6	Color pattern morphospace of PC3 (x) vs PC4 (y) with individuals and hulls colored by climate type: temperate (red) vs tropical and subtropical (blue) .	73
3.7	Color pattern morphospace of PC1 (x) vs PC2 (y) with individuals and hulls colored by depth: shallow and deep (red) vs shallow only (blue)	74
3.8	Color pattern morphospace of PC3 (x) vs PC4 (y) with individuals and hulls colored by depth: shallow and deep (red) vs shallow only (blue)	75

3.9	Color pattern morphospace of PC1 (x) vs PC2 (y) with individuals and hulls colored by reef region: Caribbean Sea (red), Coral Sea and Great Barrier Reef (green) and Red Sea (blue)	76
3.10	Color pattern morphospace of PC3 (x) vs PC4 (y) with individuals and hulls colored by reef region: Caribbean Sea (red), Coral Sea and Great Barrier Reef (green) and Red Sea (blue)	77

LIST OF TABLES

1.1	PC summary statistics	13
1.2	PC loads	13
1.3	BayesTraits results showing relative fit of discrete dependent and independent models for a simple eyespot vs ocellus, and the log Bayes Factor (logBF) for eyespot vs ocellus	16
2.1	PC summary statistics for females. Results are given for PCs 1-4 because they explain greater than 10% of the variance.	33
2.2	PC loads for females	33
2.3	PC summary statistics for males. Results are given for PCs 1-4 to match with females.	33
2.4	PC loads for males	34
3.1	PGLS results of median species latitude against colors and color pattern variables. $df = 1,274$, $*p < 0.05$	63
3.2	PGLS results of median species depth against colors and color pattern variables. $df = 1,130$, $* p < 0.05$, $** p < 0.01$	64
3.3	PC summary statistics. Results are given for PCs 1-4 because they explain greater than 10% of the variance.	64
3.4	PC loads	64

ACKNOWLEDGMENTS

I would like to thank my advisor, Dr. Michael Alfaro, for his guidance in my research and career. I thank my committee subject matter expert, Dr. Allison Shultz, for her expertise in interrogating color and pattern evolution. I also acknowledge all members of my PhD committee for their support and feedback. I thank my collaborator, Dr. Jennifer Hodge, for guiding my approach to methods and editing portions of my first chapter. I also thank Dr. Pascal Title for helping with data curating and plotting for the global-spatial analyses. I also thank other graduate students and postdoctoral researchers in the Alfaro lab for their helpful feedback.

Work completed for this dissertation was funded by the National Science Foundation Graduate Research Fellowship, as well as the UCLA Irving and Jean Stone Fellowship.

VITA

Elizabeth Anne Karan

EDUCATION

Candidate in Philosophy in Biology **2021**

University of California, Los Angeles *Los Angeles, CA*

B.A. in Organismic and Evolutionary Biology **2016**

Harvard University *Cambridge, MA*

RESEARCH EXPERIENCE

Graduate Student Researcher **2017–2023**

Alfaro Lab *Los Angeles, CA*

Summer Intern **Summer 2022**

National Institutes of Health / National Library of Medicine *Remote*

Undergraduate Student Researcher **2015–2016**

Lauder Lab / Harvard Museum of Comparative Zoology / *Cambridge, MA*

Ridcliffe Research Partnership

Research Assistant **2014**

Operation Wallacea *Wakatobi N.P., Indonesia*

TEACHING EXPERIENCE

Teaching Assistant **2018–2023**

University of California, Los Angeles *Los Angeles, CA*

REFEREED JOURNAL PUBLICATIONS

1. EA Karan, JR Hodge, ME Alfaro. Predator avoidance and defense shape the evolution of false eyespots and eye coverage in butterflyfishes (Chaetodontidae). In prep.
2. DK Wainwright, **EA Karan**, DC Collar. Evolutionary patterns of scale morphology in damselfishes (Pomacentridae). *Biological Journal of the Linnean Society*. 2021.
3. ME Alfaro, **EA Karan**, ST Schwartz, AJ Shultz. The Evolution of Color Pattern in Butterflyfishes (Chaetodontidae). *Integrative and Comparative Biology*. 2019.
4. PUPA Gilbert, KD Bergmann, CE Myers, MA Marcus, RT DeVol, C-Y Sun, AZ Blonsky, J Zhao, **EA Karan**, E Tamre, N Tamura, AJ Giuffre, S Lemer, G Giribet, JM Eiler, AH Knoll. Nacre tablet thickness records formation temperature in modern and fossil shells. *Earth and Planetary Sciences Letters*. 2017.

CONFERENCE PRESENTATIONS

1. EA Karan, ST Schwartz, M Perillo, ME Alfaro. It's not just a phase: evolutionary and functional consequences of sexually dimorphic color pattern diversity in labrid fishes. *Society of Integrative and Comparative Biology*. Virtual meeting. January 2021.
2. EA Karan, ME Alfaro. Evolution of False Eyespots in Butterflyfishes: Testing Eye Camouflage and Mimicry as Anti-predator Adaptations. *Society of Integrative and Comparative Biology*. Tampa, FL. January 2019.

GRANTS AND FELLOWSHIPS

National Institutes of Health Summer Internship	2022
National Science Foundation Graduate Research Fellowship	2019
UCLA Irving and Jean Stone Fellowship	2017

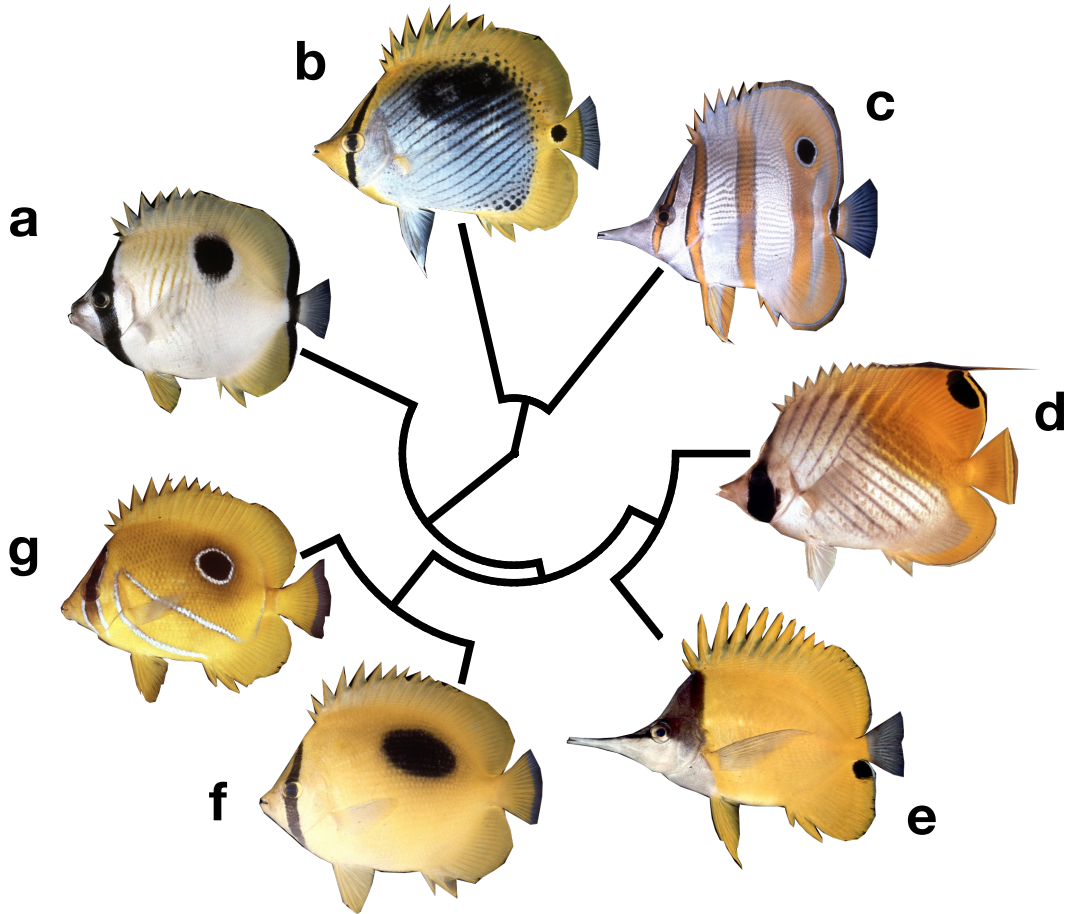
Predator avoidance and morphology shape the evolution of false eyespots and eye coverage in butterflyfishes (Chaetodontidae)

1.1 Introduction

Reef fishes are some of the most colorful communities of vertebrates on the planet. A diverse array of colors and distinct color patterns can be observed on the bodies of most reef fishes. However, it is unclear what drives the evolution of color pattern diversity and specific patterns hypothesized to serve ecologically and behaviorally significant functions. Specifically, it is unclear what functions specific color patterns or motifs may serve, especially those that are utilized by different species.

One of the most conspicuous aspects of the color pattern of butterflyfishes are eyespots, round, pigmented patches that give the impression of an eye. Butterflyfishes (Chaetodontidae) are an ideal group to study the evolution of eyespots because many species display what could be considered an eyespot. Eyespots within this family are remarkably diverse, ranging from large, darkly pigmented ovals on the dorsal and posterior of the portions of the body (e.g., Fig. 1.1a,f-g) to smaller circles on the fin or tail (e.g., Fig. 1.1b-e), with some species displaying multiple eyespots (e.g., Fig 1.1c). Eyespots with a high contrast peripheral ring are sometimes called an “ocellus” [Neudecker, 1989] (e.g., Fig. 1.1c,g). Additionally, most species of butterflyfish possess dark color patterns that reduce the conspicuousness of the real eye (Fig. 1.1c) [Barlow, 1972], a trait thought to enhance some of the proposed functions of

Figure 1.1: Examples of eyespot types found throughout the butterflyfish tree: (a) *C. unimaculatus* with a large oculus on the side body, (b) *C. ocellicaudus* with a small eyespot on the caudal peduncle, (c) *C. rostratus* with an ocellus on the dorsal fin, (d) *C. auriga* with an ovular eyespot on the dorsal fin, (e) *F. longirostrus* with a small eyespot on the anal fin, (f) *C. speculum* with a large, ovular eyespot on the side body, and (g) *C. bennetti* with a large ocellus on the side body.



eyespot patterns [Neudecker, 1989]. Lastly, butterflyfishes tend to have very little significant color pattern variation within species when compared to between-species variation [Hemingson et al., 2018], easily allowing for color pattern elements to be measured for individuals of each species and then aggregated for a cross-species comparative analysis.

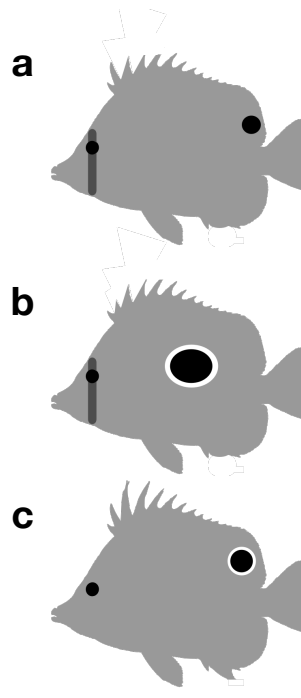
Like insect and amphibian species with eyespots [Stevens, 2005, Arbuckle and Speed, 2015], the controls on eyespot diversity in butterflyfishes are broadly thought to be related

to predation [Meadows, 1993]. However, butterflyfishes exhibit high diversity in other predation related traits including body depth, dorsal and anal fin spine length, and caudal fin shape [Hodge et al., 2018]. For example, some species exhibit deep, laterally compressed bodies and long fin spines that make them too tall for the gape of some predators. Others may lack have a more squat and less spiny body; however, they may depend more on their more rounded caudal fins and maneuverable shallower bodies for better evasive swimming performance when confronted with a predator. Spines and deep bodies appear to be more common in species that forage in open water, consistent with the idea predation pressure is an important selective force on species with risky foraging strategies. However, we still do not understand whether eyespots and other related color-pattern traits reflect a co-evolving suite of characters to divergent ecological pressure. Here we build on a comparative approach to test whether eyespots are part of a larger suite of characters that reflect divergent responses to predation pressure.

There are three main ways that eyespots are thought to serve as anti-predator displays: automimicry, predator mimicry, and aposematism (Fig. 1.2). The automimicry hypothesis posits that eyespots divert attacks to peripheral regions of the body by creating the illusion of a head on the posterior end of the fish, thus increasing evasion success [Meadows, 1993, Kjærnsmo et al., 2016]. Eyespot and other ‘false head’ elements have been shown to incur more peripheral wing damage in butterflies [Robbins, 1981]. Stickleback fishes have been shown to direct their attacks at the large eyespots of prey items [Kjærnsmo and Merilaita, 2013]. This deceptive automimicry has not been experimentally tested within butterflyfishes. However, color patterns that disrupt the outline of the true eye such as dark bars have been suggested to enhance the effectiveness of automimicry strategies, and these patterns tend to co-occur within species of butterflyfish [Neudecker, 1989, Kelley et al., 2013].

Eyespots might also deter predation by allowing butterflyfish to mimic the appearance of a larger predator. Predator mimicry strategies are well documented in moths and butterflies

Figure 1.2: Hypothesized eyespot properties, eye covering color patterns, and defensive morphology involved in aposematism, predator mimicry, and automimicry.



	Strategy	Eyespot size	Eyespot position	Eyespot type	Eye coverage	Morphology	Ecology
a	Automimicry	Small	Peripherally located; opposite of the real eye	Spot	Robust coverage of the real eye essential for deception	Short fin spines; rounded caudal fin	Close to the reef; coralivore/ benthic invert feeder
b	Predator mimicry	Very large	Centrally located on the body	Spot with ring	Obscured real eye could add to deception but not necessary	Short fin spines; rounded caudal fin	Close to the reef; coralivore/ benthic invert feeder
c	Aposematism	Large	No prediction	Spot with or without ring, although contrasting ring may be more conspicuous	Not essential	Large fin spines and/ or deep body; emarginate caudal fin	Pelagic; planktivore

where eyespot patterns on wings mimic the appearance of the eyes of larger birds, such as owls [Vallin et al., 2007]. While many insects display eyespots that resemble the lensed eyes of their vertebrate predators more than their own compound eyes, fish eyes often appear similar to those of their predators, making it difficult to parse predator mimicry from other strategies [Kjernsmo et al., 2016]. However at least some butterflyfish such as *C. speculum* and *C. bennetti* (Fig. 1.1f,g) exhibit a startle behavior wherein the side body is flashed towards potential predators [Motta, 1983] which might serve to display their large and centered eyespots (Fig. 1.1f,g) [Neudecker, 1989].

The aposematism hypothesis posits that eyespots are a form of conspicuous coloration to warn predators that prey is unpalatable or dangerous to consume [Rojas et al., 2015]. False eyespots are proposed to boost the warning signal to potential predators by increasing overall conspicuousness [Stevens, 2007]. Although this hypothesis has been most tested in species that are toxic such as butterflies [Forsman and Merilaita, 1999] and or frogs [Arbuckle

and Speed, 2015], its predictions may extend to any species that is unpalatable in some way [Stevens, 2005]. The long fin spines and deep bodies of several butterflyfishes including *C. rostratus* (Fig. 1.1b) may deter predation through the threat of inflicting painful injury [Hoogland et al., 1956], providing one scenario for the evolution of aposematic coloration in this group.

The functional and ecological differences among these modes of predation mitigation provide a framework for investigating the causes of eyespot diversity within butterflyfishes. We hypothesize that if eyespots are automimetic, they should be closer in size to the true eye and should be positioned on the posteriorly on the body to facilitate misdirection of predatory strikes (Fig. 1.2a). Automimetic eyespots should not be associated with mechanical morphological defenses because the deception is in service of evasion rather than defense. We expect automimetic eyespots to instead correlate with morphological traits and foraging strategies that would facilitate evasion such as more broad, round caudal fin shapes that allow for greater maneuverability in swimming [Blake, 2004]. We also predict that automimetic fishes should be associated with high reef cover because the ability to escape to shelter following a startle response should increase the chances of escaping a larger predator [Cole et al., 2008]. We predict that predator mimicry should select for large, conspicuous eyespots. We expect that, unlike automimicry, predator mimicry should shape these eyespots to more closely resemble the eyes of a large animal (Fig. 1.2b). Like in automimicry, we expect predator mimic eyespots to correlate with morphological traits and foraging strategies that would facilitate evasion. These also include rounded caudal fins and feeding behavior in close proximity to the reef.

We predict that aposematism should select for eyespots that maximize conspicuousness when morphological defense such as fin spines are present (Fig. 1.2c). In contrast to predator mimicry and automimicry, we predict that aposematic eyespots could be more irregular since there is presumably not selection to resemble a natural eye. We expect aposematism to

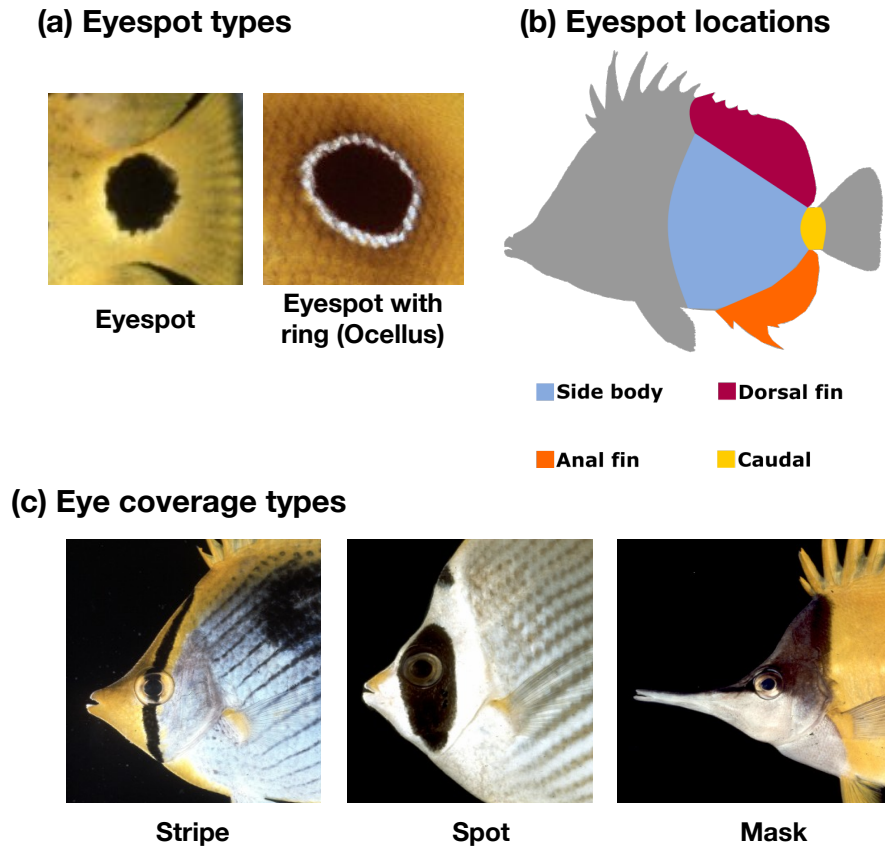
correlate with morphological defenses such as long fin spines and deep body shape. Since aposematism is presented to deter predation, it should not have a strong association with evasive traits such as caudal fin shape. We also expect fishes with this strategy to forage further from reef cover since they are not dependent on escape strategies. Here we investigate the evolutionary basis of eyespot diversity in butterflyfishes. We quantify the diversity of eyespots across the family to reconstruct the evolutionary history of eyespots and associated color pattern traits. We then adopt a comparative approach to test whether eyespot diversity in butterflyfishes reflects an evolutionary response to one of three broad predation mitigation strategies. We investigate the evolutionary relationships between eyespot size and positioning with body size, fin spine length, eye coverage, and eye size in the context of a phylogenetic tree. Our results shed new light on the forces shaping the origins and subsequent evolution of eyespot diversity and how it relates to other traits that mitigate predation risk.

1.2 Methods

Image sources We obtained images of 116 butterflyfish species from the Bishop Museum [Randall, 2023] and used the published standard and/or total length for scaling. We also analyzed images from fishbase.org [Froese and Pauly., 2023] (16 species) and reefs.com [reefs.com, 2023] (1 sp.). However, as these sources lacked information on body size, we excluded them from analyses that required scaling for linear measurements. For all sources, we included only adults and excluded hybrids, uncommon color morphs, and melanistic individuals. A full listing of image sources and the number of species per individual is given in S1. An average of 1.7 ($N = 1-5$) images were used per species.

Quantification of eyespots and related traits We explored the variability of eyespot traits within 156 chaetodontid species (S2). We recognized two eyespot types: simple eyespots and eyespots with rings (ocelli). We defined simple eyespots as circular, uniformly

Figure 1.3: (a) The two types of eyespots we considered: simple eyespots (round and uniformly dark) and ocelli (dark spots surrounded by a ring of a lighter color). (b) Possible locations of eyespots on the butterflyfish body. (c) Eye coverage color pattern types included: a vertical stripe, spot, and mask.



dark black, dark grey, or brown spots on the body that do not overlap with the true eye of the fish (Fig. 3a). We coded eyespots as ocelli if they were surrounded by a concentric ring of a light, contrasting color (Fig. 3a). We coded eyespots as occurring on four regions of the body: posterior side-body, the dorsal fin, the anal fin, and the caudal peduncle (Fig. 3b). We recorded the presence and absence of eyespots, body position, and whether the eyespot was an ocellus as discrete binary traits (S2). We coded three types of coverage of the true eye: vertical stripes, spots, and masks (Fig. 3c). A vertical stripe included a stripe of color extending from near marginal dorsal and ventral edges of the head if it passed directly

through the eye center. Eyespots were any contrasting pattern that overlapped with the true eye, could be of any color, and had to be roughly circular or oval. Masks were large, non-circular, and typically uniform areas of dark pigment covering the eye that connected across the frontal region of the face.

To quantify the relationship between eye size and eyespot size, we measured the diameters (cm) of eyes and false eyespots in ImageJ [Schneider et al., 2012]. Images were scaled using either the standard length (SL) or total length (TL), depending on which was available for each image. Some species of butterflyfishes have extremely long jaws (e.g., *Forcipiger*, *Chelmon*) that can bias size-standardized measures of eye size. To mitigate against these effects, we also measured corrected standard length (corrSL) from the posterior-most edge of the orbit to the posterior edge of the hypural plate. We took the following measures on each individual image: largest diameter of the real eye, largest diameter of the largest eyespot, and corrSL; we also measured the linear distance from the center point of corrSL to the center of the largest eyespot, from here out referred to as eyespot distance from body center (Eyespot distance from body center). To minimize measurement error, we took each measure three times and used the average value for each for each individual fish (S3). Species values were based upon the average of each measure for all individuals of the same species. We used phylogenetic residuals of eye and eyespot measurements for analyses where size correction was necessary but did not size correct in analyses that involved taking ratios of the two.

Morphometrics We used a previously published, time-calibrated maximum-clade credibility phylogeny of butterflyfishes [Hodge et al., 2014] to perform phylogenetic comparative analyses (97 sp.). We used previously published data on the defensive/evasive morphology of butterflyfishes [5] and followed the same procedures for size correction and phylogenetic principal component analysis (PPCA) of the morphological trait data (87 sp.). To account for variation in body size [Collar et al., 2014], measurements of eye and eyespot diameter were size corrected prior to comparative analyses using the `phyl.resid` function in the “phytools”

package in R [Revell, 2012]. Each diameter measurement was regressed against the average total length for each species, which was calculated from the published measurements used to scale the images. We used previously published data on the defensive/evasive morphology of butterflyfishes [Hodge et al., 2018] and followed the same procedures for size correction and PPCA of the morphological trait data (87 sp.). This included a size correction of all linear measurements of body parts using the SL measured in the morphology dataset. All scalar factors, such as caudal fin shape, were not included in size correction. All morphological measures from Hodge et al. [5] were included in the phylogenetic principal component analysis. Resulting principal components (PCs; S4) were used to represent morphology in all subsequent analyses. We also ran a normal principal component analysis (S4) using the `prcomp` function from the “stats” package in R to control for potential component selection bias [Uyeda et al., 2015].

Evolutionary model fitting Several downstream analyses required a choice of evolutionary model for continuous and discrete states. To test if the evolution of a trait was more likely to be represented by a stochastic random walk versus evolution towards an optimum, we tested the fit of Brownian Motion (BM) versus Ornstein–Uhlenbeck (OU) models using AIC scores based upon the `FitContinuous` function in the `geiger` package in R [Pennell et al., 2014]. For discrete states, we compared the fits of symmetric vs asymmetric models using `fitDiscrete` in `geiger` to estimate transition rates for eyespots, eyespots with rings, eyespot placements, eye coverage, and eye coverage types. We predicted strong correlations among continuous traits according to the automimetic, predatory mimicry, and aposematic hypotheses (Fig. 1.2). To test for these associations, we used phylogenetic least-squares regression (PGLS) using the “nlme” package in R [Pinheiro et al., 2021] with the appropriate trait model (BM or OU).

Trait distribution and ancestral states We quantified the frequency and diversity of eyespots, ocelli, and eye coverage type by averaging data across individuals of each species.

We visualized these trait distributions by plotting them on the butterflyfish tree. To understand the major transitions associated with eyespot evolution, we performed an ancestral state reconstruction of all these discrete characters using the `make.simmap` function from the `phytools` R package [Revell, 2012].

Testing Automimicry We hypothesized that an automimetic evolutionary strategy should involve an eyespot that is similar in size to the true eye of the organism and be coupled with camouflage or covering of the true eye to better divert attacks towards the eyespot. To test for dependent evolution of eyespots and true eye coverage we used `BayesTraits` [Meade and Pagel, 2016]. Ocelli are hypothesized to mimic a true eye more closely than simple eyespots [De Bona et al., 2015]. Therefore, we predicted that ocelli would aid an automimetic strategy and tested for an association between ocelli and eye coverage using `BayesTraits`. Each run used an exponential prior with a mean of 10. The stepping-stone sampler used 100 stones and 1000 iterations per stone to estimate the marginal likelihood with discrete unordered states, such that the probability of transitioning from any given state to another is equal. The marginal likelihoods were calculated for discrete dependent and discrete independent models of trait evolution between eye coverage and eyespots (97 sp.). Separating ocelli from simple eyespots, we calculated the log marginal likelihoods of dependent and independent models of trait evolution between presence/absence of eye coverage and ocelli, excluding simple eyespots (97 sp.). Estimates of log Bayes Factors (BF) were calculated from the likelihood ratio statistic, which is $2(\text{marginal log likelihood of the complex model} - \text{marginal log likelihood of the simplest model})$. A log BF of less than 2 is interpretable as very weak evidence that the more complex model is favored, whereas a log BF greater than two is interpreted as positive evidence in favor of the more complex model [Gilks et al., 1995].

An automimetic evolutionary strategy should produce a positive relationship between eyespot size and eye size. To test this, we performed phylogenetic least squares regression

(PGLS) on eye diameter and eyespot diameter (97 sp.) using the “nlme” package in R [Pinheiro et al., 2021]. We also predicted that these eye-sized eyespots evolving under automimicry should be positioned on peripheral areas of the body and fins (Fig. 2c). Among species with eyespots (24 sp.), we performed a PGLS of eyespot size against eyespot distance from body center. To account for the relative size of the eyespot to the real eye, we also ran PGLS with the ratio of eyespot diameter/eye diameter against eyespot distance from body center. In cases where a species exhibited multiple eyespots, only the diameter of the largest eyespot was used. We also ran PGLS of eyespot diameter against eye diameter with discrete coded eyespot positions (Fig. 1.3b) as interaction terms.

Under automimicry we could expect a significant relationship between eye size and eyespot size to occur with more robust forms of eye coverage that effectively obscure the eye, such as a stripe or mask rather than a spot over the eye (Fig. 1.3c). We hypothesize that these more extensive forms of eye coverage are advantageous because they extend to the marginal edges of the head, possibly concealing the profile of a real eye more effectively. To test this hypothesis, we ran a PGLS of eyespot diameter against eye diameter with discrete eye coverage types (Fig. 1.3c) as interaction terms (97 sp.).

We expected that automimetic eyespots and eye coverage should be accompanied by morphological and ecological traits that facilitate evasion once a predator attack has been diverted (Fig. 1.2a). For example, rounded caudal fins may enhance evasive maneuverability [Blake, 2004], and foraging close to the reef within a territory, as some obligate corallivores do, may improve the chances of finding refuge from predators. To test whether species with eyespots have more rounded caudal fins, we performed a Phylogenetic Logistic Regression (PLR) of eyespot presence/absence versus PCs of defensive/evasive morphology traits, caudal fin shape, and max body depth (body depth + dorsal fin spine length + anal fin spine length) using the ape R package [Paradis and Schliep, 2019]. We also performed a PGLS among species of eyespot (19 sp.) of eyespot diameter against PCs of defensive/evasive mor-

phology traits of caudal fin shape and max body depth (body depth + dorsal fin spine length + anal fin spine length) to test if eyespots of varying size showed a significant relationship with these morphological traits. To test if reef proximity via feeding ecology corresponded to morphological traits, we added interaction terms of discrete categories of feeding ecology [Hodge et al., 2018] - obligate corallivore, facultative corallivore, benthic invertebrate feeder, or pelagic planktivory - to PGLS of eyespot diameter against PCs of defensive/evasive morphology traits.

Testing Predator Mimicry Eyespots that mimic the eyes of predators should be large (much larger than the true eye) and centrally located (Fig. 1.2b) for the most conspicuous presentation. To test these predictions, we performed a PGLS of eyespot size against distance from body center (24 sp.), as well as PGLS with the ratio of eyespot diameter/eye diameter against eyespot distance from body center and PGLS of eyespot diameter against eye diameter with discrete coded eyespot positions (Fig. 1.3b) as interaction terms. Like automimicry, we expect eyespots to co-occur with morphological and ecological traits that facilitate evasion once a predator attack has been diverted, including rounded caudal fins and a close association with the reef. To test these relationships, we ran PGLS of eyespot diameter against PCs of defensive/evasive morphology traits with added interaction terms of discrete categories of feeding ecology (87 sp.).

Testing Aposematism Under aposematism we predicted that a large, conspicuous eyespot would be associated with robust morphological defensive traits. We furthermore predicted that aposematism would allow species to employ more risky foraging behaviors since predators would ignore aposematic species in favor of less defended meals. To test for a relationship between eyespot presence/absence and morphological defenses, we ran a PLR of eyespot presence/absence against caudal fin shape and max body depth (body depth + dorsal fin spine length + anal fin spine length) for 78 sp. To test if eyespot size was positively associated with defensive morphology, we ran PGLS of eyespot diameter against principal

components of defensive morphology traits (87 sp.). To test whether riskier feeding strategies such as planktivory and benthic invertivore feeding were associated with large eyespots and defensive traits, we added interaction terms of discrete categories of feeding ecology to the PGLS of eyespot diameter against principal components of defensive morphology traits.

1.3 Results

Morphometrics Phylogenetic PCs 1-3 of morphometrics data were used for downstream analyses and account for 27.68%, 16.55% and 15.04% of the variance respectively (Table 1.1; S4). Dorsal fin spine length, anal fin spine length, and pelvic fin spine length load most heavily on PC1 (Table 1.2; S4). Body depth loads most heavily on PC2. Dorsal-anal fin spine offset and caudal fin shape load most heavily on PC3.

var	PC1	PC2	PC3
Standard deviation	1.49	1.15	1.10
Proportion of Variance	0.277	0.166	0.150
Cumulative Proportion	0.277	0.442	0.593

Table 1.1: PC summary statistics

var	PC1	PC2	PC3
AnalFinSpineLength	0.740	0.247	0.081
BodyDepth	0.208	-0.832	-0.08504086
DorsalAnalFinSpineOffset	0.073	-0.099	-0.817
DorsalFinSpineLength	0.855	0.109	-0.03698879
EyeDiameter	0.591	0.438	0.13458019
PelvicFinSpineLength	0.698	-0.379	-0.18865732
CaudalFinShape	0.205	-0.461	0.621
MaximumBodySize	0.095	0.044	-0.283

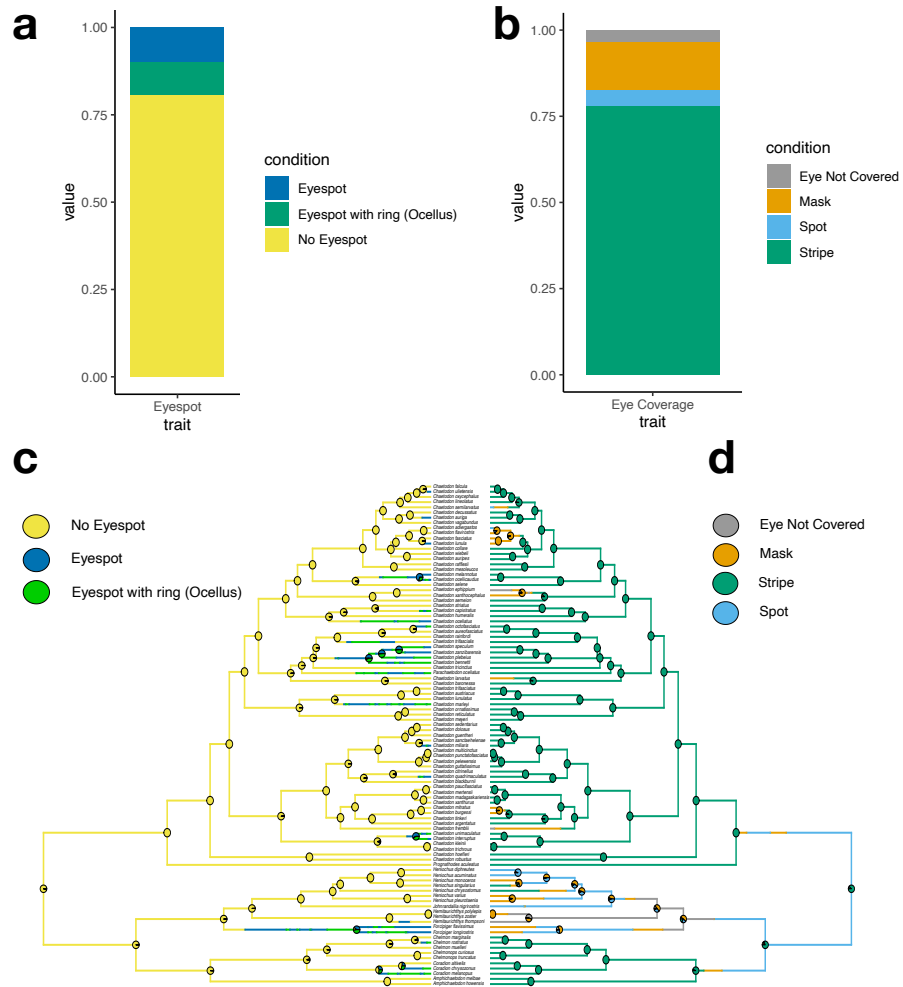
Table 1.2: PC loads

Evolutionary analyses of eyespots All continuous characters – diameters, spine lengths and body size measurements – best fit the OU model and all discrete characters

– presence/absence measures – best fit the symmetric rates model (Table S5). As a result, all PGLS analyses were performed assuming an OU model for the trait of interest. We found that most butterflyfishes do not have eyespots (Fig 1.4a). The common ancestor of butterflyfishes did not possess eyespots and this trait has evolved independently multiple times (18 times) across the tree (Fig. 1.4c). Among those that have eyespots, simple eyespots (13 sp.) are as common as ocelli (10 sp.) throughout the family (97 sp.). Conversely, eye coverage is the most common state throughout butterflyfishes, with a stripe being the most common pattern covering the eye (Fig 1.4b). Our ancestral state reconstruction suggests that the most recent common ancestor of butterflyfishes possessed a stripe covering the eye but no eyespots. Eye coverage was likely present in the common ancestor of all butterflyfishes and is only lost about 3 times on the tree. Eye coverage transitions from stripes to patches or masks have occurred at least 7 times but eye coverage within this clade has only been lost 3 times (Fig 1.4d).

Automimicry We found no evidence for the dependent model of eye coverage evolution in our BayesTraits analyses (Table 1.1), with results favoring the independent model for eyespots ($\log\text{BF} = -70.29$) and ocelli ($\log\text{BF} = -49.93$). This suggests that eyespots and eye coverage have evolved independently, contrary to the predictions of the automimicry hypothesis. Our PGLS analysis recovered a significant negative relationship between eyespot diameter and the presence of eye stripes ($t_{1,87} = 0.7729$, $p = 0.0036$). Eyespots are smaller when eye stripes are present and larger when eye stripes are absent. PGLS did not recover a significant relationship between eyespot distance from body center and eyespot diameter ($t_{1,21} = -1.228817$, $p = 0.2341$; Fig. 1.5a). despite the negative relationship, we do observe a 1:1 ratio of eyespot diameter to eye diameter at distances close to the body center. There was a significant relationship between eyespot distance from body center and the ratio of eyespot diameter / eye diameter ($t_{1,21} = -2.195171$, $p = 0.0408$), where eyespots closer in size to the real eye tend to be further from the body center (Fig. 1.5b).

Figure 1.4: The proportional distribution of (a) eyespots and (b) eye coverage across butterflyfishes (97 sp.). Ancestral state reconstructions of (c) eyespots and (d) eye coverage (97 sp.) Eyespots emerge multiple times on the tree. The stripe type eye coverage is ubiquitous and ancestral for most of the family.



trait	Discrete Dependent	Discrete Independent	log Bayes Factor
Eyespot	-72.44	-70.29	-4.30
Ocellus	-51.73	-49.93	-3.60

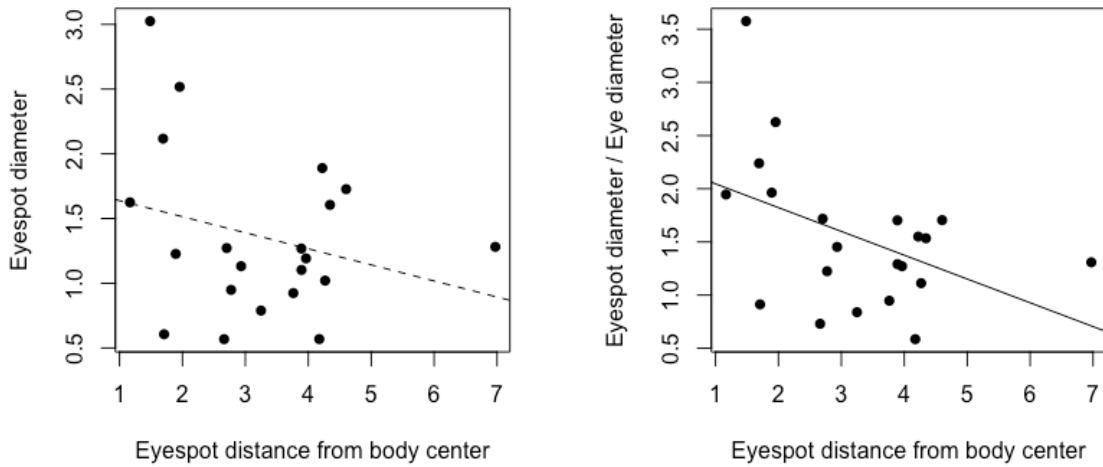
Table 1.3: BayesTraits results showing relative fit of discrete dependent and independent models for a simple eyespot vs ocellus, and the log Bayes Factor (logBF) for eyespot vs ocellus

PLR found a positive correlation between PC3 of the morphological variables and the presence of an eyespot in the caudal region (SE = 0.063446, Z = 2.3766, p = 0.01747). Caudal fin shape loaded strongly in the positive direction on PC3, while dorsal-anal fin spine offset loaded strongly in the negative direction. Species with eyespots in the caudal region tended to have rounded caudal fins and a smaller offset of their longest dorsal and anal fin spines. These results support our hypothesis that peripheral eyespots would correlate with evasive traits rather than defensive ones.

Predator Mimicry In an inverse interpretation the PGLS results' support of an automimicry scenario, eyespots much larger than the real eye tend to fall closer to the body center in eyespot distance from body center vs eyespot/eye size ratio (Fig. 1.5b), supporting the predator mimicry hypothesis. PGLS also found a positive correlation between eyespot diameter and caudal fin shape for obligate ($t_{1,78} = 2.64251$, p = 0.0101) and facultative corallivores ($t_{1,78} = 2.64251$, p = 0.0400).

Aposematism PGLS found a positive correlation between eyespot diameter and max body depth for obligate ($t_{1,78} = -2.705625$, p = 0.0086) and facultative corallivores ($t_{1,78} = -3.168524$, p = 0.0023). This points to a trend where larger eyespots tend to be present on deeper-bodied fishes with longer fin spines that feed close to the reef. PLR showed PC1 was positively correlated with the presence of a spot type eye coverage (SE = 0.046985, Z = 2.5313, p = 0.01137), where species with longer fin spines have spots as eye coverage. This supported the prediction that under aposematic scenarios robust eye coverage that disrupt the outline of the real eye is not necessary.

Figure 1.5: Phylogenetic regression (PGLS) of distance of eyespot from the body's center (eyespot distance from body center) against (a) eyespot diameter and (b) eyespot diameter / eye diameter (all raw trait values, not size-standardized), with lines representing linear models fit to PGLS. The dashed line (a) is a nonsignificant relationship between eyespot distance from body center and eyespot diameter ($t_{1,21} = -1.228817$, $p = 0.2341$). The solid line (b) represents a significant relationship between eyespot distance from body center and the ratio of eyespot diameter over eye diameter ($t_{1,21} = -2.195171$, $p = 0.0408$).



1.4 Discussion

Overview We explored the evolutionary history and patterns of co-occurrence of eyespots and eye markings in butterflyfishes to better understand the relative importance of aposematism, automimicry and predator mimicry in shaping the diversity of these traits. We demonstrate that eyespot diversity is widespread and includes a rich history of co-occurrence with eye coverage. We evaluated comparative phenotypic, morphological, and ecological evidence that eyespots could serve each of these ecological functions (Fig 2) and considered whether color pattern elements can be part of complexes alongside morphological traits that function in display and/or defense. We found support for automimicry, predator mimicry, aposematism.

We compare eyespot instance and size against other color pattern traits, eye coverage types, as well as measures of defensive/evasive morphology. Our results provide insight into the evolutionary dynamics of eyespots and eye markings and assert the importance of position and size of eyespots with co-occurrence of other phenotypic traits when determining function of eyespots. We argue that different placements of eyespots emerge independently for different functions. This spatial aspect of eyespot function has not been previously evaluated in fishes, but its importance has been empirically tested in insects through experimental manipulations [Skelhorn et al., 2014].

Evolutionary history of eyespots and related traits Eye coverage as the estimated ancestral state of butterflyfishes and its wide distribution among extant species is consistent with the findings of Kelley et al. [Kelley et al., 2013], who found a high proportional likelihood for eye stripe presence. These results suggest that eye coverage was present ancestrally, and it could have functioned to deter predators independently of eyespots by breaking up the outline of the body [Barlow, 1972]. The presence of eye coverage is not contingent on the presence of an eyespot; however, an eyespot may emerge in an instance where the eye

is covered. Butterflyfishes may have been predisposed to evolve automimicry or predator mimicry displays from this condition more than aposematism since gaining an eyespot on the body would accomplish both or one predation avoidance strategy because eye coverage bolsters the former two strategies. The multiple emergences of simple eyespots and ocelli (Fig 1.4c) support the idea of multiple functions emerging across species over time.

The loss of eye coverage within the genus *Hemitaurichthys* provides an interesting test of the idea that eyespots co-occur with evasive locomotory traits. *Hemitaurichthys* species are planktivores but unlike most other planktivores in the family, feed away from the reef [Hodge et al., 2018] and mostly associate with outer reefs and reef slopes [Lieske and Myers, 1994]. Eye coverage was likely lost within this genus due to their feeding ecology taking them further from reef coverage than most other butterflyfishes. The loss of eye coverage within this genus may reflect the reduced effectiveness of eye coverage without a nearby refuge for flight.

The evolution of ocelli The significance of ocelli has been emphasized by some authors who argue that only this state sufficiently mimics a true eye to confuse predators and that while eyespots without rings may serve anti-predator functions, their vague and simplistic nature make it likely that they could also facilitate other behaviors like signaling conspecifics [Kelley et al., 2013]. Others have considered that both eyespots with or without rings could achieve similar functions [Kodandaramaiah, 2011], and we followed this rationale in our own analyses. Ringed and unringed eyespots occur in several other fish species [Hemingson et al., 2020], as well as in marine invertebrates like octopus [Norman and Reid, 2000], amphibians including frogs [Arbuckle and Speed, 2015], and most famously insects including butterflies and moths [Kodandaramaiah, 2011]. Ringed eyespots have been suggested to function most effectively in anti-predator displays in these species, all with different hypothesized functions [Stevens et al., 2008]. We were curious what the potential function of contrasting ring could be because it is hypothesized the evolution of a high contrast ring enhances anti-predator

display [Endler, 2012, Endler et al., 2018]. However, we uncovered no significant relationship between the presence of ocelli among eyespot bearing species and any of the traits we tested.

Eyespot function in butterflyfishes Our analyses suggest that diversity in eyespots and related traits within butterflyfishes reflects an adaptive response to different evolutionary pressures. For automimicry, there is the evolution of small, peripherally located eyespots. Predator mimicry which drives the evolution of large, centrally located eyespots larger than the real eye. We also found that large eyespots are found on deeper-bodied, spinier fishes that feed closer to the reef. This deviated from our expectation that fishes displaying aposematic eyespots would be less associated with the reef. Overall, our results suggest that eyespots are part of strategies that weakly defended butterflyfishes use to mitigate predation pressure by either intimidating or confusing potential predators.

We found fishes with deep bodies and longer fin spines that feed close to the reef display large eyespots, possibly as an aposematic warning. However, there are two important caveats to our analysis. First, we did not assess chemical unpalatableness. Although there are no reports of chemically defended butterflyfishes, several species of pufferfish are toxic and possess eyespots or other patterns that are potentially aposematic [Santhanam, 2017]. Skin thickness could be considered a physical defense as well, but it has not been investigated the context of aposematism. Second, our analysis points to a significant association between physical defense and eye patches. Although we did not treat eye patches as eyespots since the patches occur over the true eye, it is possible that the eyepatch itself is aposematic.

Eyespots as an evasive-defensive tradeoff We observe that both deep-bodied, long-spined fishes and fishes with more rounded caudal fins rely more on large eyespots. This contradicts with an observed trend across fishes where eyespots tend to be less common with increasing body size [Hemingson et al., 2020]. Larger and deeper bodied butterflyfishes may not employ larger eyespots strategies simply because they cannot easily escape into and maneuver as easily within reef cover. Smaller fish species, like shallower bodied butterfly-

fishes, may be more easily swallowed by predators so distraction and evasion could buy time against quick predation. A larger eyespot could buy precious time through intimidation in an escape scenario. Additionally, both smaller fish species and shallower bodied butterflyfishes should have an easier time escaping into and maneuvering high-cover reef environments when evading predators with more rounded caudal fins.

1.5 Conclusion

We assert the diverse presentations of false eyespots have different functions, predominantly automimicry and predator mimicry based on evidence of their evolutionary relationships to other phenotypic and ecological traits. While we found no evidence for aposematism in our analyses, more holistic support of “unpalatableness” outside of physical defenses could be explored in future work. More broadly, however, we hope our approach of associating color pattern diversity to other traits opens a more nuanced framework for testing functional hypotheses of color patterns. We also emphasize the need to recognize and not reduce potential diversity of appearance and function within seemingly discrete color pattern elements like eyespots.

Comparative evolution of color pattern across sexual strategies in wrasses (Labridae)

2.1 Introduction

Colors and color patterns that fish display are significant because they are part of visual communication. Sexual color dimorphism, also known as sexual dichromatism, is largely attributed to sexual selection, where different sexes will broadcast distinct displays to conspecifics to convey information such as mating availability and fitness for reproduction. There are fishes that only display specific colors within the context and duration of mating-related activity. Temporal variation can function both in courtship and in antagonistic interactions between competing males, often in species with seasonal reproduction [Kodric-Brown, 1998]. Some species display conspicuous patches of bright color as a signal for mating. Carotenoid-based color is hypothesized to be signal of foraging success and mate quality because carotenoids can only be acquired through diet and the pigments are costly to produce [Grether et al., 2001, Lozano, 2001]. Therefore different elements of color and pattern can transmit different signal between the sexes that display them. Sexual dichromatism is of particular interest in wrasses and parrotfishes (Labridae) because of its common frequency across species in the family. The conspicuous colors and patterns among, usually male, breeding adults within the family suggested to be the result of sexual selection [Choat and Robertson, 1975, Robertson and Hoffman, 1977]. Adults usually keep a consistent pattern once they reach maturity or their most terminal phase [Robertson and Warner, 1978].

Color and pattern are not only considered within the context of sexual selection and intraspecific communication, but also balanced by the effects of natural selection, where colors that allow an organism to mitigate conspicuousness to potential predators may also contribute to fitness [Endler, 1983]. Colors themselves contribute to conspicuousness, but so can overall pattern through the juxtaposition of adjacent or other co-occurring colors [Endler, 1983, 2012, Endler et al., 2018]. Among species that exhibit sexual color dimorphism, disparity in color pattern geometry contributes to differences in relative conspicuousness towards both predators and conspecifics among sexes. The final color and pattern is a compromise between the forces of sexual and natural selection [Endler, 1978, 1983]. Therefore, color and color pattern geometry are important traits to consider within the context of sexual dichromatism and its evolution.

Factors like depth and water clarity can distort how visual signals are broadcast and received. Low visibility in turbid environments can reduce the perceived threat of predation [Gregory, 1993] and can reduce scrutiny in mate choice, relaxing the influence of sexual selection [Seehausen et al., 1997]. Habitat variation can also produce variation in diet among populations; differences in the abundances of carotenoid-rich food [Grether et al., 2001] could potentially produce both spatial and temporal variation in observed color phenotypes. Wrasses are mostly reef-associated, but the level of association varies widely among the many species. At the scale of cross-species comparative analyses, wrasses can be placed within three broad categories of habitat association: coral reef associated, coral reef exclusive, and non-reef associated [Hodge et al., 2020a,b]. All of these factors could shape color pattern evolution across wrasses. It can be hypothesized the reefs may drive complexity in color and pattern due to more inter and intraspecific competition with higher density and proximity on coral reefs.

Sex allocation type varies among wrasses, producing very distinct differences in temporal variation in color pattern among species. There are three main sex allocation types among

wrasses: gonochorism, diandric protogyny, and monandric protogyny [Hodge et al., 2020a,b]. Gonochorous species have static sexes, where individuals reproduce as once sex for the rest of their lives once they reach maturity [De Mitcheson and Liu, 2008]. Diandric species are ones where males are either born directly (primary males) or derived from females going through a sex change (secondary males) [De Mitcheson and Liu, 2008]. Monandric species only derive males via sex change from females, meaning all individuals begin life as functional females [De Mitcheson and Liu, 2008]. In diandric and monandric species, a single individual will display different colors and patterns throughout their lives. Secondary males tend to grow much larger upon sex change [McCormick et al., 2010]. Coloration and mating behavior can also differ of males of different body sizes [Taborsky et al., 1987], especially smaller males who may employ certain mating strategies dependent on the color pattern that they display. Therefore, it can be hypothesized that color pattern complexity is more important for smaller primary males.

Mating strategy varies among wrasse species and can have profound effects on the colors and patterns displayed by males vs females of the same species. There are three main categories of mating strategy among wrasses: promiscuity, lek-like polygyny, and harem polygyny [Hodge et al., 2020a,b]. Promiscuous species have females freely mating with males without territories, therefore there is no pressure for males to defend territories with the purpose of attracting mates [Colin and Bell, 1991]. Lek-like species involve terminal males establishing and defending *temporary* territories that are visited by females for reproduction [Colin and Bell, 1991]. Harem species involve terminal males maintaining *permanent* territories where a single male can monopolize all females that reside within the territory [Colin and Bell, 1991]. Harem males may be under less sexual selective pressure to be conspicuously colorful than males of lek-like or promiscuous species due to the latter two having fewer and fleeting mating opportunities, increasing the demand to better attract female attention through flashy displays. Between lek-like and promiscuous species, it can be hypothesized the promiscuous species would have the most pressure to be the most

conspicuously colorful.

The relationship between evolutionary rates and the presence of dichromatism in wrasses has been investigated in previous studies. The influence of sexual selection on diversification rates in parrotfishes, a subfamily within wrasses with clear sexual dichromatism, has been estimated along with the influence of feeding functional morphology; while innovations in feeding morphology occurred earlier in the tree, inferred location of a more recent rate shift on the parrotfish tree suggests that sexual selection played a major role in diversification [Alfaro et al., 2009, Kazancioglu et al., 2009, Streelman et al., 2002]. However, many of these studies focus on terminal males and ignore female coloration when considering other traits. Other work has shown that dichromatism has evolved adaptively dependent on life history traits, including habitat, sexual allocation types, and mating strategies, to contribute to the family’s widespread success on coral reefs [Hodge et al., 2020b]. Still, all of these studies classify dichromatism broadly across species and do not focus on specific color and pattern differences between males and females.

Quantifying the differences in color patches and pattern between males and females provides more information than simply quantifying dimorphism. Patches of color and patterns are complex traits that encompass many evolutionary processes [Grether et al., 2004, Endler, 1983]. Additionally, color and pattern give us more axes of diversity to quantify and test when compared to binary classification of dichromatism presence or absence within a species [Salis et al., 2019], giving us a more complete picture of the evolution, ecology, and behavior. A major limitation in our knowledge is that color and color pattern diversity have not been rigorously quantified within and across most families, including Labridae. Additionally, simple visual classifications of the frequency and positional relationships of colors and color patterns are not enough to adequately support hypotheses about observed levels of diversity due to biases the human visual system. Previously collection of these data was extremely tedious and time consuming, but new advances in computation and computer vision allow

for mass analyses with readily available image data. I have developed methods for rapidly extracting categorical color data from images. In this chapter, I will use these methods to measure discrete colors and metrics of color pattern geometry in different species of wrasses. I will then take the measures to test what color and pattern elements have different evolutionary patterns between males and females across species, examining how these elements factor into the evolution of dichromatism across wrasses. I test the general hypothesis that males are more colorful or have more complex patterns than females. Finally, I will examine how male-female differences in color pattern correlate with the different sex allocation types, mating strategies, and habitats used in different species of wrasses. I test the hypotheses of 1. if competition on reefs driving complexity in color and pattern, 2. if color pattern diversity is more important in species with competing primary males than species with secondary males, and if 3. if promiscuity in mating producing more colorful males with more complex patterns.

2.2 Methods

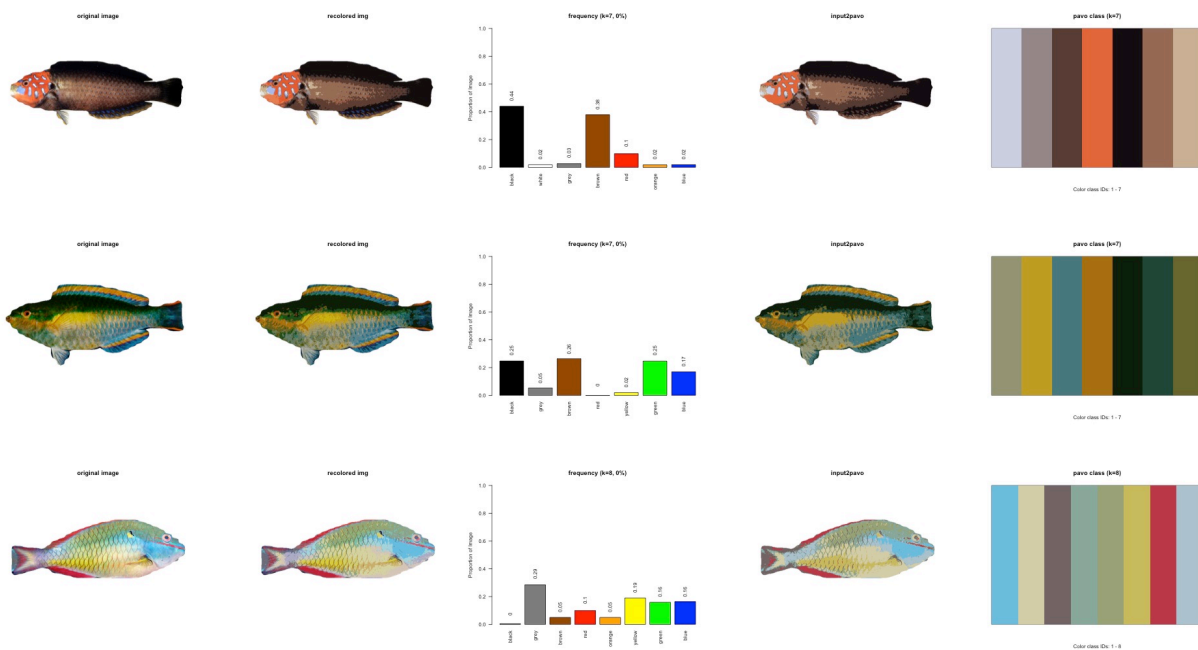
Image sourcing and processing I aggregated images of males and females for 94 wrasse species, with most from the Bishop Museum [Randall, 2023] and fishbase.org [Froese and Pauly., 2023]. One representative image was selected for a male and female of each dichromatic species, and one image represented species that were not dichromatic. There was a total of 150 images; a detailed list of all image sources can be found in Supplementary Table 7. All individual images were visually identified as male or female based on appearance, and I separated all images into separate male and female sets for all following analyses. Image backgrounds were removed using sashimi [Schwartz and Alfaro, 2021], a tool for removing image backgrounds from animal subjects using image segmentation with a neural network. The segmented images were used for all color pattern analyses.

Color pattern analyses The first step in color pattern analysis typically requires the classification of each pixel in the image to a discrete number of color classes. Many popular color pattern analysis pipelines such as the pavo package in R [Maia et al., 2013] require users to input the number of dominant color classes (k) before computing color pattern geometry measures. Traditionally this determination has fallen on people visually apprising images to manually assign discrete color classes. Visual classification is time consuming, where sampling a single family requires hundreds of images to be processed and each image takes several minutes. Visual classification can also be biased because the classification of traits can vary among individuals and the human visual system has inherent biases when classifying dominant colors. Subjectivity can be removed to a degree by using a spectrometer to measure color [Stoddard and Prum, 2011], however, our sample includes existing photographs because live spectrometry of fish for the number species required for macroevolutionary analyses would be extremely difficult to obtain. Others have obtained colors by processing images with cone-capture models to simulate the colors that would be perceived by a given organism [Troschianko and Stevens, 2015]. However, determining k for large-scale, cross-species analyses can be cumbersome and inconsistent due to variance in visual spectral sensitivity across species. Previous studies have avoided this bottleneck by choosing one, overarching k -value to account for the typically observed variation within that group [Alfaro et al., 2019]; However, this naive approach fails to account for differences in color pattern geometry statistics when color diversity within species is large.

Our research group has worked collaboratively to create charisma [Schwartz et al., In prep], an R tool to automatically determine the number of distinct color classes within an image or image set, substantially limiting the need to generalize k for large-scale color class determination. Charisma uses earth mover's distance [Rubner and Tomasi, 2001, Weller et al., 2022], a metric that uses pairwise comparisons of histograms to summarize color distance scores. One can also set minimum thresholds for amount of color present to be considered a discrete color class to avoid small negligible amounts of color or image artifacts

on photographs. Additionally, currently color class determination can be toggled between RGB and HSV perceptual color spaces. Once k is established, each of the identified color classes are matched to a database of known colors and can be assigned to one of 10 broad color classes. Color categories were determined with charisma, which aggregates pixels in the image based on chromatic proximity using clustering to classify colors present in an image into k categories. To check to see if the number of color classes and color categories I appropriate, I produced a diagnostic plot for each image (Fig. 2.1).

Figure 2.1: Diagnostic plots of *Anampses chrysocephalus*, *Sparisoma aurofrenatum*, and *Scarus taeniopterus*. Each includes the original image, the discrete color categories determined, the image input for 'pavo' color pattern analysis, and the number of colors (k) to input into 'pavo'



Color geometry statistics were calculated in pavo package in R [Maia et al., 2013] with inputs of the segmented image and k . The geometry statistics are based upon the colors of the sampled pixels, the frequency of color transitions to adjacently sampled pixels, and the color distance between adjacent pixels.[Endler, 2012, Endler et al., 2018]. I calculated the overall pattern transition density (m), the aspect ratio (ratio of row-wise to column-wise

transitions, A), the scaled Simpson color class diversity (J_c), the scaled Simpson transition diversity (J_t), and the mean chromatic and achromatic boundary strength (m_{dS} and m_{dL}) using pavo [Maia et al., 2013]. Transition complexity quantifies the number of unique transitions across the image. Aspect ratio describes a scale of complexity cross the horizontal vs vertical axis, where $A < 1$ is closer to vertical banding) and $A > 1$ is closer longitudinal stripes. J_c normalizes the proportion of colors by the number of colors present. J_t is the transition complexity normalized by number of colors present. Chromatic boundary strength describes the intensity of transition between color patches. Achromatic boundary strength describes the intensity of transition between patches divorced from color.

Boundary strength analyses are ideally done using color distances calculated by the photoreceptor outputs of the appropriate observer [Endler, 2012]. These distances can be calculated by obtaining data on reflectance per wavelength for each color region using a reflectance spectrometer or a color and luminance calibrated digital photograph, and then applying a visual model [Endler, 2012]. I could not perform these calculations because our data were not collected with a calibrated camera, therefore I could not obtain calculations of reflectance per wavelength. Additionally, while some species from this family have had their visual systems described, these data do not exist for all species and may vary. Finally, the evolution of these color patterns may be the product of selection not only from conspecifics, but also other organisms (e.g. predators) with different visual systems [Winters et al., 2018]. Although the image data used in our study does not necessarily incorporate information about the visual system of a particular aquatic viewer, I argue that they describe empirical aspects of the color patterns.

Evolutionary model fitting I used a wrasse phylogenetic tree extracted from fish tree of life [Rabosky et al., 2018] for all comparative analyses. For the discrete color class categories (84 sp.), I compared the fits of symmetric vs asymmetric models using the `fitDiscrete` function in the `geiger` package in R [Pennell et al., 2014] to estimate transition rates. I tested the fit

of Brownian Motion (BM) versus Ornstein–Uhlenbeck (OU) models using AIC scores based upon the `FitContinuous` function in `geiger` for color pattern geometry metrics (81 sp.). This was to test if the evolution of a trait was better represented by a stochastic random walk versus evolution towards an optimum for these continuous values.

Comparing male vs female color traits I used `charisma` to extract discrete color categories and color pattern geometry statistics for males and females of each species in the tree (84 sp.) in RGB color space. To determine how the continuous color pattern geometry traits change differently through time between males and females, I performed ancestral state reconstructions on male and female trees (81 sp.) with `fitContinuous` (`geiger` in R) [Pennell et al., 2014]. The trees were plotted using the `contMap` function in the `phytools` package in R [Revell, 2012].

To determine if there was a significant difference between the rates of evolution for color and pattern geometry traits between males and females, I calculated the rates for the number of colors (k) and each color pattern geometry metric for separate sexes using `RRphylo` (81 sp.) [Silvia Castiglione et al., 2018]. I compared the rates between sexes using phylogenetic reduced major axis regression (`phyloRMA`) with the function `phyl.RMA` (“lambda” method) in the `phytools` R-package [Revell, 2012], with values for males as x-variable and values for females as y-variable (Babarović et al. 2023)

Color pattern morphospace To combine the the color pattern statistics into a single morphospace, I performed a phylogenetic principal component analysis (PPCA) using the `phytools` package in R [Revell, 2012] separately for male and female data sets. This was done to holistically explore different aspects of color pattern diversity at once. I also ran a normal principal component analysis (S9) using the `prcomp` function from the `stats` package in R to control for potential component selection bias [Uyeda et al., 2015]. I plotted the PCs against each other and see how different life history traits fall within the color pattern trait morphospace (75 sp.). Additionally, I calculated convex hull areas for each life history

category within the morphospace using the `chull` function from the `grDevices` package in R [R Core Team, 2023].

Life history and color pattern evolution I obtained life history traits from Hodge et al. [Hodge et al., 2020a], including the proportion of color dimorphism within each species, habitat, sex allocation type, and mating strategy. Proportion of color dimorphism is a numerical proportion, therefore I compared it against continuous traits. I used these discrete categories of habitat, sex allocation type, and mating strategy as interaction terms for some analyses and to segment data for others. To examine the relationship between color pattern geometry and life history traits strongly tied to sexual dichromatism, I performed a phylogenetic least-squares regression (PGLS) of the color pattern geometry PCs and proportion of color dimorphism with habitat, sex allocation type, and mating strategy added as interaction terms (75 sp.) using the “nlme” package in R [Pineiro et al., 2021].

2.3 Results

Evolutionary model fitting All continuous characters fit the OU model and all discrete characters fit the symmetric rates model (S8). As a result, all PGLS were fit with an OU model.

Comparing male vs female color traits All color classes are represented across male and female trees (Fig. 2.2). There tends to be a lot more brown among the females (Fig. 2.2b), which may give the impression that they are duller. However, a lot of males have brown too (Fig. 2.2b).

The ancestral state reconstructions show some differences in the color pattern trait distribution and history between males and females. Males have more color transitions (m) and appear to have that trait ancestrally with it being lost within some clades (Fig. 2.3a). The

inverse pattern appears on the female tree, where lower transition complexity is widespread and ancestral with a few clades independently evolving more complexity (Fig. 2.3b). Pattern aspect ratio (A) appears to be very close in value between males and females of the same species, with only a few clades where one sex evolves a much lower value for aspect ratio (Fig. 2.4). If $A < 1$ then the pattern is simpler along the horizontal axis (closer to vertical banding) and if $A > 1$ it is simpler along the vertical axis (closer to longitudinal stripes). Most species regardless of sex have a value of $A < 1$, suggesting patterns close to vertical stripes are more common across the family. The scaled Simpson color class diversity (Jc) is relatively similar between males and female of the same species with only a few clades showing significant differences (Fig. 2.5). The scaled Simpson transition diversity (Jt) shows that some clades of both sexes have independently evolved significantly different diversity values than the opposite of the same species (Fig. 2.6). Chromatic boundary strength (m_dS) shows no overall strong pattern across male and female trees (Fig. 2.7). Achromatic boundary strength (m_dL) shows that most species have similarity between the sexes with a few instances of the sexes evolving to extremes that are both inverse of the opposite sex, but also far from values of the same sex of closely related species (Fig. 2.8).

Phylogenetic reduced major axis regression shows male and female rates for number of color classes are strongly correlated ($R^2=0.85776$; Fig. 2.9). Between sexes, color pattern traits are strongly correlated for the patterns metrics of Simpson scaled transition diversity ($R^2=0.837534$; Fig. 2.10) and achromatic boundary strength ($R^2=0.98114$; Fig. 2.11).

Color pattern morphospace The phylogenetic PCs 1-4 were calculated from the female color pattern traits (Table 2.1; S9). Scaled Simpson transition diversity (Jt), achromatic boundary strength (m_dL), and scaled Simpson color class diversity (Jc) load the most heavily on PC1 (Table 2.2). Chromatic boundary strength (m_dS) and aspect ratio (A) load the most on PC2. Transition complexity (m) loads most heavily on PC3. Aspect ratio (A) and chromatic boundary strength (m_dS) load most heavily on PC4.

var	PC1	PC2	PC3	PC4
Standard deviation	1.54	1.18	0.982	0.840
Proportion of Variance	0.397	0.232	0.161	0.118
Cumulative Proportion	0.397	0.630	0.790	0.908

Table 2.1: PC summary statistics for females. Results are given for PCs 1-4 because they explain greater than 10% of the variance.

var	PC1	PC2	PC3	PC4
m	-0.278	0.040	0.956	0.057
A	-0.298	0.706	-0.082	0.622
Jc	0.809	0.425	-0.010	0.030
Jt	0.912	-0.075	0.126	0.201
m_dS	-0.068	-0.831	-0.064	0.523
m_dL	0.852	-0.130	0.153	0.034

Table 2.2: PC loads for females

The phylogenetic PCs 1-4 were calculated from the male color pattern traits (Table 2.3; S9). Scaled Simpson transition diversity (Jt), achromatic boundary strength (m_dL), transition complexity (m), and scaled Simpson color class diversity (Jc) load the most heavily on PC1 (Table 2.4). Chromatic boundary strength (m_dS), scaled Simpson color class diversity (Jc), and aspect ratio (A) load the most on PC2. Chromatic boundary strength (m_dS) loads the most on PC3 and achromatic boundary strength (m_dL) the most on PC4.

var	PC1	PC2	PC3	PC4
Standard deviation	1.57	1.29	0.892	0.662
Proportion of Variance	0.414	0.277	0.133	0.073
Cumulative Proportion	0.414	0.692	0.824	0.897

Table 2.3: PC summary statistics for males. Results are given for PCs 1-4 to match with females.

PC1 vs PC2 for habitat type did not show any recognizable pattern across either axis (Fig. 2.12). When the morphospace of PC3 vs P4 is categorized by habitat type, the male space does not show any significant patterns (Fig. 2.13a). The Female morphospace shows three species as extreme outliers with high values on the PC3 axis with each representing

var	PC1	PC2	PC3	PC4
m	0.677	-0.552	-0.049	0.284
A	0.505	-0.590	-0.506	-0.024
Jc	-0.601	-0.684	-0.140	-0.102
Jt	-0.835	-0.047	-0.393	-0.198
m_dS	0.188	0.729	-0.602	0.162
m_dL	-0.823	-0.102	0.0138	0.531

Table 2.4: PC loads for males

each of the three potential habitat types (Fig. 2.13b). The rest of the species inhabit the lower bound of the PC3 axis. Transition complexity loads most heavily on PC3 for females, suggesting that most species' females have relatively low transition complexity other than the three outliers. All habitat types show wide spread across the PC4 axis for females.

PC1 vs PC2 for sex allocation type did not show any recognizable pattern across either axis (Fig. 2.14). When categorizing the morphospace of PC3 vs P4 by sex allocation type, the male space does not show any clear patterns (Fig. 2.15a). The female morphospace shows three species as extreme outliers with high values on the PC3 axis, all of them diandric species (Fig. 2.15b). With the exception of the outliers, all other females of any mating strategy occupy the lower bound of the PC3 axis. This suggest that most species' females, including all gonochorous and monandric females, have low transition complexity.

The morphospace of PC1 vs PC2 categorized by mating strategy shows promiscuous species inhabiting a small area of the morphospace for both males and females (Fig. 12.16). The promiscuous males are only within small bounds of both the PC1 and PC2 axes (Fig. 12.16a). Scaled Simpson transition diversity, achromatic boundary strength, transition complexity, and scaled Simpson color class diversity load the most heavily on PC1 for males. Chromatic boundary strength and scaled Simpson color class diversity load the most heavily on PC2 for males. The restricted area of the morphospace that promiscuous males inhabit suggests they have low transition complexity, high color class diversity, low chromatic boundary strength and high achromatic boundary strength. Promiscuous females have spread

across the PC1 axis but are restricted within smaller bounds higher on the PC2 axis (Fig. 12.16b). Chromatic boundary strength and pattern aspect ratio load the most on PC2 for females. This suggests promiscuous females with lower chromatic boundary strength and higher values of color pattern aspect ratio. The morphospace of PC3 vs PC4 categorized by mating strategy also shows promiscuous species inhabiting a small area of the morphospace for both males and females (Fig. 12.17). The area of the morphospace occupied by promiscuous female species is exceptionally restricted, and the area of harem females is restricted to the lower bounds of the PC3 axis (Fig. 12.17b). Most species' females, including all harem and promiscuous females, have low transition complexity.

Life history and color pattern evolution The PGLS of the color pattern geometry PCs against proportion of dichromatism with habitat as an interaction term reveals a significant positive relationship ($t_{1,87} = 1.9982578$, $p = 0.0496$) between PC4 and proportion of dichromatism for reef exclusive species of males. Since achromatic boundary strength loads most heavily on PC4 (S9), there is support for achromatic boundary strength being higher when rate of dichromatism is higher in reef exclusive male species. For females, there is significant positive correlation ($t_{1,87} = 2.2896665$, $p = 0.0251$) between PC3 and proportion of dichromatism for reef exclusive species. Chromatic boundary strength and pattern aspect ratio load the most on PC2 for females (S9). A low chromatic boundary strength and a high pattern aspect ratio correlate with higher rate of dichromatism for non coral reef females.

When sex allocation type is added as an interaction in PGLS, there is a significant positive relationship between PC2 and proportion of dichromatism for gonochorous ($t_{1,87} = -2.344109$, $p = 0.0220$) males. Chromatic boundary strength, scaled Simpson color class diversity, and pattern aspect ratio load the most heavily on PC2 for males. A high chromatic boundary strength, a low color class diversity, and a low pattern aspect ratio correlate with higher rate of dichromatism for gonochorous males. There is a significant negative relationship between PC3 and proportion of dichromatism for gonochorous ($t_{1,87} = -2.5283757$, $p = 0.0138$) and

monandric ($t_{1,87} = -2.5131482$, $p = 0.0143$) females. Since transition complexity loads the most on PC3, a low transition complexity correlates with higher rates of dichromatism for gonochorous and monandric female species.

With mating strategy as an interaction, there is a significant ($t_{1,87} = -2.1486846$, $p = 0.0352$) negative relationship between PC3 and proportion of dichromatism for promiscuous males. Chromatic boundary strength loads the most on PC3 for males, suggesting promiscuous males have higher chromatic boundary strength with higher rates of dichromatism.

2.4 Discussion

Male vs female color and pattern traits Color categories are widely represented across species of both sexes. One distinction I think is that more species' females tend to display the color brown than males overall. Surprisingly females of many species do display conspicuous carotenoid-derived colors - red, orange, yellow - often associated with male fitness. Male and female rates for color pattern traits are strongly correlated for color classes, Simpson scaled transition diversity, and achromatic boundary strength. This suggests that, broadly across wrasses, both sexes are under similar amounts of selective pressure when it comes to these color pattern traits. Most interestingly, rate of evolution for the number of colors is correlated between the sexes. The reason for this should be further tested in future work. Correlated rates between sexes may be due to the pressure to keep color consistent enough to maintain intraspecific recognition across sexes. Alternatively, the correlation may also potentially be due to developmental constraints within species fixing the number of color producing mechanisms, especially in cases of sequential hermaphroditism found in many species.

Life history and color pattern evolution In terms of habitat, it appears the reef

exclusive males tend to have high achromatic boundary strength at high proportions of dichromatism. This metric captures the strength of conspicuous transitions absent of color [Endler et al., 2018], so it makes sense for reef exclusive species because reefs tend to have a lot of conspicuous transitions across their cover and the males have to stand out. The strong achromatic color transitions of these males may serve to be eye catching to a proximal potential mate while not attracting the attention from the distant predator due not being too colorful [Endler, 1992]. Reef exclusive females display low chromatic boundary strength and a high pattern aspect ratio correlating with higher proportions of dichromatism. It is intuitive that females would display less conspicuous color transition color transitions because they do not have to attract male attention in many mating scenarios. By not displaying large patches of very conspicuous colors often associated with males, the females avoid attracting attention from predators.

Gonochoruous males tend be more conspicuous with less complex patterns at high proportions of dichromatism. As hypothesized, these primary males may have to be more conspicuous because they may rely more on colorful than being larger. This may also be because a lifetime male has more overall mating opportunities through time, so there is limited sexual selective pressure for a more complex color pattern. However, the males still need to remain conspicuous to attract female attention. Gonochorous and monandric females both have low transition complexity. Diandric females may not fit this pattern since there tends to be a lot of variation among females across the PC3 axis (Fig. 12.15).

Promiscuous males have higher chromatic boundary strength at high proportions of dichromatism. This supports the hypothesis that promiscuity would drive more conspicuous color. Among different mating strategies, all harem and lek-like males tend to have extremely variable color patterns across species (Fig. 2.16a, 2.17a). However, promiscuous males seem to be more restricted in their color pattern geometry, suggesting a promiscuous mating strategy puts strong sexual selective pressure on male coloration. It seems that

promiscuous female color patterns are also not very diverse (Fig. 2.16b, 2.17b). It may be that sexual selection for color pattern among promiscuous species is so strong that it tightly restricts which types patterns are displayed.

Female outliers PCA analyses consistently showed three females occupied distinct regions of color geometry space than all other species. These species (*Thalassoma hardwicke*, *Thalassoma lucasanum*, and *Symphodus melanocercus*) all share the same mating strategy: diandric with lek-like mating. However, they occupy very different habitat types: *T. hardwicke* is coral reef exclusive, *T. lucasanum* is coral reef associated, and *Symphodus melanocercus* is not associated with a coral reef habitat. Additionally, most species' females have relatively low transition complexity other than the three outliers. It is unclear what other life history traits contribute to these species being outliers. Further investigation is required to determine what selective pressures shape color pattern evolution within the females of these species.

2.5 Conclusion

Sexual dichromatism is a result of different color and pattern elements coming together to signal conspecifics. These pattern elements are shaped both by sexual and natural selection, and many life history traits play in to how these selective pressures act. I went beyond simple categorizations of dichromatism to test how color and pattern elements relate to life history traits. I demonstrated that color pattern elements can be selected by natural selection due to function within different habitats, and sexual selection through both sex allocation and mating strategies.

Figure 2.3: Continuous map of ancestral states for color pattern transition complexity (m) across the wrasse tree for (a) males vs (b) females.

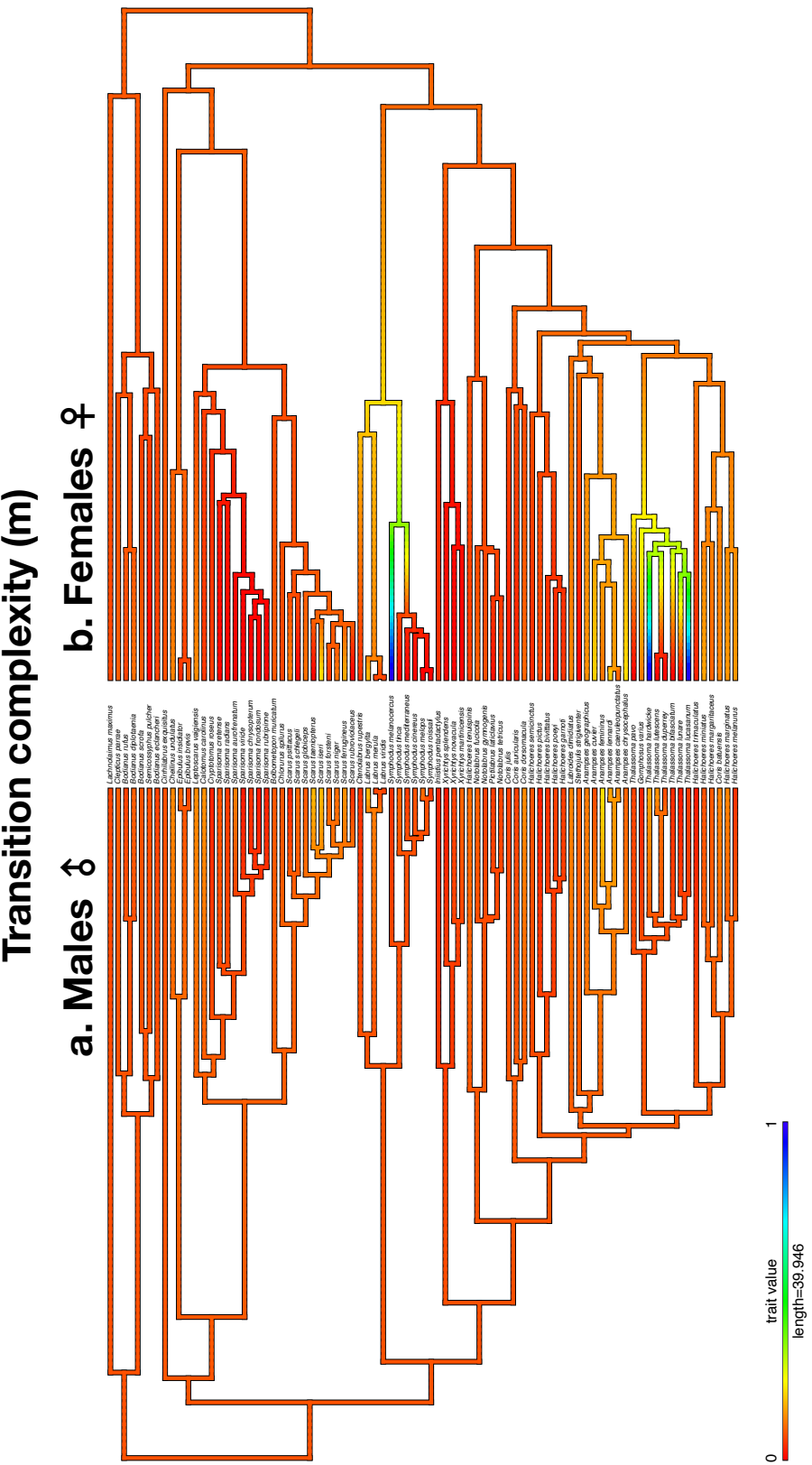


Figure 2.5: Continuous map of ancestral states for scaled Simpson color class diversity (J_c) across the wrasse tree for (a) males vs (b) females.

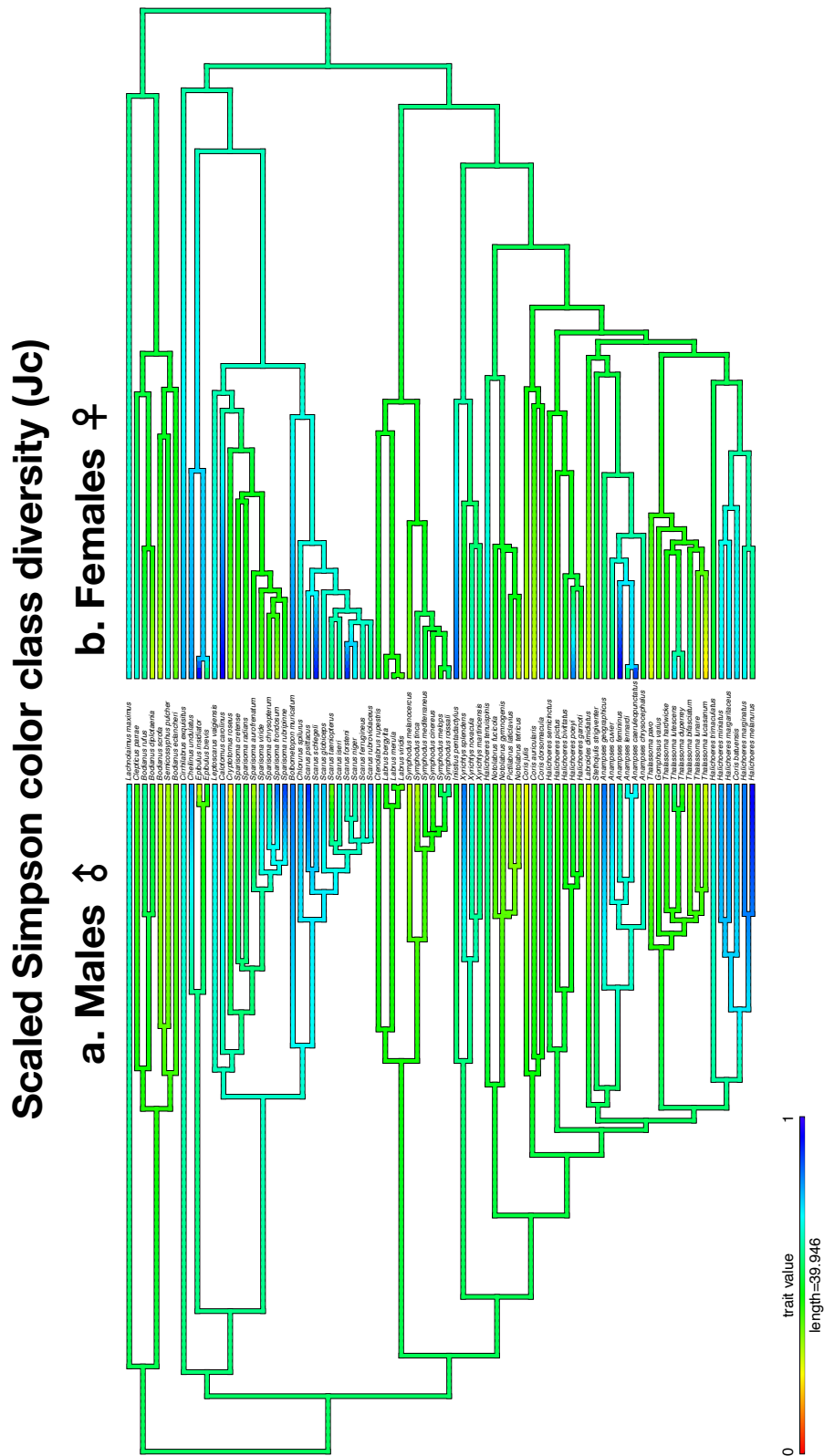


Figure 2.6: Continuous map of ancestral states for scaled Simpson transition diversity (Jt) across the wrasse tree for (a) males vs (b) females.

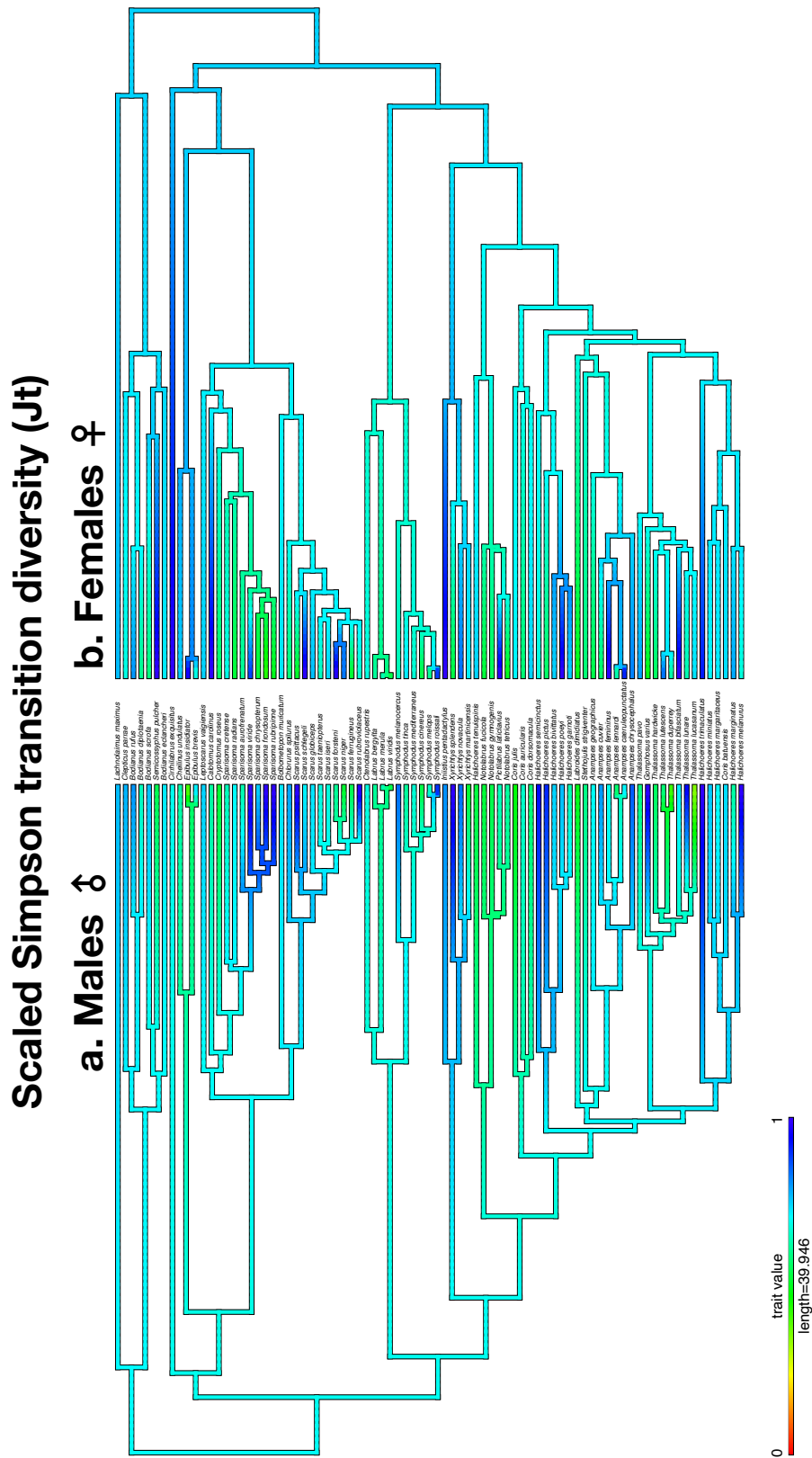


Figure 2.7: Continuous map of ancestral states for chromatic boundary strength (m_ds) across the wrasse tree for (a) males vs (b) females.

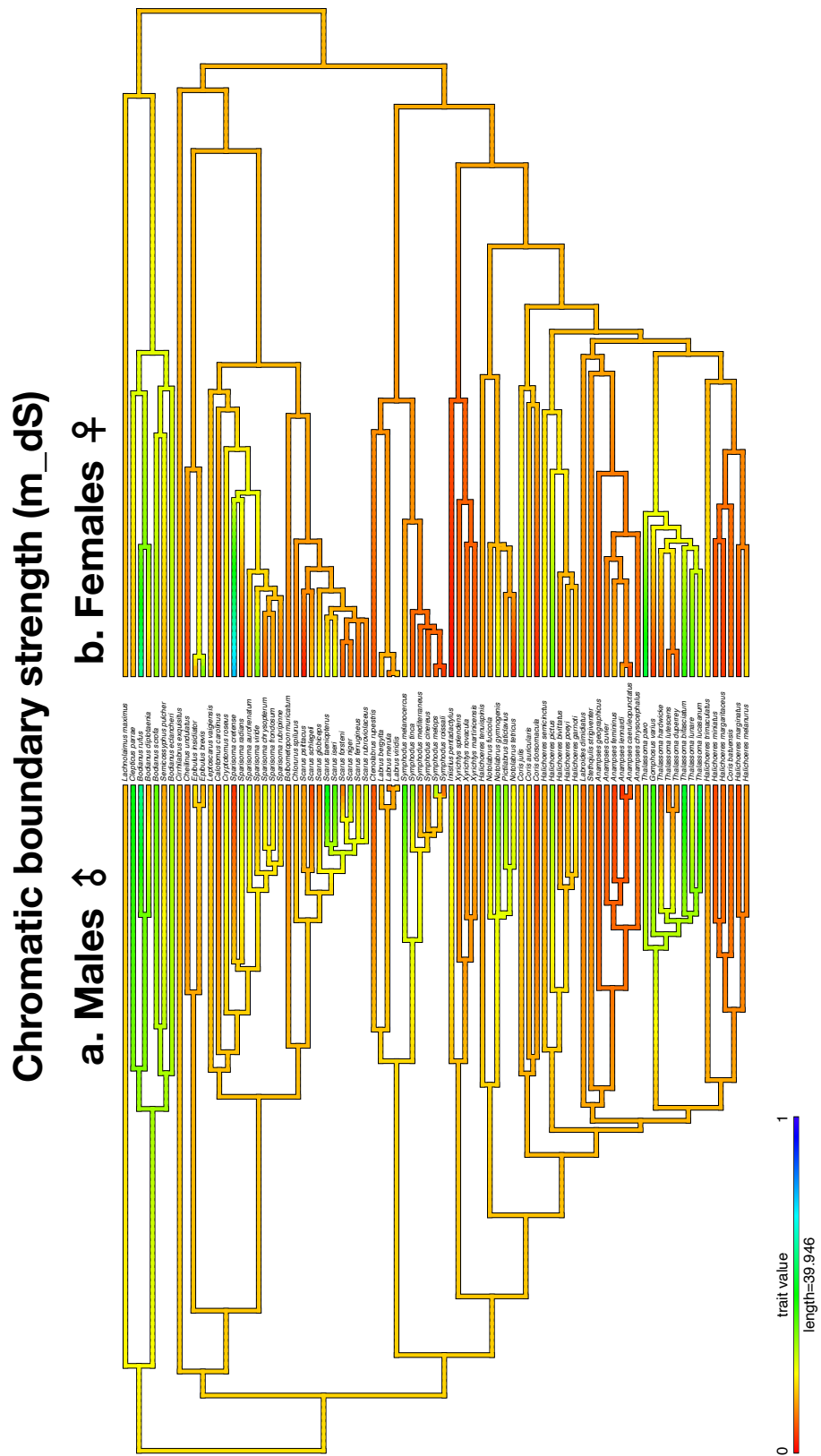


Figure 2.9: Phylogenetic reduced major axis regression of male (x) vs female (y) rates of evolution of color classes (k). Reduced major axis regression ($y = 0.449x + 0.007$; $R^2=85776$) is significant ($T = 18.86480$, $df = 57.28805$, $p \leq 0.00001$)

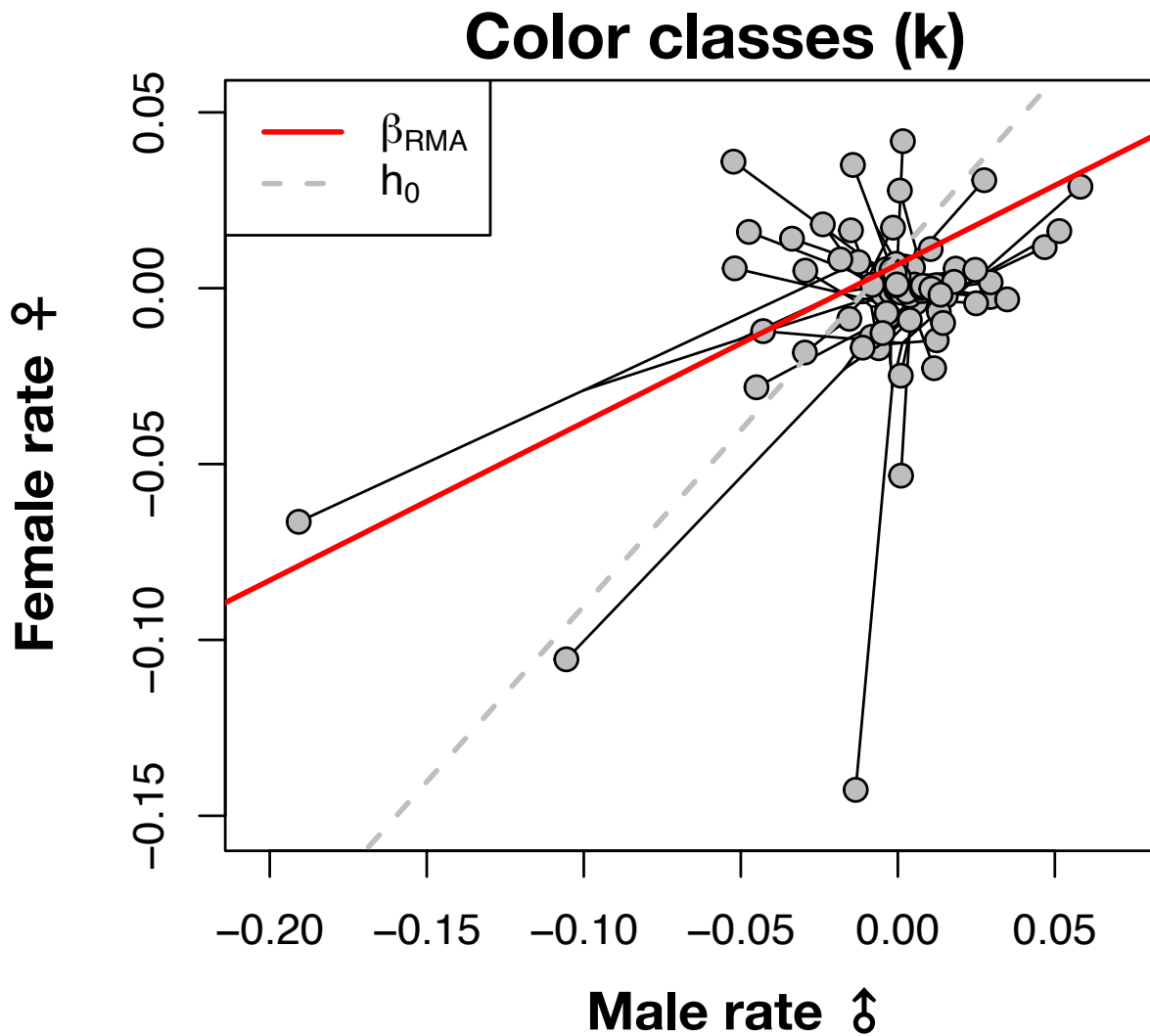


Figure 2.10: Phylogenetic reduced major axis regression of male (x) vs female (y) rates of evolution of scaled Simpson transition diversity (Jt). Reduced major axis regression ($y = 0.791x - 0.001$; $R^2=0.838$) is significant ($T = 5.179$, $df = 57.682$, $P = 3 \cdot 10^{-6}$.)

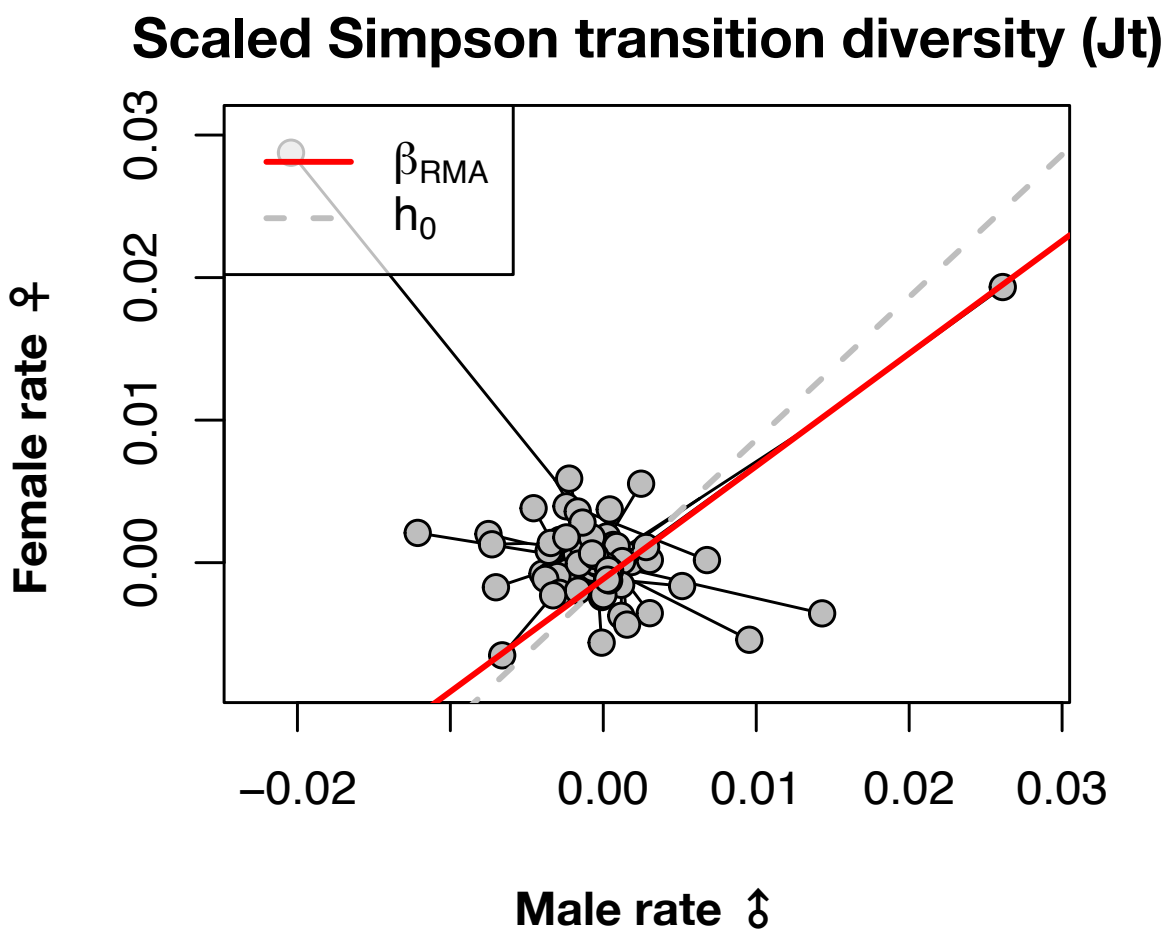


Figure 2.11: Phylogenetic reduced major axis regression of male (x) vs female (y) rates of evolution of achromatic boundary strength (m_dL). Reduced major axis regression ($y = 0.757x - 6.73 \times 10^{-4}$; $R^2=0.981$) is significant ($T = 18.049$, $df = 54.999$, $P < 0.0001$.)

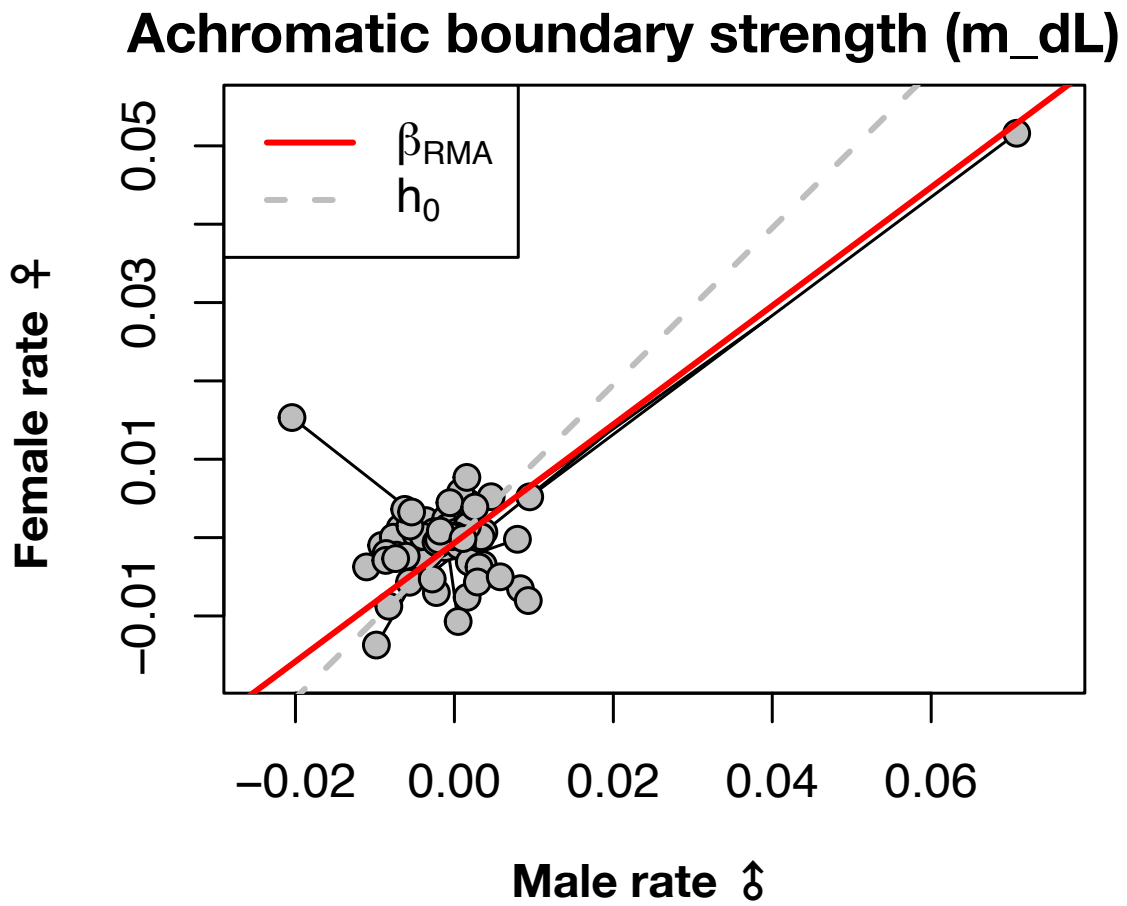


Figure 2.12: Color pattern morphospace of PC1 (x) vs PC2 (y) for (a) males and (b) females with individuals and hulls colored by habitat type: coral reef associated (red), coral reef exclusive (green), and non coral reef (blue)

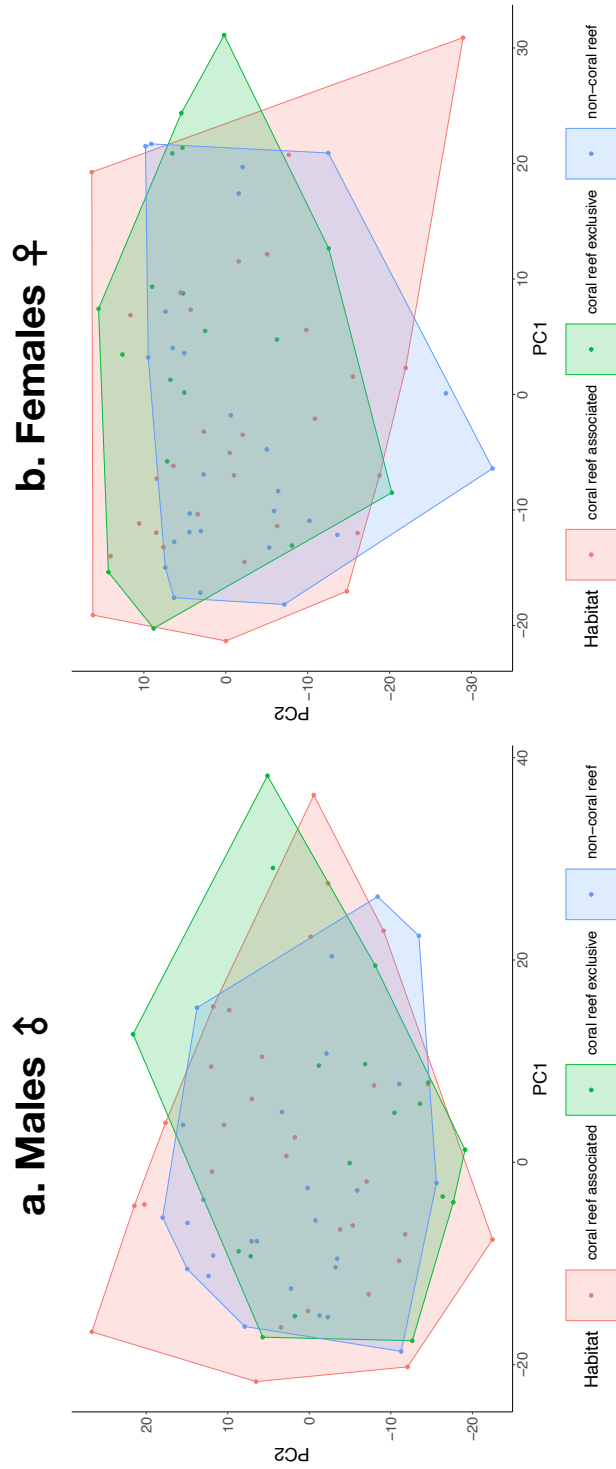


Figure 2.13: Color pattern morphospace of PC3 (x) vs PC4 (y) for (a) males and (b) females with individuals and hulls colored by habitat type: coral reef associated (red), coral reef exclusive (green), and non coral reef (blue)

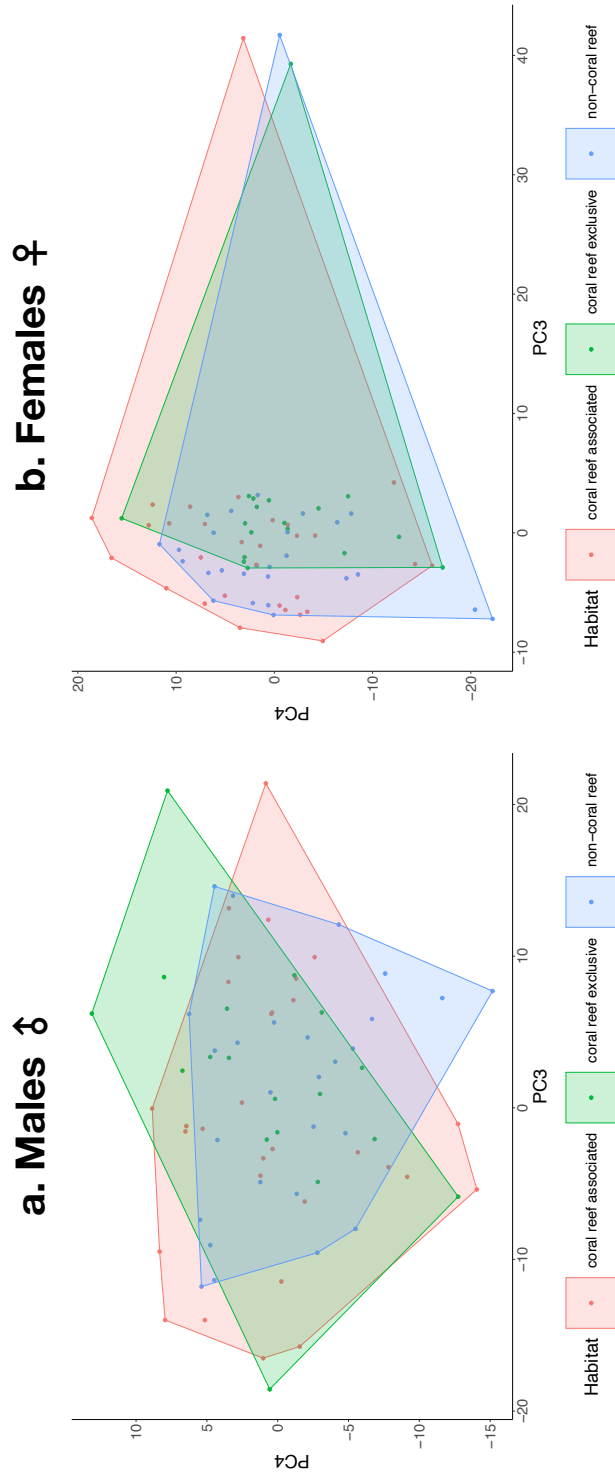


Figure 2.14: Color pattern morphospace of PC1 (x) vs PC2 (y) for (a) males and (b) females with individuals and hulls colored by sex allocation type: diandric (red), gonochorous (green), and monandric (blue)

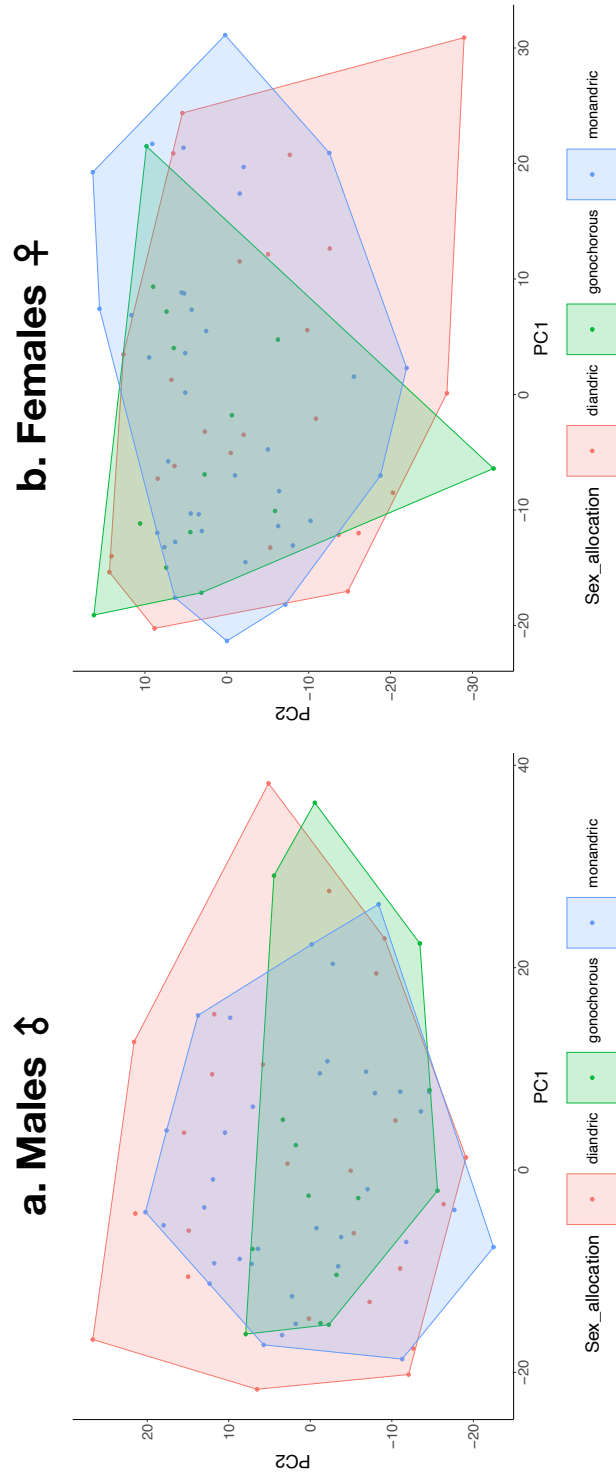


Figure 2.15: Color pattern morphospace of PC3 (x) vs PC4 (y) for (a) males and (b) females with individuals and hulls colored by sex allocation type: diandric (red), gonochorous (green), and monandric (blue)

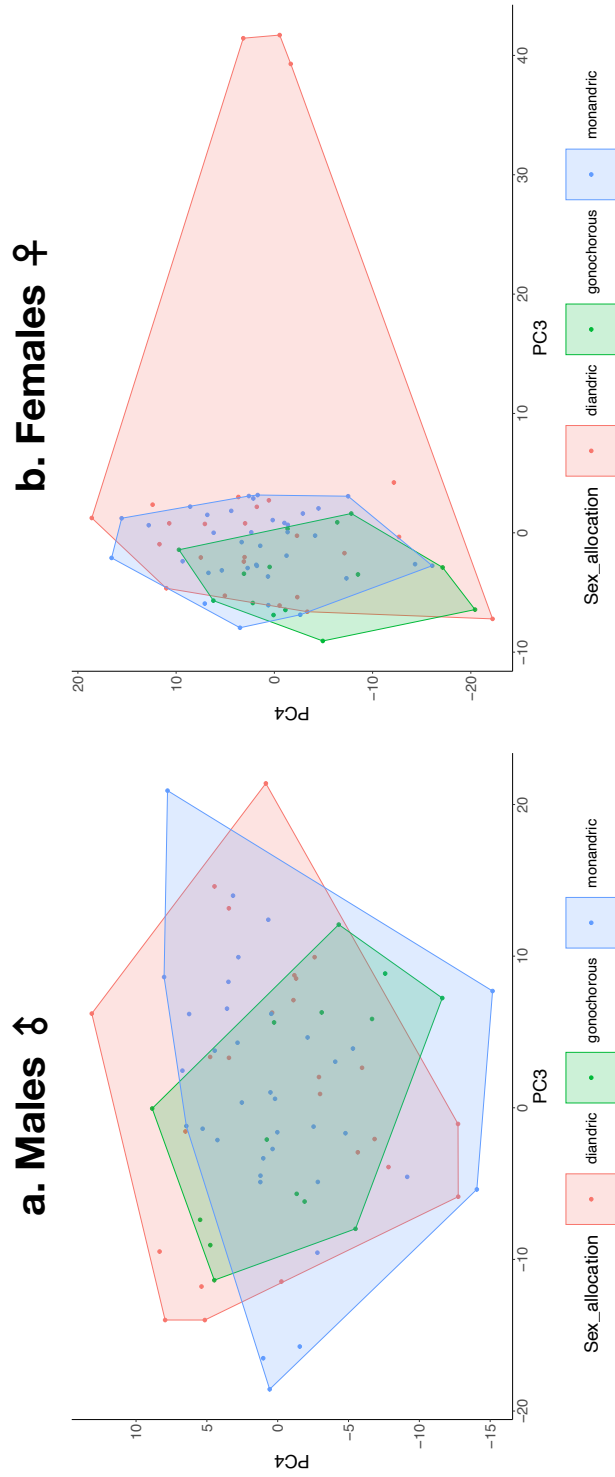


Figure 2.16: Color pattern morphospace of PC1 (x) vs PC2 (y) for (a) males and (b) females with individuals and hulls colored by mating strategy: harem (red), lek-like (green), and promiscuous (blue)

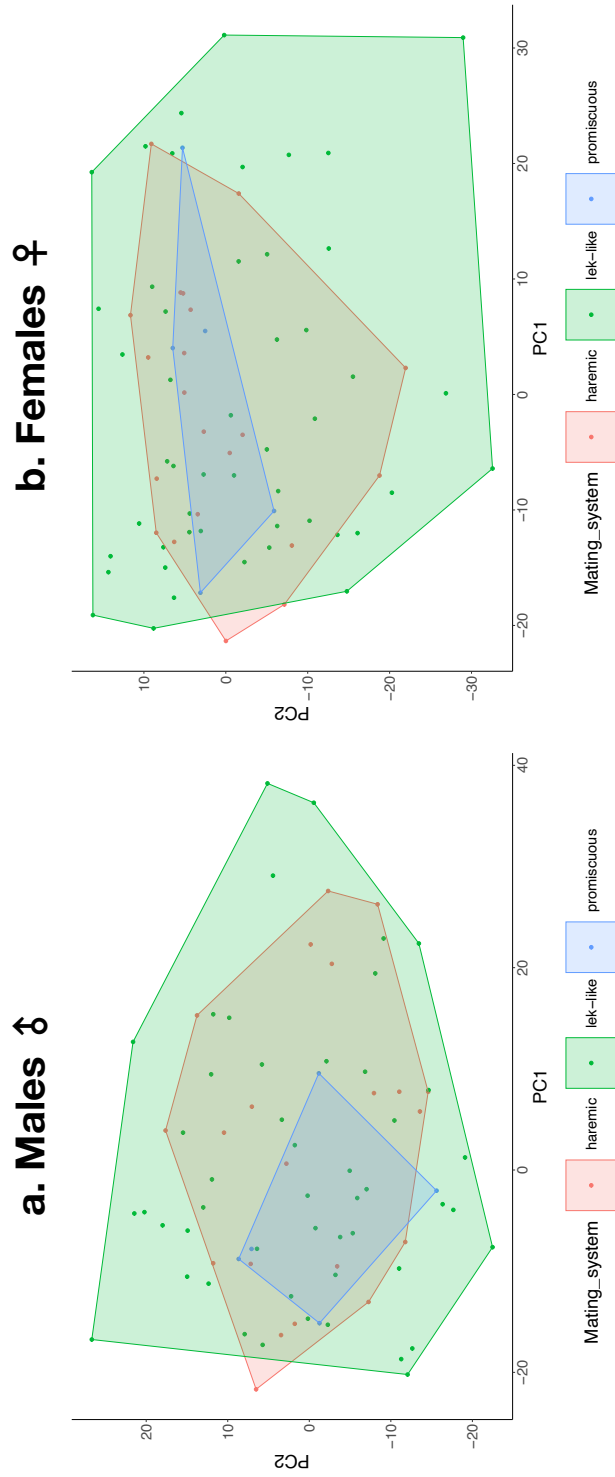
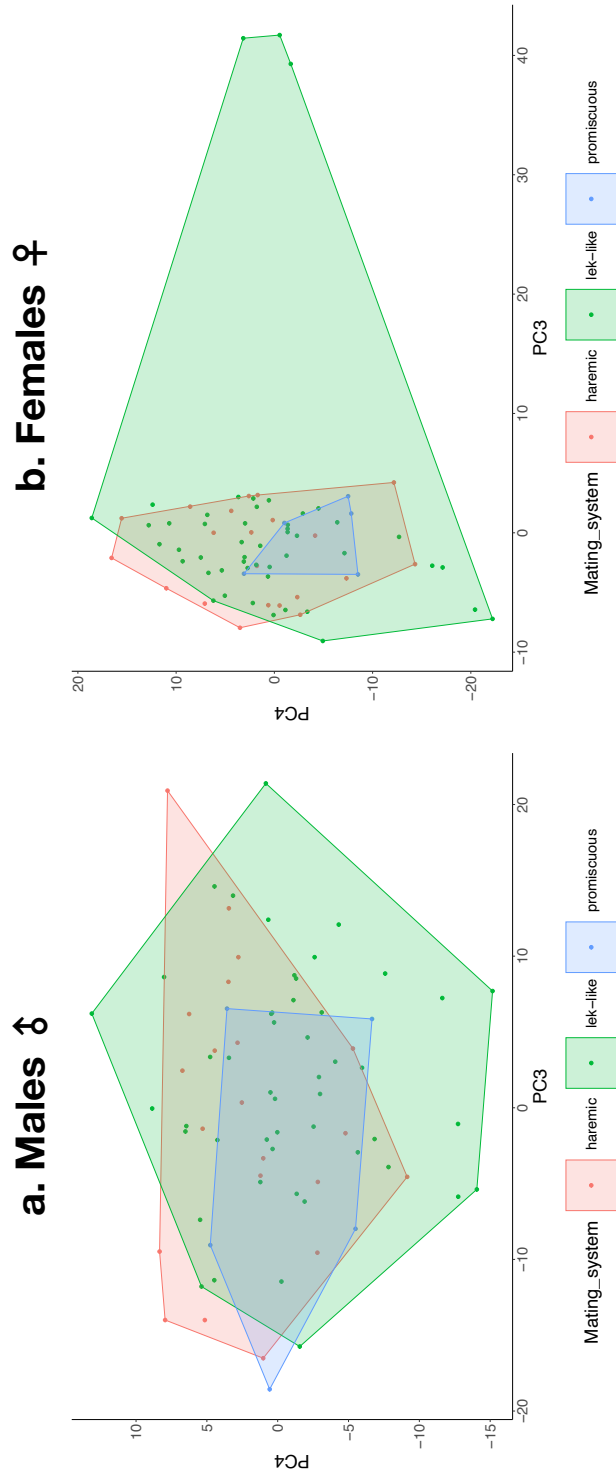


Figure 2.17: Color pattern morphospace of PC3 (x) vs PC4 (y) for (a) males and (b) females with individuals and hulls colored by mating strategy: harem (red), lek-like (green), and promiscuous (blue)



Global spatial patterns and phylogeography of color and color pattern diversity across fishes

3.1 Introduction

Global spatial patterns of diversity are important to consider in the evolution and ecology of fishes. Color is perhaps one of the most conspicuous axes of diversity in reef fish habitats, however we have a poor understanding of what shapes this diversity at global scales. Analyses of species abundance and functional traits have revealed a latitudinal gradient in fish diversity where tropical regions tend to be global "hotspots" for diversity [Tittensor et al., 2010, Stuart-Smith et al., 2013, Diamond and Roy, 2023]. These analyses try to capture functional diversity, however they mostly include common morphological and ecological traits. Color and pattern are underutilized but very valuable metrics of diversity to consider because they can compliment and capture aspects of diversity outside of other phenotypic or ecological traits [Salis et al., 2019]. Previous work has attempted to quantify the distribution of color and pattern across fishes [Miyazawa, 2020, Zapfe, 2021, Langlois et al., 2022], but the spatial distributions of these traits have not been explored. The tropics and subtropics are anecdotally recognized for their exceptionally colorful fish assemblages, but it is unknown if they are truly exceptionally colorful when compared to all regions. Birds, a large and diverse group, show a latitudinal gradient where tropical species are more colorful [Cooney et al., 2022]. The total global distribution of color and color pattern among fishes remains largely unknown because the latitudinal distributions of color and pattern have not been widely

quantified across fishes.

Color and patterns displayed and perceived by fishes are largely dependent on habitat [Seehausen et al., 1999]. Factors like depth [Schweikert et al., 2018] and water clarity [Wright et al., 2017] can produce inconsistencies in visibility and distort how visual signals are broadcast and received. Coral reefs are characterized by their shallow, clear waters that could result in clearer signaling for intraspecific recognition and mate choice. Habitat variation can also produce variation in diet among populations; differences in the abundances of carotenoid-rich food could potentially produce both spatial and temporal variation in observed color phenotypes [Svensson and Wong, 2011]. Aside from differences in resource availability, depth also interacts with the physical properties of light. Longer wavelengths of the visual spectrum, starting with red and working through the spectrum, are absorbed and removed as a signal with increasing depth [Levine and MacNichol, 1979]. Very short wavelengths in the UV and violet range are also limited in depth [Chou et al., 2021], meaning the overall range of visible light is constrained at both ends of the visible spectrum with increasing depth. The different light conditions, combined with trophic constraints, may lead to species that live in deeper or murkier temperate waters to produce less longer-wavelength producing carotenoid pigments. There also may be differences in color pattern across habitats. The bright, clear waters of shallow reefs can theoretically transmit more color combinations due to more colors being visible. We would predict that if available wavelength is a primary control on color pattern diversity, then measures of color and color pattern diversity should be negatively correlated with depth.

Sexual selection and range size are drivers of color evolution in some fishes [Montanari et al., 2012, 2014, Hemingson et al., 2018], where color and pattern play a part in enforcing species boundaries through assortative mating. Even though reefs are often seen as biodiversity hotspots in general, there may be differences between reef regions in species richness and endemism [Hughes et al., 2002]. Endemic species are usually defined by their very

small geographic range [Myers et al., 2000]. High endemism is not concordant with high species richness among reef fishes [Hughes et al., 2002] and different reef regions will possess different degrees of each due to a myriad of factors [Cowman et al., 2017]. These factors can contribute to similarities and differences in traits, including color, within and between these regions [Drew et al., 2008], where smaller endemic populations can evolve distinct differences. Therefore, it can be hypothesized that there are differences in the diversity of color and pattern between these regions. Reef regions differences may also be attributed to the phylogenetic dissimilarity [Cowman et al., 2017]. If endemism is a driving force in color pattern evolution at a global spatial scale we should expect the regions with the most endemism to have the most color pattern diversity. Additionally, local differences should produce regional differences of reef fish color pattern diversity. Therefore, an alternative hypothesis could be that if wide ranging species are common or convergence/saturation in color space has occurred, then we do not expect regional differences

The global spatial distribution of color and color pattern among marine fishes has not been widely quantified. We aim to evaluate broad patterns of color and pattern diversity across a wide sample of marine fishes. We test if color and pattern diversity align with other established diversity gradients. We investigate if there are latitudinal gradients in color and pattern diversity, testing the hypothesis of tropical/subtropical species closer to the equator being more colorful than temperate species at higher latitudes. We also investigate depth gradients through two hypothesis: 1. that the frequency of colors should correspond to depths where they are visible (ie. red should be more frequent at shallower depths because the wavelengths are absorbed in deeper waters) and 2. complex color patterns should be found at shallower depths where they would have higher visibility. Additionally, we explore regional differences in color and pattern to begin to understand if factors like endemism and species richness increase or decrease color and pattern diversity within regions. We test the hypothesis that if color is functioning mostly in species recognition, color and pattern diversity should be positively correlated with species number and local diversity within

regions.

3.2 Methods

Image sourcing and processing We aggregated images of 6,781 fishes across 2,523 species from the Bishop Museum [Randall, 2023]. Anywhere from about 1 to 10 images were processed for each species depending on availability. Images were included for both sexes when possible, if not terminal males were mostly available to represent a species. For this analysis, only ray-finned fishes (Actinopterygii) were used due to their stereotypical fish body shape. Elasmobranchs were excluded due to being more distantly related having vastly different structures on the surface of the body. Groups with extreme elongate body forms such as eels (Anguilliformes) and Pipefishes/Seahorses (Syngnathidae) were also excluded. Due to AI image processing models improving significantly over the course of the PhD, we opted to use automated background removal software which surpassed functionality of our sashimi program that we used for previous instances of background removal [Schwartz and Alfaro, 2021]. Instead we used Photoroom, remove.bg, and Adobe express to remove backgrounds from all images.

Color pattern analyses We used our R tool charisma [Schwartz et al., In prep] to automatically classify the number of color categories (k) and to assign each of 10 discrete potential colors present on a fish within an RGB color space. For all species, the proportion of each color category sampled was calculated. We then inserted each k value and the mean color of each category into functions in the pavo package in R [Maia et al., 2013] to calculate color pattern geometry statistics for each fish. Of these statistics, we focused on overall pattern transition density (m), the aspect ratio (ratio of row-wise to column-wise transitions, $A < 1$ is closer to vertical banding and if $A > 1$ is closer to longitudinal stripes; A), the scaled Simpson color class diversity (J_c), the scaled Simpson transition diversity

(Jt), and the mean chromatic and achromatic boundary strength (m_dS and m_dL) in our analyses.

Evolutionary model fitting We used a phylogenetic tree extracted from fish tree of life [Rabosky et al., 2018] for all comparative analyses. 1,311 species (~10% of species in the fish tree of life) encompassing 119 families (S10 and S11) from the color pattern analyses matched the tree and were used for subsequent comparative analyses. To test if the evolution of a trait was more likely to be represented by a stochastic random walk versus evolution towards an optimum for these continuous values, I tested the fit of Brownian Motion (BM) versus Ornstein–Uhlenbeck (OU) models using AIC scores based upon the FitContinuous function in geiger for species color proportions and color pattern geometry metrics.

Latitudinal and depth gradients of color and pattern To test for a latitudinal gradient in color pattern while controlling for statistical non independence through phylogenetic relatedness, we used phylogenetic least-squares regression (PGLS) using the nlme package in R [Pineiro et al., 2021]. All measures of species median latitude were acquired from FishBase [Froese and Pauly., 2023] through the rfishbase package in R [Boettiger et al., 2012]. To test relationship between the proportion of each color category surveyed for each species and latitude, we ran PGLS of species color proportions (the fraction of individuals sampled within a species that express the color) and median latitude (1274 sp.). We also performed PGLS for each color pattern geometry metric against median latitude (1,274 sp.). To test relationships between color and pattern against depth, we performed PGLS for all color proportions and color pattern geometry metrics against average species depth (1,130 sp.). Average depth was calculated from the shallow and deep depth available for each species from FishBase [Froese and Pauly., 2023] through the rfishbase package in R [Boettiger et al., 2012].

Estimation of geographic distributions We used an expanded dataset of species range estimates building off of Rabosky et al. [Rabosky et al., 2018] to match species

coverage with the sampled species (1,311 sp.). In the same manner as in Rabosky et al., we used the AquaMaps algorithm [Ready et al., 2010, Kaschner et al., 2016] to simulate species geographic ranges on a global spatial grid. This allowed us to estimate geographic ranges for marine fishes based on available species-specific occurrence records along with environmental predictors of depth, sea surface temperature, salinity, proportional ice cover and primary productivity. The species values for k and the color pattern geometry statistics were projected onto the species presence/absence data on the global spatial grid. Shallow and deep depth categories [Miller et al., 2022] were also assigned for each species, where each species was assigned a binary value for presence or absence at deep and shallow depth categories (some species were present in both categories).

Color pattern morphospace To combine the the color pattern statistics into a single morphospace, we performed a phylogenetic principal component analysis (PPCA) using the phytools package in R [Revell, 2012] (1,311 sp.). We also ran a normal principal component analysis (S12) using the prcomp function from the “stats” package in R to control for potential component selection bias [Uyeda et al., 2015] (S12).

Color pattern and habitat All species in the morphospace were assigned to different habitat categories of climate and reef region acquired from FishBase [Froese and Pauly., 2023] through the rfishbase package in R [Boettiger et al., 2012]. For climate (1,258 sp.), species were designated as “subtropical and tropical” or “temperate”. All “boreal” (4 sp.) and “polar” (1 sp.) species were discarded due to low sampling. The compared reef regions (905 sp.) included “Caribbean Sea”, “Coral Sea and Great Barrier Reef (GBR)”, and “Red Sea”. We also assigned shallow and deep depth categories [Miller et al., 2022] for each species (1,296 sp.). The species sampled were able to be assigned to “shallow and deep” vs “shallow only” categories. There were no deep water only species in the sample. For each habitat designation, principal components (PCs) were plotted against each other to see how different habitat categories fall within the color pattern morphospace. Convex hull areas for

each habitat category within the morphospace were calculated using the chull function from the `grDevices` package in R [R Core Team, 2023].

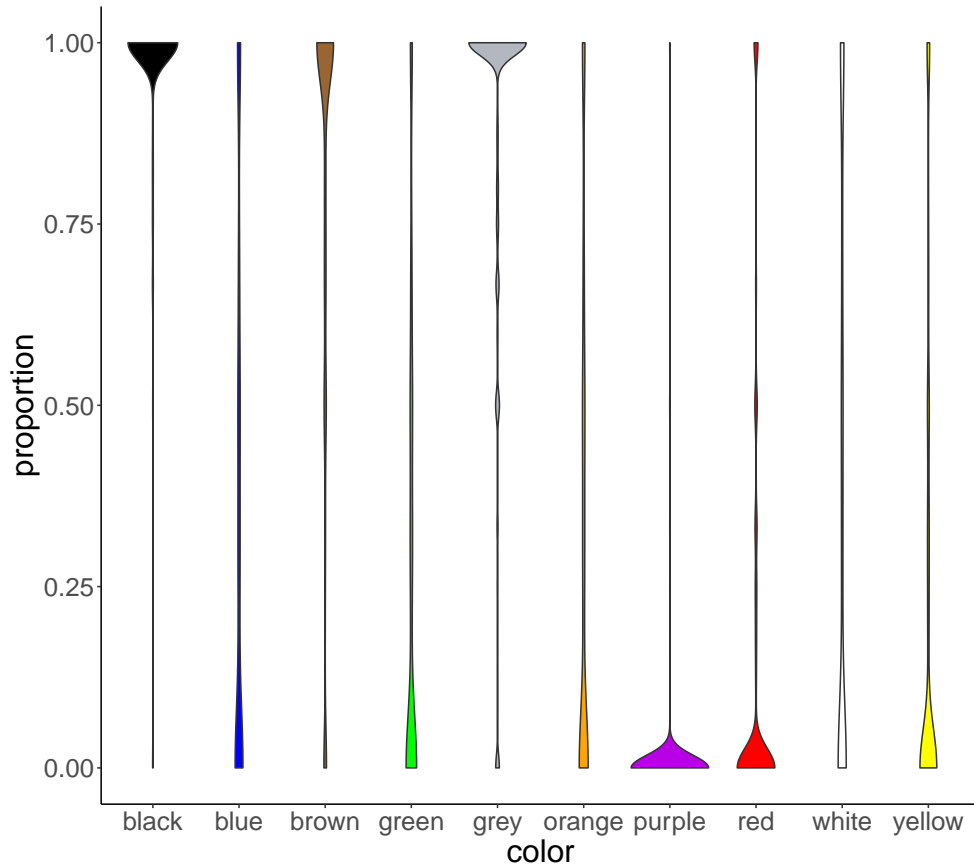
3.3 Results

Distribution of color and pattern Black, brown, grey were present among most individuals across all species, while other colors were displayed at lower frequencies within species (Fig. 3.1). PGLS revealed a significant negative relationship between median latitude and a high proportion of red sampled within the species (Table 3.1). This means that species at lower latitudes showed a higher proportion of the color red and species at higher latitudes showed a lower proportion of the color red. There was no other significant correlation found between median latitude and any of the other sampled color proportions. There was also no significant correlation found between median latitude and any of color pattern geometry metrics.

A significant negative relationship was found between pattern aspect ratio (A) and depth through PGLS (Table 3.2). A significant negative relationship was also found between number of colors (k) and depth. In testing depth against color proportions, PGLS found a significant positive relationship between depth and the species proportion of red and purple. There was a significant negative relationship between depth and the species proportion of green and blue.

The global spatial distribution of number of colors (k) and color pattern geometry metrics all show a general pattern of coastal species being distinct from pelagic species (Fig. 3.2). Coastal and reef species have more colors (k), with the highest values concentrated around the Indo-Pacific. Some northern latitude species also seem to have a somewhat high number of colors. Pattern transition complexity (m) appears to be somewhat higher in reef regions

Figure 3.1: Violin plot of the proportions of each color class (k) displayed by individuals sampled within each species.



and mostly very low at high latitudes. Most species tend to be simpler along the horizontal axis, but reef and coastal species seem to have higher complexity along this axis; coastal species have patterns closer to horizontal stripes. Scaled Simpson color class diversity (J_c) and scaled Simpson transition diversity (J_t) have high values in species in the southern Indian Ocean. J_t is low in coastal and reef regions, especially the Indo-Pacific reefs. Chromatic boundary strength (m_{dS}) is higher in nearshore communities, including the Caribbean Sea, patches the southern Indian Ocean, and the Arctic Ocean. Achromatic boundary strength (m_{dL}) tends to be lower in coastal and reef regions than pelagic ones.

The pattern of k being higher for coastal and reef region species is consistent across shallow and deep depths (Fig. 3.3, 3.4). Deep vs shallow species also generally follow

var	Estimate	SE	t-value	p-value
red	-1.99e-3	8.43e-4	-2.36	0.0187*
orange	-7.62e-4	-1.06e-3	-0.720	0.472
yellow	-1.31e-3	1.10e-3	-1.19	0.234
green	1.19e-3	1.04e-3	1.145	0.252
blue	1.35e-3	1.14e-3	1.19	0.234
purple	2.74e-4	2.60e-4	1.05	0.292
brown	-1.03e-3	9.35e-4	-1.10	0.272
black	1.28e-4	3.11e-4	0.412	0.680
white	2.16e-4	1.27e-3	0.170	0.865
grey	1.23e-3	8.21e-4	1.50	0.134
k	-6.93e-4	-3.43e-3	-0.202	0.840
m	1.83e-4	1.26e-4	1.45	0.147
A	-6.22e-4	4.66e-4	-1.33	0.183
Jc	-2.99e-4	3.06e-4	-0.977	0.329
Jt	3.36e-4	3.31e-4	1.01	0.311
m_dS	-2.19e-4	1.63e-4	-1.34	0.179
m_dL	-2.97e-4	5.45e-4	-0.545	0.586

Table 3.1: PGLS results of median species latitude against colors and color pattern variables. df = 1,274, *p <0.05

similar patterns for all metrics. However, deep water species tend to skew higher in values than shallow for almost all metrics except for chromatic boundary strength. There are very different global spatial patterns of chromatic boundary strength when it comes to shallow vs deep water species. Shallow water species tend to have very low chromatic boundary strength in the southern oceans, whereas deep water species tend to have low chromatic boundary strength in across the Atlantic ocean and in the western Indian Ocean.

Color pattern and habitat Consistent with the PGLS results, there appears to be significant overlap between temperate vs tropical and subtropical species in color pattern morphospace (Fig. 3.5, 3.6). When comparing shallow and deep vs shallow only species, the shallow and deep species tend to have less spread, especially across the PC2 axis (Fig. 3.7). Species that live shallow and deep also have less spread across PC axes 3 and 4 than shallow only species (Fig. 3.8). There tends to be a lot of overlap between reef regions, particularly between the Coral Sea GBR and the Red Sea (Fig. 3.9, 3.10). However, the morphospace of

var	Estimate	SE	t-value	p-value
red	6.49e-4	1.47e-4	4.414101	0.000**
orange	-1.54e-4	1.86e-4	-0.829	0.407
yellow	-1.83e-4	1.97e-4	-0.927	0.354
green	-8.12e-4	1.78e-4	-4.57	0.000**
blue	-9.73e-4	1.96e-4	-4.96	0.000**
purple	3.38e-4	4.15e-5	8.15	0.000**
brown	-2.09e-4	1.60e-4	-1.31	0.191
black	-8.00e-6	5.77e-5	-0.138	0.890
white	2.65e-5	2.25e-4	0.117	0.906
grey	1.71e-5	1.46e-4	0.117	0.907
k	-1.31e-3	6.06e-4	-2.16	0.0309*
m	-4.19e-5	2.20e-5	-1.91	0.0567
A	-2.43e-4	8.18e-5	-2.98	0.003**
Jc	-1.05e-4	5.38e-5	-1.95	0.0516
Jt	6.96e-5	5.83e-5	1.20	0.2323
m_dS	3.84e-5	2.89e-5	1.33	0.1841
m_dL	4.43e-4	9.38e-5	4.72	0

Table 3.2: PGLS results of median species depth against colors and color pattern variables. df = 1,130, * p < 0.05, ** p < 0.01

var	PC1	PC2	PC3	PC4
Standard deviation	1.5	1.1	0.94	0.85
Proportion of Variance	0.38	0.21	0.15	0.12
Cumulative Proportion	0.38	0.59	0.74	0.86

Table 3.3: PC summary statistics. Results are given for PCs 1-4 because they explain greater than 10% of the variance.

var	PC1	PC2	PC3	PC4
m	-0.720	0.290	-0.091	-0.550
A	-0.420	0.590	-0.520	0.350
Jc	0.570	0.580	-0.240	-0.043
Jt	0.730	0.240	-0.047	-0.500
m_dS	0.058	-0.660	-0.730	-0.160
m_dL	0.850	-0.021	-0.085	0.170

Table 3.4: PC loads

Caribbean Sea species tends to be more constrained than the other reef regions, especially along the PC2 (Fig. 3.9) and PC4 axes (Fig. 3.10).

3.4 Discussion

Latitudinal gradients We found no relationship between latitude and color pattern geometry statistics (k , m , A , J_c , J_t , $m.dS$, $m.dL$; Table 3.1). No color showed a significant change in proportion with changing latitude except for red which was negatively associated (Table 3.1). The ecological factors contributing to this are likely complex and cannot be discerned from an analysis of this scale. There was no significant relationship between the number of colors (k) and median latitude. Tropical species not being more colorful than temperate species is consistent with similar results found for butterflies and flowers [Dalrymple et al., 2015]. However, this is different from birds which have more colorful species in tropical latitudes [Cooney et al., 2022]. Pattern geometry also doesn't show any patterns across latitude as well. Color pattern morphospaces show considerable overlap between the tropical and subtropical vs temperate regions (Fig. 3.5, 3.6). Color pattern diversity is comparable across latitude and climate.

Depth restricts color and pattern diversity There was a significant negative relationship between the number of color classes (k) and average species depth (Table 3.2). Shallower species tend to have more colors. This may be because shallower species live in light conditions where more wavelengths of light are available than in deep water, ensuring that each different color can be interpreted as a distinct signal [Levine and MacNichol, 1979]. There was a significant positive relationship between depth and the species proportion of red and purple, and there was a significant negative relationship between depth and the species proportion of green and blue (Table 3.2). Red loss at depth may act as camouflage because red wavelengths are not present in the environment, so the fish does not reflect light and is inconspicuous [Herring, 1988, Johnsen, 2005]. The images used for these analyses were illuminated by artificial light and are not reflective of natural light conditions at depth. Therefore a fish that appears red under flash photography may appear as dark as the sur-

rounding water and be nearly invisible at depth. Green and blue may be abundant among shallower species for similar reasons to blend into a well-lit, blue environment.

A significant negative relationship was found between pattern aspect ratio (A) and depth, however no other color pattern metrics seem to correlate with depth. Shallow-only species display a wider variability in color pattern morphospace (Fig. 3.7, 3.8), however the factors underlying this pattern are unclear.

Differences between reef regions The morphospace showed considerable overlap in color pattern diversity between all reef regions (Fig. 3.9, 3.10). However, Caribbean Sea species tend to occupy a smaller area of the morphospace than Red Sea, Coral Sea and Great Barrier Reef Species. Caribbean species show greater phylogenetic dissimilarity from other Atlantic or Eastern Pacific regions [Cowman et al., 2017]. A split between extant Atlantic and the Indo-Pacific reef fishes is seen in occurrence data [Floeter et al., 2008, Kulbicki et al., 2013a,b] and in phylogenetic analyses [Barber and Bellwood, 2005, Cowman and Bellwood, 2013, Hodge et al., 2013] as well. Some Atlantic genera also have highly skewed distributions, with more genera being localized to the eastern Atlantic near the Caribbean [Floeter et al., 2008]. Caribbean species being highly localized and phylogenetically dissimilar to other regions may be related why their color pattern diversity is not as wide as other regions. This does not fit with the general hypothesis that endemism drives color pattern diversity. Instead, it could fit with the alternative hypothesis where endemism has driven saturation and limited diversity due to common contact in this scenario.

Red sea species may display great pattern diversity due to relatively high rates of regional endemism [DiBattista et al., 2015]. Great barrier reef species have low endemism, however pattern diversity may be explained by having high species richness combined with wide-ranging taxa [Roberts et al., 2002, Cowman et al., 2017]. There could be more small, endemic ranges on either side of biogeographic boundaries, with more similarity between sister species in overlapping regions [Gaither and Rocha, 2013]. There are even instances of

color pattern differences within species across regions [Drew et al., 2008, DiBattista et al., 2015]. However, this nuance is not available to be investigated at this scale of analysis. In our data, all species data is pooled.

Caveats This work attempts to explore global spatial patterns of color and color pattern, however there were some instances where the data and analyses can be improved. These analyses only capture 10% of the diversity sampled in the fish tree of life, and more should be added in future work to capture a wider sample. The image data used in these analyses were not calibrated to capture fish visual space, and they do not capture colors such as UV that fish can see but are outside of the range of traditional human color space represented in the images. All images were taken with artificial lighting that does not accurately represent the natural environment, especially for deeper water species. Color and pattern data were aggregated from anywhere from about 1-10 individuals for each species. Males and females were pooled together to get species averages for sampled color proportions and color pattern statistics. This was done to get a representative average that captured color variation present within each species. However, the ratio of males to females vary in each species sample, potentially effecting species color proportions and averaged pattern statistics. Separating males from females and conducting separate analyses for each may produce different spatial trends.

3.5 Conclusion

We have quantified diversity of color and pattern across a wide taxonomic sample of marine fishes. We tested if these color and pattern traits formed similar latitudinal and depth gradients as other evolutionary and ecological traits. We also found no significant difference in pattern diversity among tropical vs temperate labeled species. While most color and pattern traits do not show latitudinal gradients, we found that these traits vary across

depth, habitat and eco-region. This exploratory analysis has revealed broad patterns of color and pattern diversity, however the evolutionary and ecological factors that shape these patterns require further investigation.

Figure 3.2: Mean species transition complexity (m), pattern aspect ratio (A), scaled Simpson color class diversity (J_c), scaled Simpson transition diversity (J_t), chromatic boundary strength (m_{dS}), achromatic boundary strength (m_{dL}), and number of color classes (k) for marine fish assemblages at the global scale.

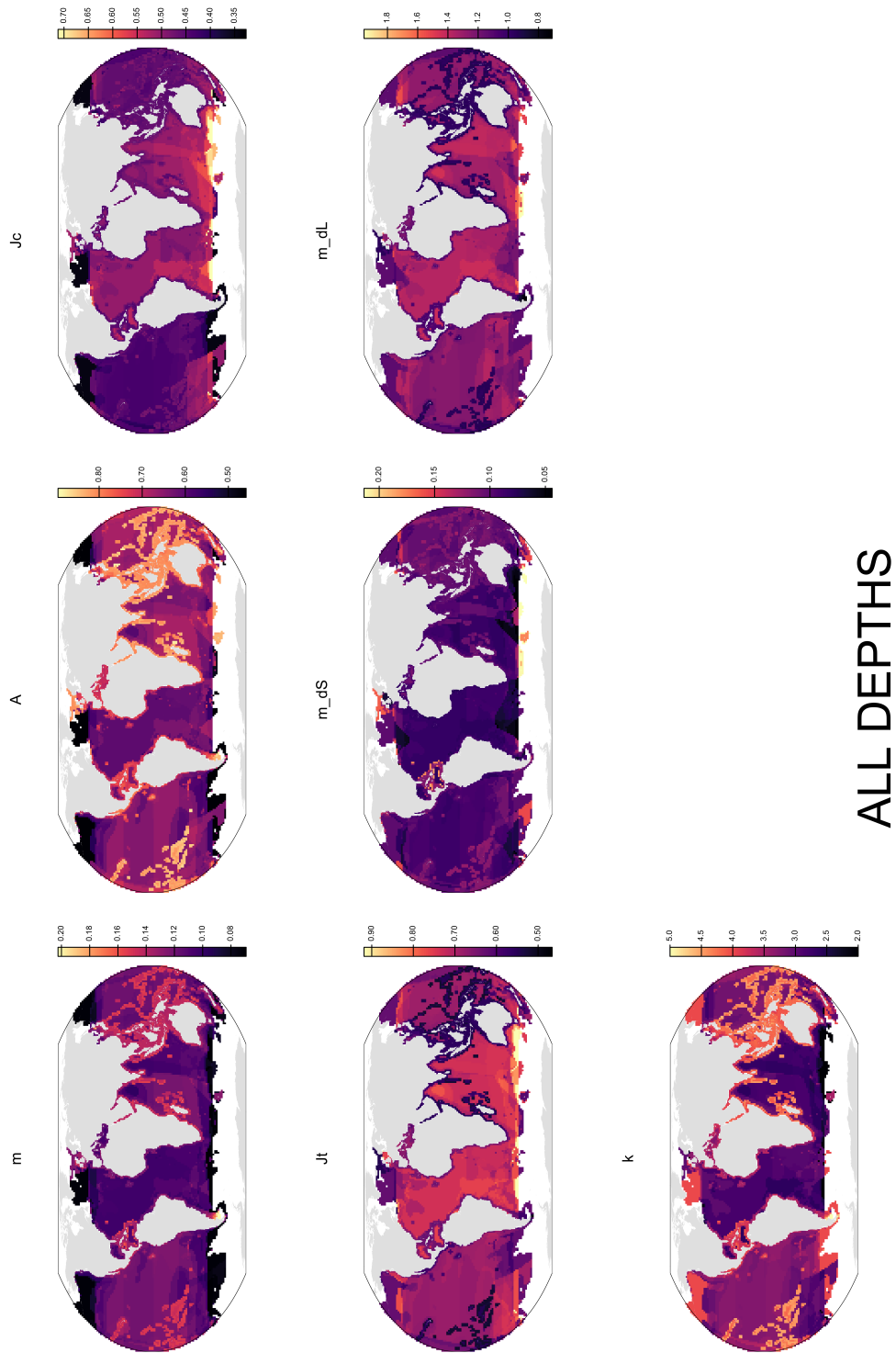


Figure 3.3: Mean species transition complexity (m), pattern aspect ratio (A), scaled Simpson color class diversity (J_c), scaled Simpson transition diversity (J_t), chromatic boundary strength (m_{dS}), achromatic boundary strength (m_{dL}), and number of color classes (k) for marine fish assemblages at the global scale for shallow water species only.

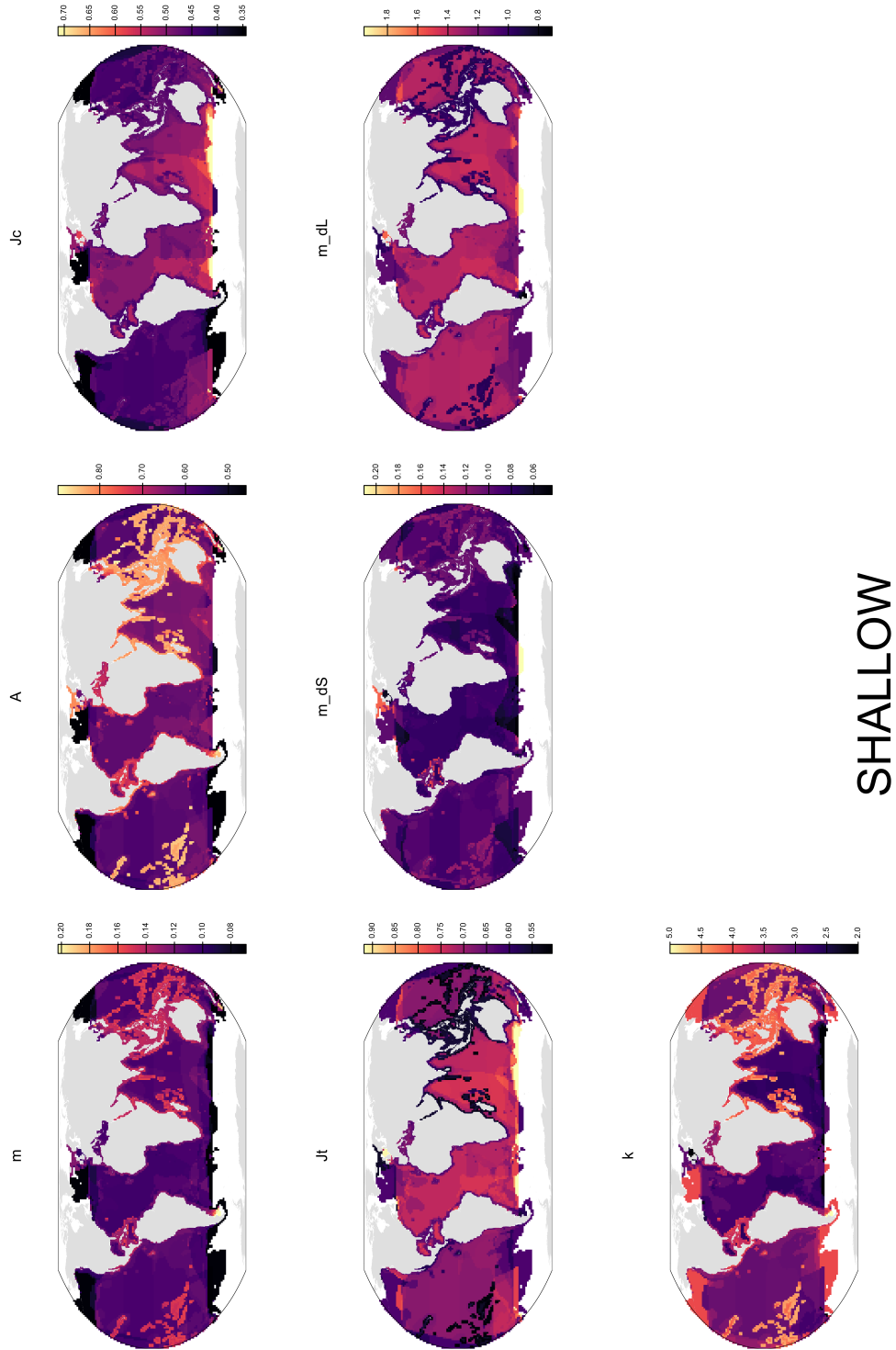


Figure 3.4: Mean species transition complexity (m), pattern aspect ratio (A), scaled Simpson color class diversity (J_c), scaled Simpson transition diversity (J_t), chromatic boundary strength (m_{dS}), achromatic boundary strength (m_{dL}), and number of color classes (k) for marine fish assemblages at the global scale for deep water species only

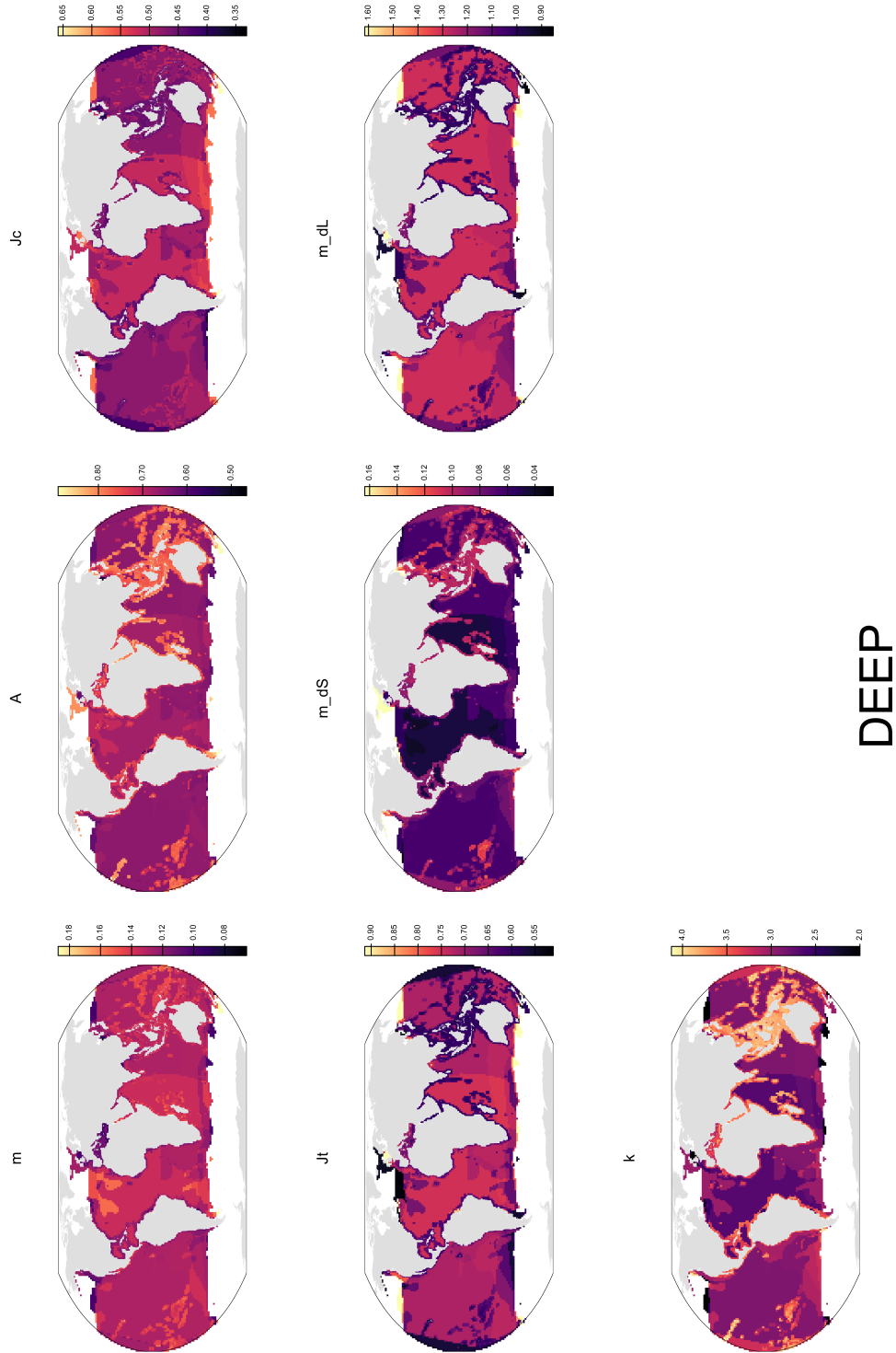


Figure 3.5: Color pattern morphospace of PC1 (x) vs PC2 (y) with individuals and hulls colored by climate type: temperate (red) vs tropical and subtropical (blue)

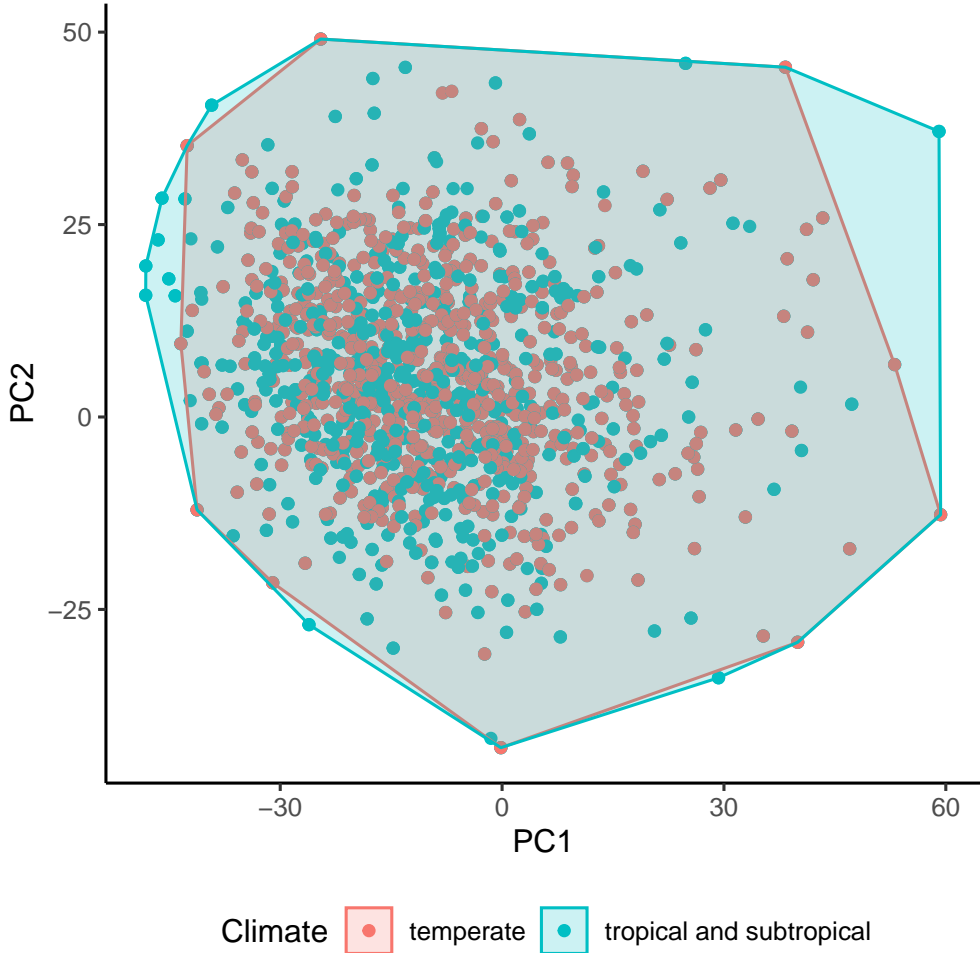


Figure 3.6: Color pattern morphospace of PC3 (x) vs PC4 (y) with individuals and hulls colored by climate type: temperate (red) vs tropical and subtropical (blue)

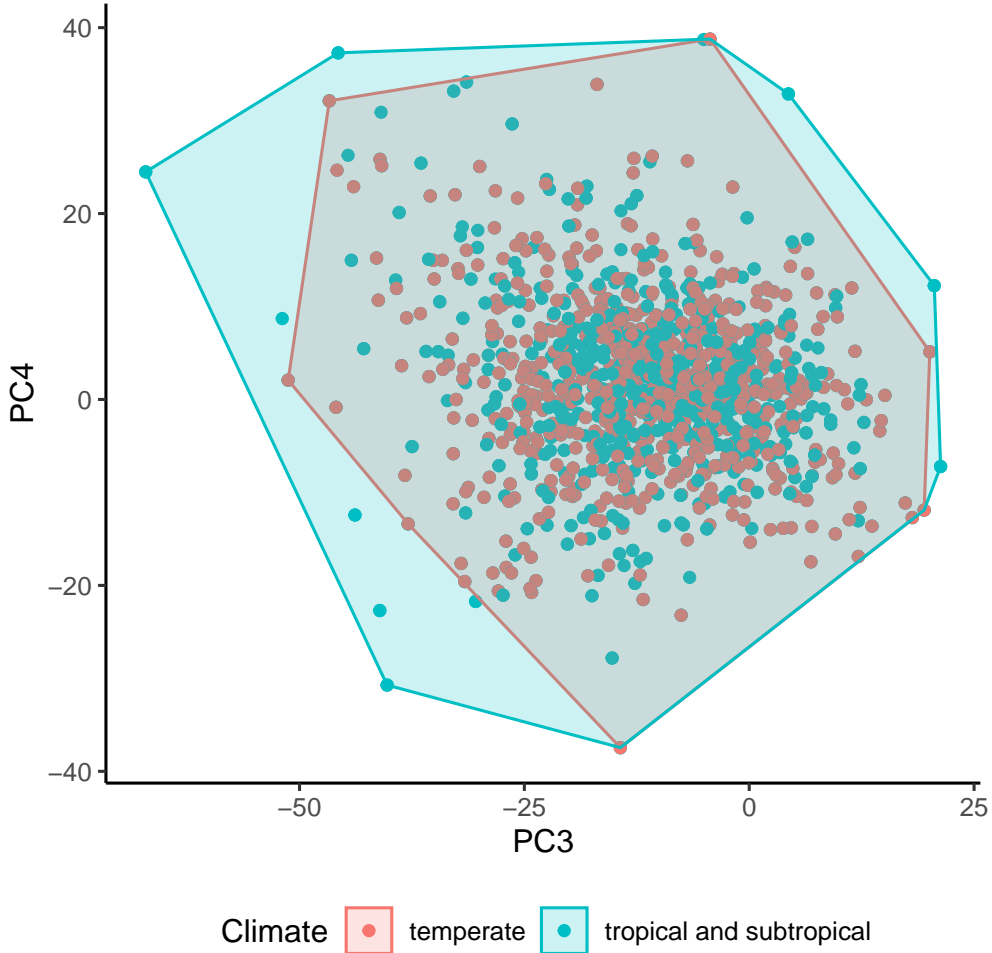


Figure 3.7: Color pattern morphospace of PC1 (x) vs PC2 (y) with individuals and hulls colored by depth: shallow and deep (red) vs shallow only (blue)

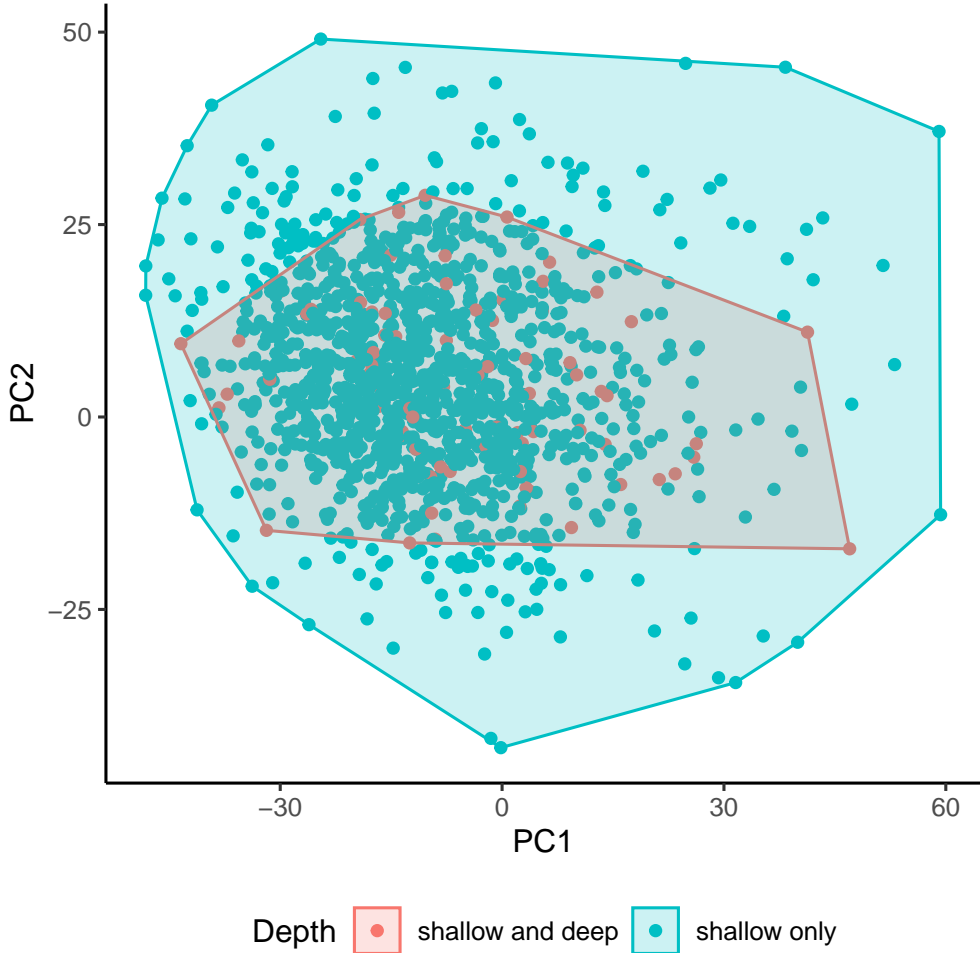


Figure 3.8: Color pattern morphospace of PC3 (x) vs PC4 (y) with individuals and hulls colored by depth: shallow and deep (red) vs shallow only (blue)

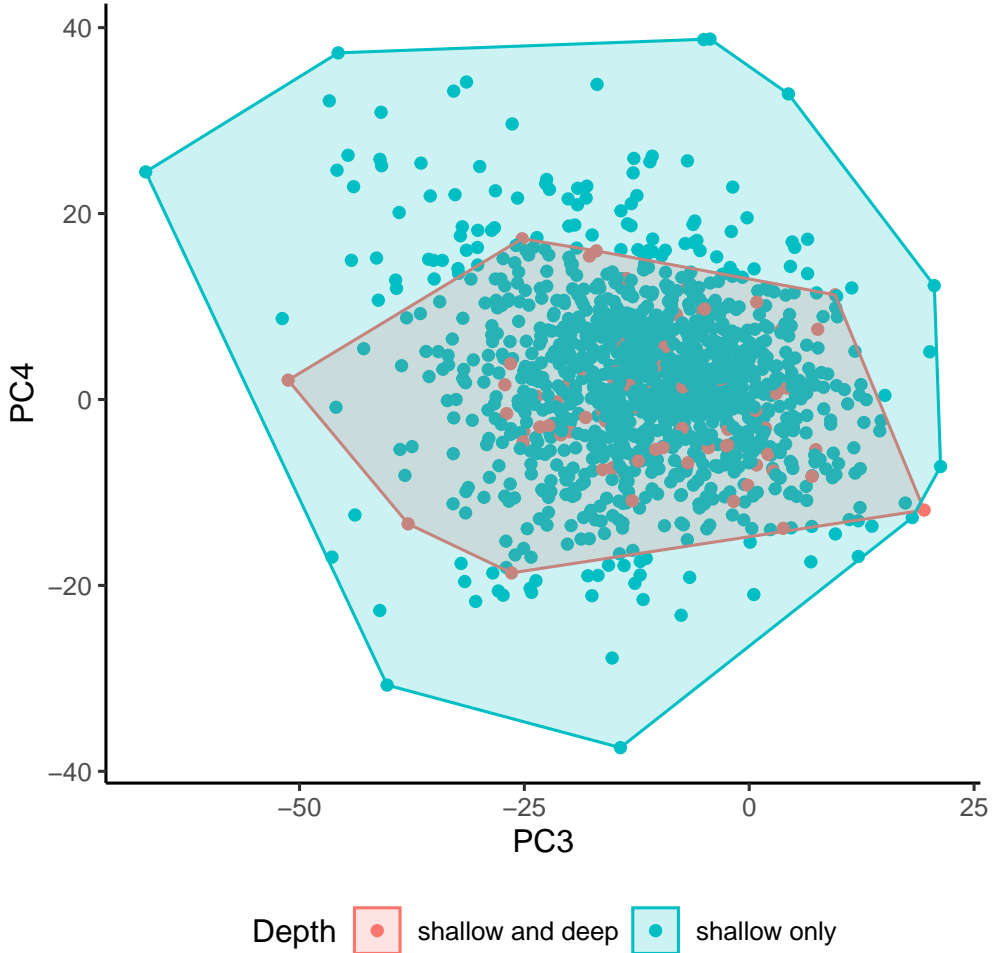


Figure 3.9: Color pattern morphospace of PC1 (x) vs PC2 (y) with individuals and hulls colored by reef region: Caribbean Sea (red), Coral Sea and Great Barrier Reef (green) and Red Sea (blue)

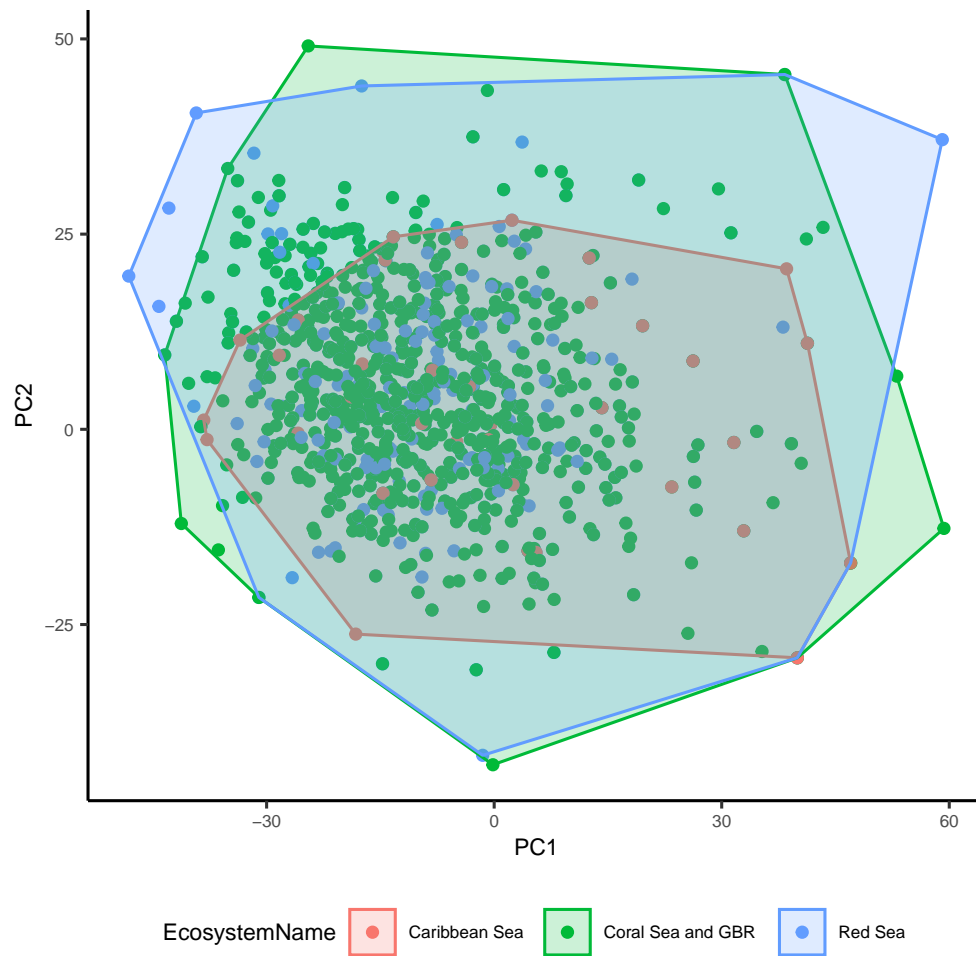
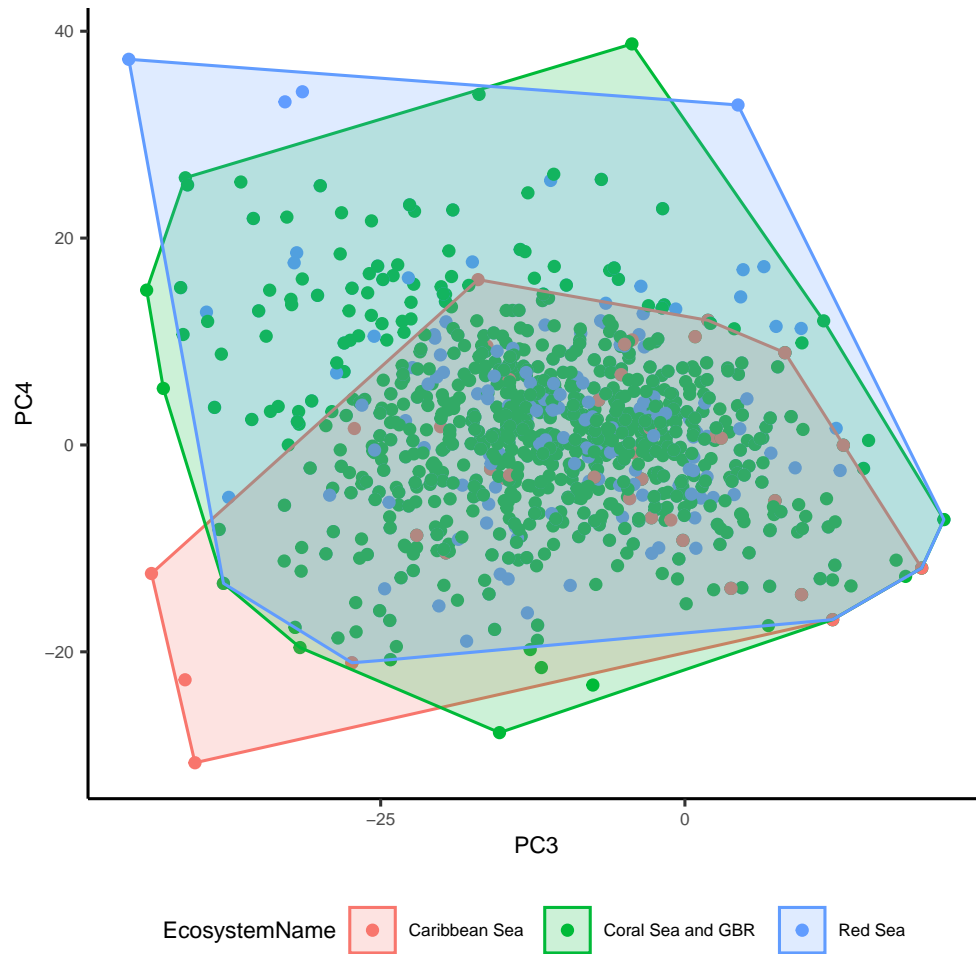


Figure 3.10: Color pattern morphospace of PC3 (x) vs PC4 (y) with individuals and hulls colored by reef region: Caribbean Sea (red), Coral Sea and Great Barrier Reef (green) and Red Sea (blue)



Bibliography

- Stephen Neudecker. Eye camouflage and false eyespots: chaetodontid responses to predators. *Environmental Biology of Fishes*, 25(1-3):143–157, 1989. ISSN 03781909. doi: 10.1007/BF00002208. arXiv: 1011.1669v3 ISBN: 9788578110796.
- George W Barlow. The attitude of fish eye-lines in relation to body shape and to stripes and bars. *Copeia*, 1972(1):4–12, 1972. ISSN 00458511. doi: 10.2307/1442777. URL <http://www.jstor.org/stable/1442777>. ISBN: 00458511.
- Christopher R. Hemingson, Peter F. Cowman, Jennifer R. Hodge, and David R. Bellwood. Colour pattern divergence in reef fish species is rapid and driven by both range overlap and symmetry. *Ecology Letters*, 2018. ISSN 14610248. doi: 10.1111/ele.13180.
- Martin Stevens. The role of eyespots as anti-predator mechanisms, principally demonstrated in the Lepidoptera. *Biological Reviews of the Cambridge Philosophical Society*, 80(4): 573–588, 2005. ISSN 14647931. doi: 10.1017/S1464793105006810. ISBN: 1464-7931.
- Kevin Arbuckle and Michael P. Speed. Antipredator defenses predict diversification rates. *Proceedings of the National Academy of Sciences*, 112(44):13597–13602, 2015. ISSN 0027-8424. doi: 10.1073/pnas.1509811112. URL <http://www.pnas.org/lookup/doi/10.1073/pnas.1509811112>. ISBN: 1091-6490 (Electronic) 0027-8424 (Linking).
- Dwayne W . Meadows. Morphological Variation in Eyespots of the Foureye Butterflyfish (*Chaetodon capistratus*): Implications for Eyespot Function. *Copeia*, 1(1):235–240, 1993.

- Jennifer R Hodge, Chidera Alim, Nick G. Bertrand, Wesley Lee, Samantha A Price, Binh Tran, and Peter C. Wainwright. Ecology shapes the evolutionary trade-off between predator avoidance and defence in coral reef butterflyfishes. *Ecology Letters*, 21(7):1033–1042, 2018. ISSN 14610248. doi: 10.1111/ele.12969.
- Karin Kjernsmo, Miranda Grönholm, and Sami Merilaita. Adaptive constellations of protective marks: Eyespots, eye stripes and diversion of attacks by fish. *Animal Behaviour*, 111: 189–195, 2016. ISSN 00033472. doi: 10.1016/j.anbehav.2015.10.028. ISBN: 0003-3472.
- Robert K. Robbins. The "False Head" Hypothesis: Predation and Wing Pattern Variation of Lycaenid Butterflies. *The American Naturalist*, 118(5):770–775, November 1981. ISSN 0003-0147, 1537-5323. doi: 10.1086/283868. URL <https://www.journals.uchicago.edu/doi/10.1086/283868>.
- Karin Kjernsmo and Sami Merilaita. Eyespots divert attacks by fish. *Proceedings of the Royal Society B: Biological Sciences*, 280(1766):20131458–20131458, 2013. ISSN 0962-8452. doi: 10.1098/rspb.2013.1458. URL <http://rspb.royalsocietypublishing.org/content/280/1766/20131458.short%5Cnhttp://rspb.royalsocietypublishing.org/cgi/doi/10.1098/rspb.2013.1458>.
- Jennifer L. Kelley, John L. Fitzpatrick, and Sami Merilaita. Spots and stripes: Ecology and colour pattern evolution in butterflyfishes. *Proceedings of the Royal Society B: Biological Sciences*, 280(1757), 2013. ISSN 14712954. doi: 10.1098/rspb.2012.2730.
- Adrian Vallin, Sven Jakobsson, and Christer Wiklund. "An eye for an eye?" - On the generality of the intimidating quality of eyespots in a butterfly and a hawkmoth. *Behavioral Ecology and Sociobiology*, 61(9):1419–1424, 2007. ISSN 03405443. doi: 10.1007/s00265-007-0374-6. ISBN: 0340-5443.
- Philip J. Motta. Response by potential prey to coral reef fish predators. *Animal Behaviour*,

- 31(4):1257–1259, November 1983. ISSN 00033472. doi: 10.1016/S0003-3472(83)80033-5. URL <https://linkinghub.elsevier.com/retrieve/pii/S0003347283800335>.
- Bibiana Rojas, Janne Valkonen, and Ossi Nokelainen. Aposematism. *Current Biology*, 25(9):R350–R351, May 2015. ISSN 09609822. doi: 10.1016/j.cub.2015.02.015. URL <https://linkinghub.elsevier.com/retrieve/pii/S0960982215001530>.
- M. Stevens. Predator perception and the interrelation between different forms of protective coloration. *Proceedings of the Royal Society B: Biological Sciences*, 274(1617):1457–1464, 2007. ISSN 0962-8452. doi: 10.1098/rspb.2007.0220. URL <http://rspb.royalsocietypublishing.org/cgi/doi/10.1098/rspb.2007.0220>. ISBN: 0962-8452 (Print)\r0962-8452 (Linking).
- Anders Forsman and Sami Merilaita. Fearful symmetry: pattern size and asymmetry affects aposematic signal efficacy. *Evolutionary Ecology*, 13:131–140, 1999. doi: 10.1023/A:1006630911975.
- R. Hoogland, D. Morris, and N. Tinbergen. The Spines of Sticklebacks (*Gasterosteus* and *Pygosteus*) as Means of Defence Against Predators (*Perca* and *Esox*). *Behaviour*, 10(1):205–236, 1956. ISSN 1568539X. doi: 10.1163/156853956X00156.
- R.W. Blake. Fish functional design and swimming performance. *Journal of Fish Biology*, (65):1193–1222, 2004. doi: 10.1111/j.1095-8649.2004.00568.x.
- Andrew J. Cole, Morgan S. Pratchett, and Geoffrey P. Jones. Diversity and functional importance of coral-feeding fishes on tropical coral reefs. *Fish and Fisheries*, 9(3):286–307, September 2008. ISSN 14672960, 14672979. doi: 10.1111/j.1467-2979.2008.00290.x. URL <https://onlinelibrary.wiley.com/doi/10.1111/j.1467-2979.2008.00290.x>.
- John E. Randall. John E. Randall’s Fish Photos, 2023. URL <http://pbs.bishopmuseum.org/images/JER/>.

R. Froese and D. Pauly. Fishbase, 2023. URL <https://fishbase.org>.

reefs.com. Reefs.com - Saltwater Aquarium Blog - Marine Aquarium Blog, 2023. URL <https://reefs.com/>.

Caroline A Schneider, Wayne S Rasband, and Kevin W Eliceiri. NIH Image to ImageJ: 25 years of image analysis. *Nature Methods*, 9(7):671–675, July 2012. ISSN 1548-7091, 1548-7105. doi: 10.1038/nmeth.2089. URL <http://www.nature.com/articles/nmeth.2089>.

Jennifer R. Hodge, Lynne van Herwerden, and David R. Bellwood. Temporal evolution of coral reef fishes: Global patterns and disparity in isolated locations. *Journal of Biogeography*, 41(11):2115–2127, 2014. ISSN 13652699. doi: 10.1111/jbi.12356.

David C. Collar, Peter C. Wainwright, Michael E. Alfaro, Liam J. Revell, and Rita S. Mehta. Biting disrupts integration to spur skull evolution in eels. *Nature Communications*, 5: 5505, 2014. ISSN 2041-1723. doi: 10.1038/ncomms6505. URL <http://www.nature.com/doi/10.1038/ncomms6505>.

Liam J. Revell. phytools: an R package for phylogenetic comparative biology (and other things): *phytools: R package. Methods in Ecology and Evolution*, 3(2):217–223, April 2012. ISSN 2041210X. doi: 10.1111/j.2041-210X.2011.00169.x. URL <https://onlinelibrary.wiley.com/doi/10.1111/j.2041-210X.2011.00169.x>.

Josef C. Uyeda, Daniel S. Caetano, and Matthew W. Pennell. Comparative Analysis of Principal Components Can be Misleading. *Systematic Biology*, 64(4):677–689, July 2015. ISSN 1076-836X, 1063-5157. doi: 10.1093/sysbio/syv019. URL <https://academic.oup.com/sysbio/article/64/4/677/1649888>.

Matthew W. Pennell, Jonathan M. Eastman, Graham J. Slater, Joseph W. Brown, Josef C. Uyeda, Richard G. FitzJohn, Michael E. Alfaro, and Luke J. Harmon. geiger v2.0: an expanded suite of methods for fitting macroevolutionary models to phylogenetic trees. *Bioinformatics*, 30(15):2216–2218, August 2014. ISSN 1367-4811, 1367-4803. doi: 10.1093/

bioinformatics/btu181. URL <https://academic.oup.com/bioinformatics/article/30/15/2216/2390619>.

Jose Pinheiro, Douglas Bates, Saikat DebRoy, Deepayan Sarkar, and R Core Team. nlme: Linear and Nonlinear Mixed Effects Models, 2021. URL <https://CRAN.R-project.org/package=nlme>.

A Meade and M Pagel. BayesTraits: Version 3.01 [manual], 2016. URL <http://www.evolution.rdg.ac.uk/BayesTraits.html>.

Sebastiano De Bona, Janne K. Valkonen, Andrés López-Sepulcre, and Johanna Mappes. Predator mimicry, not conspicuousness, explains the efficacy of butterfly eyespots. *Proceedings of the Royal Society B: Biological Sciences*, 282(1806), 2015. ISSN 14712954. doi: 10.1098/rspb.2015.0202.

Walter R Gilks, Sylvia Richardson, and David J Spiegelhalter. Introducing markov chain monte. *Markov chain Monte Carlo in practice*, 1, 1995.

E. Paradis and K. Schliep. ape 5.0: an environment for modern phylogenetics and evolutionary analyses in R. *Bioinformatics*, 35:526–528, 2019.

John Skelhorn, Giles Dorrington, Thomas J. Hossie, and Thomas N. Sherratt. The position of eyespots and thickened segments influence their protective value to caterpillars. *Behavioral Ecology*, 25(6):1417–1422, 2014. ISSN 14657279. doi: 10.1093/beheco/aru154.

E Lieske and R Myers. Collins pocket guide to coral reef fishes: Indopacific and Caribbean. *Herper Collins, London*, 1994.

Ullasa Kodandaramaiah. The evolutionary significance of butterfly eyespots. *Behavioral Ecology*, 22(6):1264–1271, 2011. ISSN 10452249. doi: 10.1093/beheco/arr123.

Christopher R Hemingson, Peter F Cowman, and David R Bellwood. Body size determines

- eyespot size and presence in coral reef fishes. *Ecology and Evolution*, (December 2019): 1–9, 2020. doi: 10.1002/ece3.6509.
- Mark Norman and Amanda Reid. *Guide to squid, cuttlefish and octopuses of Australasia*. CSIRO publishing, 2000.
- M. Stevens, C. J. Hardman, and C. L. Stubbins. Conspicuousness, not eye mimicry, makes "eyespot" effective antipredator signals. *Behavioral Ecology*, 19(3):525–531, January 2008. ISSN 1045-2249, 1465-7279. doi: 10.1093/beheco/arm162. URL <https://academic.oup.com/beheco/article-lookup/doi/10.1093/beheco/arm162>.
- John A. Endler. A framework for analysing colour pattern geometry: Adjacent colours. *Biological Journal of the Linnean Society*, 107(2):233–253, 2012. ISSN 00244066. doi: 10.1111/j.1095-8312.2012.01937.x.
- John A. Endler, Gemma L. Cole, and Alexandra M. Kranz. Boundary strength analysis: Combining colour pattern geometry and coloured patch visual properties for use in predicting behaviour and fitness. *Methods in Ecology and Evolution*, (July):1–15, 2018. ISSN 2041210X. doi: 10.1111/2041-210X.13073. ISBN: 0014-4894 (Print)\r0014-4894 (Linking).
- Ramasamy Santhanam. *Biology and ecology of toxic pufferfish*. CRC Press, 2017.
- Astrid Kodric-Brown. Sexual dichromatism and temporary color changes in the reproduction of fishes. *American Zoologist*, 38(1):70–81, 1998. ISSN 1540-7063. doi: 10.1093/icb/38.1.70. URL <http://icb.oxfordjournals.org/content/38/1/70.abstract>. ISBN: 0003-1569.
- G. F. Grether, J. Hudon, and J. A. Endler. Carotenoid scarcity, synthetic pteridine pigments and the evolution of sexual coloration in guppies (*Poecilia reticulata*). *Proceedings of the Royal Society B: Biological Sciences*, 268(1473):1245–1253, 2001. ISSN 0962-8452. doi: 10.1098/rspb.2001.1624. URL <http://rspb.royalsocietypublishing.org/cgi/doi/10.1098/rspb.2001.1624>. ISBN: 0962-8452 (Print).

- George A. Lozano. Carotenoids, Immunity, and Sexual Selection: Comparing Apples and Oranges? *The American Naturalist*, 158(2):200–203, 2001. ISSN 0003-0147. doi: 10.1086/321313. URL <http://www.journals.uchicago.edu/doi/10.1086/321313>. ISBN: 0003-0147.
- JH Choat and DR Robertson. Protogynous hermaphroditism in fishes of the family scaridae. In *Intersexuality in the animal kingdom*, pages 263–283. Springer, 1975.
- D Ross Robertson and Steven G Hoffman. The roles of female mate choice and predation in the mating systems of some tropical labroid fishes. *Zeitschrift für Tierpsychologie*, 45(3): 298–320, 1977.
- Ross Robertson and Robert R. Warner. Sexual patterns in the labroid fishes of the Western Caribbean, II, the parrotfishes (Scaridae). *Smithsonian Contributions to Zoology*, (255): 1–26, 1978. ISSN 00810282. doi: 10.5479/si.00810282.255. URL <https://repository.si.edu/handle/10088/5279>. ISBN: 0081-0282.
- John A Endler. Natural and sexual selection on color patterns in poeciliid fishes. *Environmental Biology of Fishes*, 9(2):173–190, 1983.
- John A Endler. A predator’s view of animal color patterns. In *Evolutionary biology*, pages 319–364. Springer, 1978.
- Robert S. Gregory. Effect of Turbidity on the Predator Avoidance Behaviour of Juvenile Chinook Salmon (*Oncorhynchus tshawytscha*). *Canadian Journal of Fisheries and Aquatic Sciences*, 50(2):241–246, 1993. ISSN 0706-652X. doi: 10.1139/f93-027. URL <http://www.nrcresearchpress.com/doi/10.1139/f93-027>.
- O Seehausen, J J M van Alphen, and F Witte. Cichlid fish diversity threatened by eutrophication that curbs sexual selection. *Science*, 277(September):1808–1811, 1997.

- Jennifer R Hodge, Francesco Santini, and Peter C Wainwright. Correlated Evolution of Sex Allocation and Mating System in Wrasses and Parrotfishes. *The American Naturalist*, 196(1), 2020a.
- J. R. Hodge, F. Santini, and P. C. Wainwright. Colour dimorphism in labrid fishes as an adaptation to life on coral reefs. *Proceedings of the Royal Society B: Biological Sciences*, 287(1923):20200167, March 2020b. ISSN 0962-8452, 1471-2954. doi: 10.1098/rspb.2020.0167. URL <https://royalsocietypublishing.org/doi/10.1098/rspb.2020.0167>.
- Yvonne Sadovy De Mitcheson and Min Liu. Functional hermaphroditism in teleosts. *Fish and Fisheries*, 9(1):1–43, 2008.
- Mark I. McCormick, Christopher A. Ryen, Philip L. Munday, and Stefan P. W. Walker. Differing Mechanisms Underlie Sexual Size-Dimorphism in Two Populations of a Sex-Changing Fish. *PLoS ONE*, 5(5):e10616, May 2010. ISSN 1932-6203. doi: 10.1371/journal.pone.0010616. URL <https://dx.plos.org/10.1371/journal.pone.0010616>.
- Michael Taborsky, Barbara Hudde, and Peter Wirtz. Reproductive behaviour and ecology of *symphodus (crenilabrus) ocellatus*, a european wrasse with four types of male behaviour. *Behaviour*, 102(1-2):82 – 117, 1987. doi: <https://doi.org/10.1163/156853986X00063>. URL https://brill.com/view/journals/beh/102/1-2/article-p82_6.xml.
- Patrick L Colin and Lori J Bell. Aspects of the spawning of labrid and scarid fishes (pisces: Labroidei) at enewetak atoll, marshall islands with notes on other families. *Environmental Biology of Fishes*, 31:229–260, 1991.
- Michael E. Alfaro, Chad D. Brock, Barbara L. Banbury, and Peter C. Wainwright. Does evolutionary innovation in pharyngeal jaws lead to rapid lineage diversification in labrid fishes? *BMC Evolutionary Biology*, 9(1):1–14, 2009. ISSN 14712148. doi: 10.1186/1471-2148-9-255. ISBN: 1471-2148.

- E. Kazancioglu, T. J. Near, R. Hanel, and P. C. Wainwright. Influence of sexual selection and feeding functional morphology on diversification rate of parrotfishes (Scaridae). *Proceedings of the Royal Society B: Biological Sciences*, 276(1672):3439–3446, 2009. ISSN 0962-8452. doi: 10.1098/rspb.2009.0876. URL <http://rspb.royalsocietypublishing.org/cgi/doi/10.1098/rspb.2009.0876>. ISBN: 0962-8452.
- J. T. Streebman, M. Alfaro, M. W. Westneat, D. R. Bellwood, and S. A. Karl. EVOLUTIONARY HISTORY OF THE PARROTFISHES: BIOGEOGRAPHY, ECOMORPHOLOGY, AND COMPARATIVE DIVERSITY. *Evolution*, 56(5):961–971, 2002.
- Gregory F Grether, Gita R Kolluru, and Karen Nersissian. Individual colour patches as multicomponent signals. *Biological Reviews*, 79(3):583–610, 2004.
- Pauline Salis, Thibault Lorin, Vincent Laudet, and Bruno FrÃ©dÃ©ric. Magic Traits in Magic Fish: Understanding Color Pattern Evolution Using Reef Fish. *Trends in Genetics*, pages 1–14, 2019. ISSN 13624555. doi: 10.1016/j.tig.2019.01.006. URL <https://doi.org/10.1016/j.tig.2019.01.006>. Publisher: Elsevier Ltd.
- Shawn T. Schwartz and Michael E. Alfaro. *Sashimi* : A toolkit for facilitating high throughput organismal image segmentation using deep learning. *Methods in Ecology and Evolution*, 12(12):2341–2354, December 2021. ISSN 2041-210X, 2041-210X. doi: 10.1111/2041-210X.13712. URL <https://besjournals.onlinelibrary.wiley.com/doi/10.1111/2041-210X.13712>.
- Rafael Maia, Chad M. Eliason, Pierre-Paul Bitton, StÃ©phanie M. Doucet, and Matthew D. Shawkey. pavo : an R package for the analysis, visualization and organization of spectral data. *Methods in Ecology and Evolution*, pages n/a–n/a, July 2013. ISSN 2041210X. doi: 10.1111/2041-210X.12069. URL <https://onlinelibrary.wiley.com/doi/10.1111/2041-210X.12069>.
- Mary Caswell Stoddard and Richard O. Prum. How colorful are birds? Evolution of the

avian plumage color gamut. *Behavioral Ecology*, 22(5):1042–1052, 2011. ISSN 10452249. doi: 10.1093/beheco/arr088.

Jolyon Troscianko and Martin Stevens. Image calibration and analysis toolbox – a free software suite for objectively measuring reflectance, colour and pattern. *Methods in Ecology and Evolution*, 6(11):1320–1331, November 2015. ISSN 2041-210X, 2041-210X. doi: 10.1111/2041-210X.12439. URL <https://besjournals.onlinelibrary.wiley.com/doi/10.1111/2041-210X.12439>.

Michael E Alfaro, Elizabeth A Karan, Shawn T Schwartz, and Allison J Shultz. The Evolution of Color Pattern in Butterflyfishes (Chaetodontidae). *Integrative and Comparative Biology*, 59(3):604–615, September 2019. ISSN 1540-7063. doi: 10.1093/icb/icz119. URL <https://academic.oup.com/icb/article/59/3/604/5530961>.

Shawn T Schwartz, Whitney T Nakashima, Elizabeth A Karan, and Michael E Alfaro. Charisma: An R tool to automatically determine discrete color classes for high-throughput color pattern analysis. In prep.

Yossi Rubner and Carlo Tomasi. *Perceptual metrics for image database navigation*. Springer Science & Business Media, 2001.

Hannah I Weller, Steven M Van Belleghem, Anna E Hiller, and Nathan P Lord. recolorize: improved color segmentation of digital images (for people with other things to do). *preprint*, 2022.

Anne E. Winters, Nerida G. Wilson, Cedric P. van den Berg, Martin J. How, John A. Endler, N. Justin Marshall, Andrew M. White, Mary J. Garson, and Karen L. Cheney. Toxicity and taste: Unequal chemical defences in a mimicry ring. *Proceedings of the Royal Society B: Biological Sciences*, 285(1880), 2018. ISSN 14712954. doi: 10.1098/rspb.2018.0457.

Daniel L. Rabosky, Jonathan Chang, Pascal O. Title, Peter F. Cowman, Lauren Sallan, Matt Friedman, Kristin Kaschner, Cristina Garilao, Thomas J. Near, Marta Coll, and Michael E.

Alfaro. An inverse latitudinal gradient in speciation rate for marine fishes. *Nature*, 559 (7714):392–395, 2018. ISSN 14764687. doi: 10.1038/s41586-018-0273-1. URL <http://dx.doi.org/10.1038/s41586-018-0273-1>. Publisher: Springer US ISBN: 4158601802731.

Silvia Castiglione, Gianmarco Tesone, Martina Piccolo, Marina Melchionna, Alessandro Mondanaro, Carmela Serio, Mirko Di Febbraro, and Pasquale Raia. A new method for testing evolutionary rate variation and shifts in phenotypic evolution. *Methods in Ecology and Evolution*, 9:974–983, 2018. URL <https://besjournals.onlinelibrary.wiley.com/doi/full/10.1111/2041-210X.12954>.

R Core Team. *R: A Language and Environment for Statistical Computing*. R Foundation for Statistical Computing, Vienna, Austria, 2023. URL <https://www.R-project.org/>.

John A Endler. Signals, Signal Conditions, and the Direction of Evolution. *The American Naturalist*, 139:S125–S153, 1992. ISSN 0003-0147. doi: 10.1086/285308. URL <http://www.journals.uchicago.edu/doi/10.1086/285308>. ISBN: 00030147.

Derek P. Tittensor, Camilo Mora, Walter Jetz, Heike K. Lotze, Daniel Ricard, Edward Vanden Berghe, and Boris Worm. Global patterns and predictors of marine biodiversity across taxa. *Nature*, 466(7310):1098–1101, 2010. ISSN 00280836. doi: 10.1038/nature09329. URL <http://dx.doi.org/10.1038/nature09329>. Publisher: Nature Publishing Group.

Rick D. Stuart-Smith, Amanda E. Bates, Jonathan S. Lefcheck, J. Emmett Duffy, Susan C. Baker, Russell J. Thomson, Jemina F. Stuart-Smith, Nicole A. Hill, Stuart J. Kininmonth, Laura Airoidi, Mikel A. Becerro, Stuart J. Campbell, Terence P. Dawson, Sergio A. Navarrete, German A. Soler, Elisabeth M.A. Strain, Trevor J. Willis, and Graham J. Edgar. Integrating abundance and functional traits reveals new global hotspots of fish diversity. *Nature*, 501(7468):539–542, 2013. ISSN 00280836. doi: 10.1038/nature12529. Publisher: Nature Publishing Group.

Jonathan Diamond and Denis Roy. Patterns of functional diversity along latitudinal gra-

- dients of species richness in eleven fish families. *Global Ecology and Biogeography*, 32(3):450–465, March 2023. ISSN 1466-822X, 1466-8238. doi: 10.1111/geb.13633. URL <https://onlinelibrary.wiley.com/doi/10.1111/geb.13633>.
- Seita Miyazawa. Pattern blending enriches the diversity of animal colorations. *Science Advances*, 6(49):eabb9107, December 2020. ISSN 2375-2548. doi: 10.1126/sciadv.abb9107. URL <https://www.science.org/doi/10.1126/sciadv.abb9107>.
- Katerina Zapfe. *MACROEVOLUTION OF BOLD COLOR PATTERNS ACROSS TELEOSTEAN FISHES*. PhD thesis, Clemson University, 2021.
- Juliette Langlois, François Guilhaumon, Florian Baletaud, Nicolas Casajus, Cédric De Almeida Braga, Valentine Fleuré, Michel Kulbicki, Nicolas Loiseau, David Mouillot, Julien P. Renoult, Aliénor Stahl, Rick D. Stuart Smith, Anne-Sophie Tribot, and Nicolas Mouquet. The aesthetic value of reef fishes is globally mismatched to their conservation priorities. *PLOS Biology*, 20(6):e3001640, June 2022. ISSN 1545-7885. doi: 10.1371/journal.pbio.3001640. URL <https://dx.plos.org/10.1371/journal.pbio.3001640>.
- Christopher R. Cooney, Yichen He, Zoë K. Varley, Lara O. Nouri, Christopher J. A. Moody, Michael D. Jardine, András Liker, Tamás Székely, and Gavin H. Thomas. Latitudinal gradients in avian colourfulness. *Nature Ecology & Evolution*, 6(5):622–629, May 2022. ISSN 2397-334X. doi: 10.1038/s41559-022-01714-1. URL <https://doi.org/10.1038/s41559-022-01714-1>.
- O. Seehausen, P. J. Mayhew, and J. J M Van Alphen. Evolution of colour patterns in East African cichlid fish. *Journal of Evolutionary Biology*, 12(3):514–534, 1999. ISSN 1010061X. doi: 10.1046/j.1420-9101.1999.00055.x. URL <http://doi.wiley.com/10.1046/j.1420-9101.1999.00055.x>. ISBN: 1010-061X.
- Lorian E. Schweikert, Robert R. Fitak, Eleanor M. Caves, Tracey T. Sutton, and SÃ¶nke

- Johnsen. Spectral sensitivity in ray-finned fishes: Diversity, ecology and shared descent. *Journal of Experimental Biology*, 221(23), 2018. ISSN 00220949. doi: 10.1242/jeb.189761.
- D. S. Wright, N. Demandt, J. T. Alkema, O. Seehausen, T. G.G. Groothuis, and M. E. Maan. Developmental effects of visual environment on species-assortative mating preferences in Lake Victoria cichlid fish. *Journal of Evolutionary Biology*, 30(2):289–299, 2017. ISSN 14209101. doi: 10.1111/jeb.13001.
- Svensson and Wong. Carotenoid-based signals in behavioural ecology: a review. *Behaviour*, 148(2):131–189, 2011.
- Joseph S Levine and Edward F MacNichol. Visual pigments in teleost fishes: effects of habitat, microhabitat, and behavior on visual system evolution. *Sensory processes*, 1979.
- Chun-Feng Chou, Cheng-Mu Tsai, Chao-Hsien Chen, Yung-Hao Wong, Yi-Chin Fang, Chan-Chuan Wen, Hsiao-Yi Lee, Hien Thanh Le, Shun-Hsyung Chang, and Hsing-Yuan Liao. Optical design and optimization with genetic algorithm for high-resolution optics applied to underwater remote-sensing. *Applied Sciences*, 11:10200, 10 2021. doi: 10.3390/app112110200.
- Stefano R. Montanari, Lynne van Herwerden, Morgan S. Pratchett, Jean Paul A. Hobbs, and Anneli Fugedi. Reef fish hybridization: Lessons learnt from butterflyfishes (genus *Chaetodon*). *Ecology and Evolution*, 2(2):310–328, 2012. ISSN 20457758. doi: 10.1002/ece3.83.
- Stefano R. Montanari, Jean Paul A. Hobbs, Morgan S. Pratchett, Line K. Bay, and Lynne Van Herwerden. Does genetic distance between parental species influence outcomes of hybridization among coral reef butterflyfishes? *Molecular Ecology*, 23(11):2757–2770, 2014. ISSN 1365294X. doi: 10.1111/mec.12762.
- Terry P. Hughes, David R. Bellwood, and Sean R. Connolly. Biodiversity hotspots, centres of endemism, and the conservation of coral reefs: Biodiversity of coral reefs. *Ecology Letters*,

5(6):775–784, November 2002. ISSN 1461023X, 14610248. doi: 10.1046/j.1461-0248.2002.00383.x. URL <http://doi.wiley.com/10.1046/j.1461-0248.2002.00383.x>.

Norman Myers, Russell A Mittermeier, Cristina G Mittermeier, Gustavo AB Da Fonseca, and Jennifer Kent. Biodiversity hotspots for conservation priorities. *Nature*, 403(6772): 853–858, 2000.

Peter F. Cowman, Valeriano Parravicini, Michel Kulbicki, and Sergio R. Floeter. The biogeography of tropical reef fishes: endemism and provinciality through time: Reef fish endemism and provinciality. *Biological Reviews*, 92(4):2112–2130, November 2017. ISSN 14647931. doi: 10.1111/brv.12323. URL <https://onlinelibrary.wiley.com/doi/10.1111/brv.12323>.

Joshua Drew, Gerald R. Allen, Les Kaufman, and Paul H. Barber. Endemism and Regional Color and Genetic Differences in Five Putatively Cosmopolitan Reef Fishes: *Regional Divergence of Southwestern Pacific Fishes*. *Conservation Biology*, 22(4):965–975, August 2008. ISSN 08888892. doi: 10.1111/j.1523-1739.2008.01011.x. URL <https://onlinelibrary.wiley.com/doi/10.1111/j.1523-1739.2008.01011.x>.

Carl Boettiger, Duncan Temple Lang, and Peter Wainwright. rfishbase: exploring, manipulating and visualizing FishBase data from r. *Journal of Fish Biology*, nov 2012. URL <https://doi.org/10.1111/j.1095-8649.2012.03464.x>.

Jonathan Ready, Kristin Kaschner, Andy B South, Paul D Eastwood, Tony Rees, Josephine Rius, Eli Agbayani, Sven Kullander, and Rainer Froese. Predicting the distributions of marine organisms at the global scale. *Ecological Modelling*, 221(3):467–478, 2010.

K Kaschner, K Kesner-Reyes, C Garilao, J Rius-Barile, T Rees, and R Froese. Aquamaps: Predicted range maps for aquatic species. *World wide web electronic publication, www.aquamaps.org, Version*, 8:2016, 2016.

Elizabeth Christina Miller, Christopher M. Martinez, Sarah T. Friedman, Peter C. Wainwright, Samantha A. Price, and Luke Tornabene. Alternating regimes of shallow and deep-sea diversification explain a species-richness paradox in marine fishes. *Proceedings of the National Academy of Sciences*, 119(43):e2123544119, October 2022. ISSN 0027-8424, 1091-6490. doi: 10.1073/pnas.2123544119. URL <https://pnas.org/doi/10.1073/pnas.2123544119>.

Rhiannon L. Dalrymple, Darrell J. Kemp, Habacuc Flores-Moreno, Shawn W. Laffan, Thomas E. White, Frank A. Hemmings, Marianne L. Tindall, and Angela T. Moles. Birds, butterflies and flowers in the tropics are not more colourful than those at higher latitudes. *Global Ecology and Biogeography*, 24(12):1424–1432, 2015. ISSN 14668238. doi: 10.1111/geb.12368. ISBN: 1466-8238.

Peter J Herring. The photoecology of pelagic oceanic decapods. In *Symp Zool Soc Lond*, volume 59, pages 263–290, 1988.

SÅ¶nke Johnsen. The Red and the Black: Bioluminescence and the Color of Animals in the Deep Sea. *Integrative and Comparative Biology*, 45(2):234–246, April 2005. ISSN 1540-7063. doi: 10.1093/icb/45.2.234. URL <https://doi.org/10.1093/icb/45.2.234>. eprint: <https://academic.oup.com/icb/article-pdf/45/2/234/2336134/i1540-7063-045-02-0234.pdf>.

S ergio Ricardo Floeter, Luiz A Rocha, D Ross Robertson, JC Joyeux, William F Smith-Vaniz, Peter Wirtz, AJ Edwards, Jo ao P Barreiros, CEL Ferreira, Jo ao L Gasparini, et al. Atlantic reef fish biogeography and evolution. *Journal of Biogeography*, 35(1):22–47, 2008.

Michel Kulbicki, Valeriano Parravicini, David R Bellwood, Ernesto Arias-Gonz alez, Pascale Chabanet, Sergio R Floeter, Alan Friedlander, Jana McPherson, Robert E Myers, Laurent Vigliola, et al. Global biogeography of reef fishes: a hierarchical quantitative delineation of regions. *PloS one*, 8(12):e81847, 2013a.

- Michel Kulbicki, Laurent Vigliola, Laurent Wantiez, Nicolas Hubert, Sergio R Floeter, and Robert F Myers. Biogeography of butterflyfishes: a global model for reef fishes. *Biology of butterflyfishes*, pages 70–106, 2013b.
- Paul H Barber and David R Bellwood. Biodiversity hotspots: evolutionary origins of biodiversity in wrasses (halichoeres: Labridae) in the indo-pacific and new world tropics. *Molecular phylogenetics and evolution*, 35(1):235–253, 2005.
- Peter F Cowman and David R Bellwood. Vicariance across major marine biogeographic barriers: temporal concordance and the relative intensity of hard versus soft barriers. *Proceedings of the Royal Society B: Biological Sciences*, 280(1768):20131541, 2013.
- Jennifer R Hodge, Charmaine I Read, David R Bellwood, and Lynne van Herwerden. Evolution of sympatric species: a case study of the coral reef fish genus *Pomacanthus* (Pomacanthidae). *Journal of Biogeography*, 40(9):1676–1687, 2013.
- Joseph D. DiBattista, Ellen Waldrop, Luiz A. Rocha, Matthew T. Craig, Michael L. Berumen, and Brian W. Bowen. Blinded by the bright: a lack of congruence between colour morphs, phylogeography and taxonomy for a cosmopolitan Indo-Pacific butterflyfish, *Chaetodon auriga*. *Journal of Biogeography*, 42(10):1919–1929, October 2015. ISSN 03050270. doi: 10.1111/jbi.12572. URL <https://onlinelibrary.wiley.com/doi/10.1111/jbi.12572>.
- Callum M Roberts, Colin J McClean, John EN Veron, Julie P Hawkins, Gerald R Allen, Don E McAllister, Cristina G Mittermeier, Frederick W Schueler, Mark Spalding, Fred Wells, et al. Marine biodiversity hotspots and conservation priorities for tropical reefs. *Science*, 295(5558):1280–1284, 2002.
- Michelle R Gaither and Luiz A Rocha. Origins of species richness in the indo-malay-philippine biodiversity hotspot: Evidence for the centre of overlap hypothesis. *Journal of biogeography*, 40(9):1638–1648, 2013.